MBMG Open-File Report 720 **2019**

SOUTH MEDICINE LAKE AREA OF THE CLEAR LAKE AQUIFER:

GROUNDWATER MODEL REPORT

Kevin Chandler and Jon Reiten

Montana Bureau of Mines and Geology Open-File Report 720

A Ground Water Investigation Program Project

MBMG
Montana Bureau of Mines and Geology

Cover. Sunset over Medicine Lake.

MBMG Open-File Report 720 **2019**

SOUTH MEDICINE LAKE AREA OF THE CLEAR LAKE AQUIFER: GROUNDWATER MODEL REPORT

Kevin Chandler and Jon Reiten

Montana Bureau of Mines and Geology Open-File Report 720

A Ground Water Investigation Program Project

TABLE OF CONTENTS

FIGURES

Appendix Figures:

TABLES

Appendix Tables:

PREFACE

The Ground Water Investigation Program (GWIP) at the Montana Bureau of Mines and Geology (MBMG) investigates areas prioritized by the Ground-Water Assessment Steering Committee (2-15-1523 MCA) based on current and anticipated growth of industry, housing, commercial activity, or agriculture. Additional program information and project ranking details are available at: http://www.mbmg.mtech.edu/gwip/gwip.html. GWIP also collects and compiles groundwater and surface-water data for each study area. These data are used to interpret how groundwater has responded to past stresses and to project future responses.

The final products of the Clear Lake aquifer study include:

An **Interpretive Report** (Reiten and Chandler, in review) that presents data interpretations and summarizes the project results. This report's main focus addresses potential effects to surface water and groundwater from increased use of the Clear Lake aquifer, and whether water development or other land uses have impacted water quality in the Clear Lake aquifer.

A **Groundwater Modeling Report** (this report) documents development of groundwater flow models, including a detailed description of the procedures, assumptions, and results of the models. Groundwater modelers and other qualified individuals can evaluate and use the models as a starting point to test additional water use scenarios and for site-specific analyses. The MBMG publications website includes the model files.

MBMG's Groundwater Information Center (GWIC) online database (http://mbmggwic.mtech.edu/) provides a permanent archive for the data from this study.

ABSTRACT

The Clear Lake aquifer in eastern Montana is a source of irrigation water. The MBMG prepared a groundwater flow model for a portion of this aquifer south of Medicine Lake, to characterize aquifer response to a potential increase in groundwater withdrawal for irrigation.

The model encompasses a 73 mi^2 region between Medicine Lake and Froid, Montana. The six-layer model, constructed in GMS and MODFLOW, represents the complex stratigraphy in the buried valley aquifer and the underlying Fort Union bedrock. Aquifer materials include alluvial and glacial outwash sand and gravel units interbedded with low-permeability glacial till and lake clay. These deposits form a complex groundwater system with highly variable aquifer thickness and hydrologic properties. Sources of water to the numerical model include head-dependent flux boundaries representing flow into the aquifer from adjacent areas of the Clear Lake aquifer. Recharge from direct infiltration of precipitation occurs largely within an area covered by sand hills. Groundwater sinks represented in the model include evapotranspiration from wetlands and seeps, discharge to small creeks and coulees, irrigation pumping, and outflow to adjacent areas of the Clear Lake aquifer.

A steady-state, calibrated version of the model provided a basis for a 1-year transient model. The transient model simulates the aquifer over 1 year of irrigation pumping; water levels recorded in monitoring wells during 2015 were used for calibration. Overall, the simulated transient response to irrigation pumping reasonably matches the timing and magnitude of water-level change in the calibration data set. Five simulations completed with the transient model include a current conditions scenario, wherein four existing irrigation wells pump at the rates used during the 2015 irrigation season. A simulation without irrigation pumping provides a control set of aquifer heads for comparison to irrigation pumping scenarios. Three predictive scenarios simulate increased irrigation pumping: the existing irrigation wells pumping at the maximum water rights allocations, the addition of four hypothetical irrigation wells pumping at rates similar to those used in 2015, and a simulation wherein all eight wells pump at full allocation volumes. With existing wells pumping at full allocation rates, water levels remain low for a longer period of time compared to 2015 irrigation extraction rates. With eight irrigation wells limited to 2015 pumping rates, groundwater extraction results in a 2-ft decrease in the potentiometric surface near Homestead.

Mass balance analyses from the simulations indicate that increasing irrigation pumping will increase groundwater flow into the area from upgradient portions of the Clear Lake aquifer and decrease groundwater flow from the simulated area to downgradient portions of the aquifer. Increased pumping also decreases water loss from evapotranspiration and flow to drains, which represent seepage to wetland areas.

INTRODUCTION

Background

An important water resource in eastern Montana occupies a broad, buried valley formed by the pre-glacial Missouri River. The Clear Lake aquifer contains sand and gravel deposited by the ancestral Missouri River and later by glacial meltwater streams (fig. 1). These deposits form a complex system of highly variable layer thickness and hydrologic properties, with some areas capable of supporting high-yield irrigation wells. The aquifer discharges to lakes and wetlands overlying the aquifer (Donovan, 1992). These lakes are important habitat for migratory birds and other wildlife. The U.S. Fish and Wildlife Service (USFWS) manage many of these lakes and wetlands as part of the Medicine Lake Wildlife Refuge. The USFWS is concerned that irrigation withdrawals will deplete water from the wetlands and lakes and thereby diminish the value of the habitat. In addition, the USFWS is concerned with impacts of past, current, and proposed hydrocarbon development on and near properties managed by the USFWS.

The South Medicine Lake management area was selected for development of a groundwater flow model. This area was chosen since there are long-term records of water levels and irrigation use. There is also concern that additional irrigation development may impact existing groundwater users, surface-water flows, and surface-water quality in this area. The aquifer management areas and the location of the groundwater model are shown in figure 1.

Purpose

The Clear Lake aquifer GWIP project purpose is to assist the Sheridan County Conservation District (SCCD) as they manage and allocate water resources from the aquifer. To meet this purpose, the Montana Bureau of Mines and Geology (MBMG) addressed two objectives:

(1) Evaluate potential effects on groundwater and surface-water resources resulting from increased irrigation withdrawals in the South Medicine Lake management area.

(2) Determine how water quality varies throughout the aquifer with respect to irrigation development and if water development or other land uses have affected water quality.

Tasks completed to address the objectives were:

1. Evaluate existing data, including previous geologic assessments, hydrogeologic reports, and unpublished field data.
2. Collect and compile water-quality data for the management areas and compare results to irrigation standards.
3. Develop a conceptual model for the South Medicine Lake management area.
4. Develop a numerical groundwater flow model of the South Medicine Lake management area.
5. Model future water-use scenarios in the South Medicine Lake management area.

Results from the first three tasks are presented in the interpretive report ((Reiten and Chandler, in review). This modeling report summarizes the conceptual model presented in the interpretive report, documents model construction and calibration, and presents the findings of the water-use scenarios.

MODEL OBJECTIVES

The numerical model is a tool to assess increased water development in the South Medicine Lake management area. Two objectives guided model development:

(1) <u>Simulate current aquifer conditions</u>

The first objective of the modeling exercise was to simulate the current conditions in the aquifer system. A steady-state model was developed and calibrated to average 2015 water levels. This model was subsequently modified to form a transient groundwater flow model. The transient model was calibrated to match 2015 water-level fluctuations resulting primarily from irrigation water use.

(2) <u>Simulate increased irrigation water use</u>

The second objective of the modeling was to assess effects of increased irrigation water use. Three scenarios tested increased water use by extending pumping periods and by simulating additional irrigation wells.

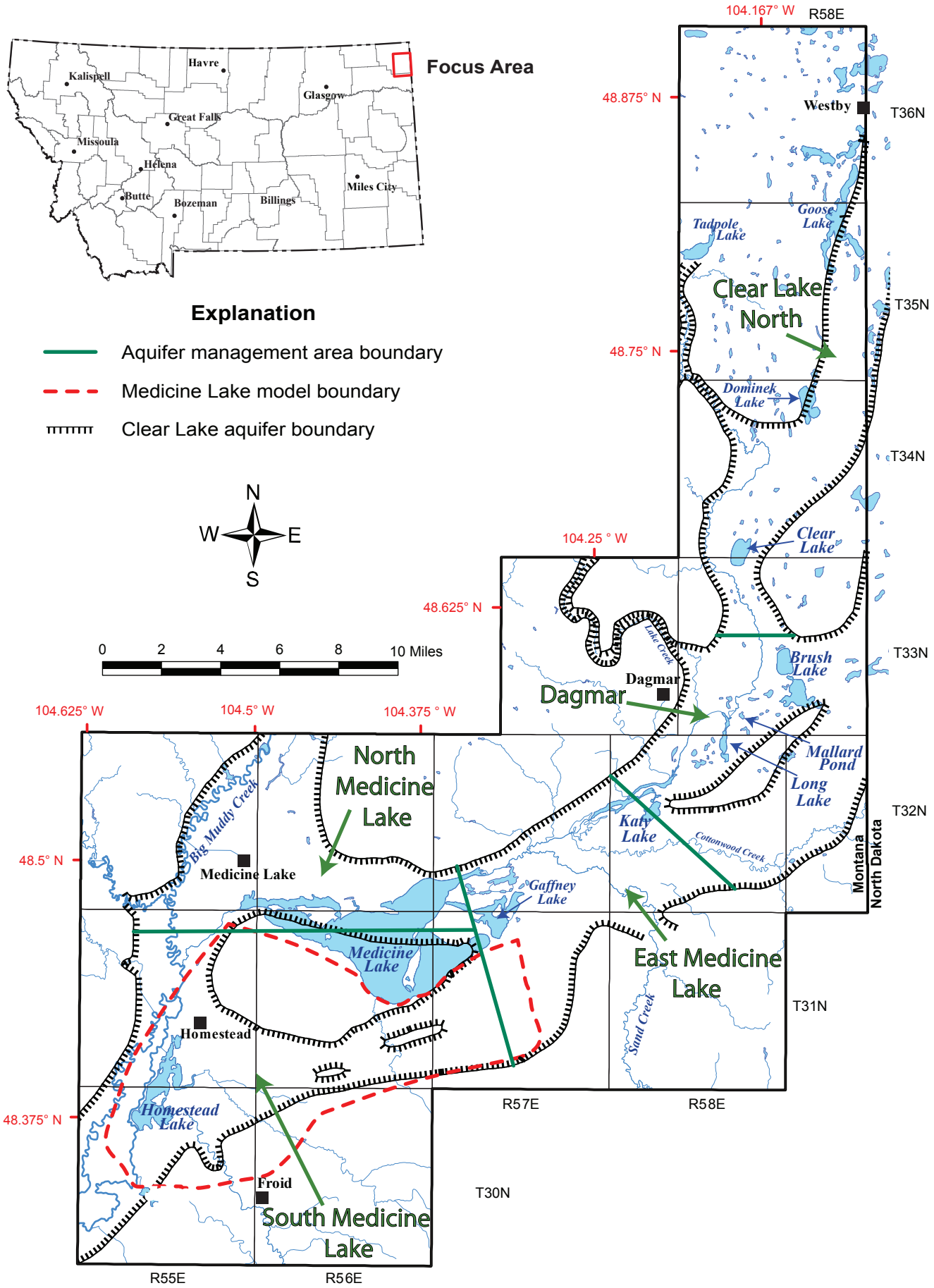

Figure 1. The Clear Lake aquifer underlies a large area in northeastern Montana.

MODEL AREA

The model area encompasses 73.2 mi^2 of farm, pasture, and wildlife refuge lands between Medicine Lake and Froid, Montana. The northern model boundary is approximately the shoreline of Medicine Lake, excluding an area where Fort Union bedrock crops out along the southwest edge of the lake (fig. 2). The western boundary was selected at an area of aquifer discharge near the center of the Big Muddy Creek Valley. The southern model boundary was established south of where the buried valley aquifer has been mapped, with the goal of including the valley edge where the Fort Union Formation bedrock is near the surface. The eastern boundary was located to include part of the sand dunes area (Eolian deposit, fig. 2), an important local recharge area for the aquifer.

PREVIOUS INVESTIGATIONS

The Clear Lake aquifer system has been studied for over three decades, providing a wealth of background information. The surficial geology was studied by the MBMG in the late 1980s, and detailed hydrogeologic data and interpretations are reported in Donovan and Bergantino (1987) and Donovan (1988). Schuele (1998) produced a groundwater model to evaluate the impacts of the irrigation development on the water balance and surface waters. Additionally, groundwater monitoring data are stored in the MBMG Ground Water Information Center (GWIC) system. These data provide background to the SCCD as part of the water permit application process (SCCD, unpublished file data). Reiten (2002) summarized the results of the monitoring program.

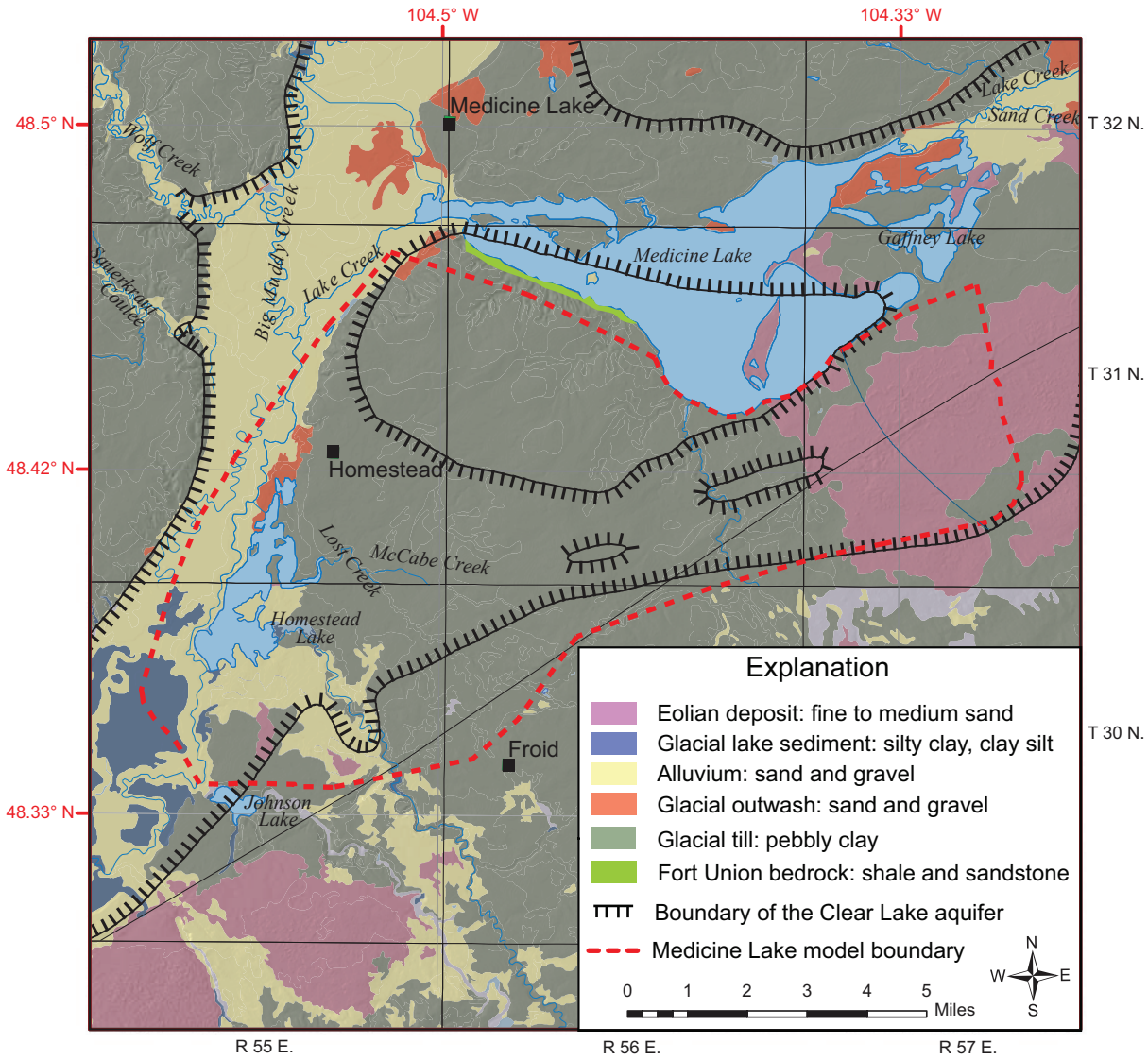

Figure 2. Surficial geology of the South Medicine Lake model area shows the sand hills (Eolian deposit) recharge area in the east, the glacial till in the middle, and the alluvium along Big Muddy Creek in the west. The Fort Union Formation bedrock outcrop on the southwest shore of Medicine Lake forms vertical faces (the extent is exaggerated by the mapped polygon).

As part of his investigation of the Clear Lake aquifer system, Donovan (1988) developed a two-dimensional groundwater flow model to evaluate a water budget for the entire aquifer. The one-layer model with 508 active cells was too simplistic to simulate water-level changes induced by irrigation, and was calibrated to average water levels and the average drawdown from irrigation use. Transient simulations used estimated pumping volumes for 1986 and then doubled that volume in a predictive simulation. The model simulation doubling the pumping volume predicted a decrease in evapotranspiration (ET) and outflow from Medicine Lake. Donovan concluded that the evaporative loss from the aquifer system was more than five times greater than the increased pumping volume.

A second groundwater flow model was developed for the entire Clear Lake aquifer, including channels of the aquifer in North Dakota (Schuele, 1998). The two-layer model assumed uniform aquifer properties over large areas, high levels of recharge, and a direct connection between surface-water bodies and the aquifer. Assumptions of the Schuele model are not valid in the South Medicine Lake model area, and Schuele's model area was too large and the grid too coarse to simulate the conditions relative to this project.

HYDROGEOLOGIC SETTING

Climate

Eastern Sheridan County has a semiarid continental climate, characterized by cold, dry winters, moderately hot and dry summers, and cool, dry falls. Cold winters are often interrupted by warming trends, with summers dominated by hot days and cool nights. January is generally the coldest month and July the warmest. Near the northern extent of the aquifer the average precipitation at Westby is about 14.2 in/yr [1937–2016, Western Regional Climate Center (WRCC, 2017)] with about 65% of the precipitation falling from May through August. Near the southern extent of the aquifer at Medicine Lake, the average precipitation is about 13.8 in/yr (1911–2016, WRCC), with the majority falling during the summer. June is typically the wettest month.

Although potential evaporation is typically much higher than precipitation is in this area, estimates of evaporation vary widely. The Medicine Lake 3 SE weather station (48.29°, -104.27°) reports a long-term pan evaporation average of 39.30 in, period of record (1911–2005,WRCC). A comparable station with a long-term Class A evaporation pan at Sidney, 50 mi south, was used in previous studies. Long-term data from the Sidney site report average annual evaporation of 33.14 in, period of record 1910–2005 (WRCC, 2017). Evaporation from a Class A pan at the U.S. Department of Agriculture research farm near Froid indicated 53% higher evaporation rates than at Sidney. The average evaporation at the Froid station was 52 in/yr from 1984 to 1988, but that was during an extreme drought. In contrast, the Sidney station reported 34 in of annual evaporation over the same time period (Donovan, 1988). Wind and hot temperatures contribute to an average of 6 to 12 in of monthly evaporation from May to August at the Froid site. For this modeling effort, the potential evapotranspiration was assumed to be approximately 3 ft/yr.

Physiography

Sloan (1972) characterized the landscape covering a large portion of the Clear Lake aquifer as prairie pothole type with rolling low-relief hills, wide valleys, and scattered closed drainage basins. Eolian sand hills dominate the east end of the model area, creating a hummocky landscape with small rounded hills and numerous potholes. The sand hills are sparsely covered with grasses, shrubs, and occasional trees near small potholes (fig. 3). The potholes hold water briefly

Figure 3. The sand hills southeast of Medicine Lake form an important recharge area for the Clear Lake aquifer (inset; sparse vegetation cover on dunes).

during snowmelt and large precipitation events. Aerial photos show crescent-shaped dunes and the lack of any clear drainage patterns, as precipitation produces little or no runoff in this area.

To the west of the sand hills, the land surface in the model area is mainly covered by glacial till. Piles of glacial erratic boulders can be found along section lines and at field corners where they have been removed from farmed fields. The fields have been tilled and rock-picked for many years, altering the geologic features. The glacial erratics are more visibly scattered on the surface of pasture lands and in coulees. The non-farmed areas help to identify the glacial surface deposits at many locations.

The Fort Union Formation is exposed at the surface in the northwestern part of the model area along the shores of Medicine Lake (fig. 4). This elevated bedrock area forms a low-permeability ridge between the model area buried valley aquifer and the lake. This bedrock ridge is likely an erosional remnant surrounded by incised buried valleys and capped with a sand and gravel alluvial terrace (fig. 5). Reiten and Chandler (in review) provide more detailed discussion on the physiography of the model area.

LAND USE AND WATER INFRASTRUCTURE

Approximately 63% of the land surface in the model area is farmed, and much of this area has been leveled. Crops are rotated, and large areas of gently sloping tilled land are often without vegetation during

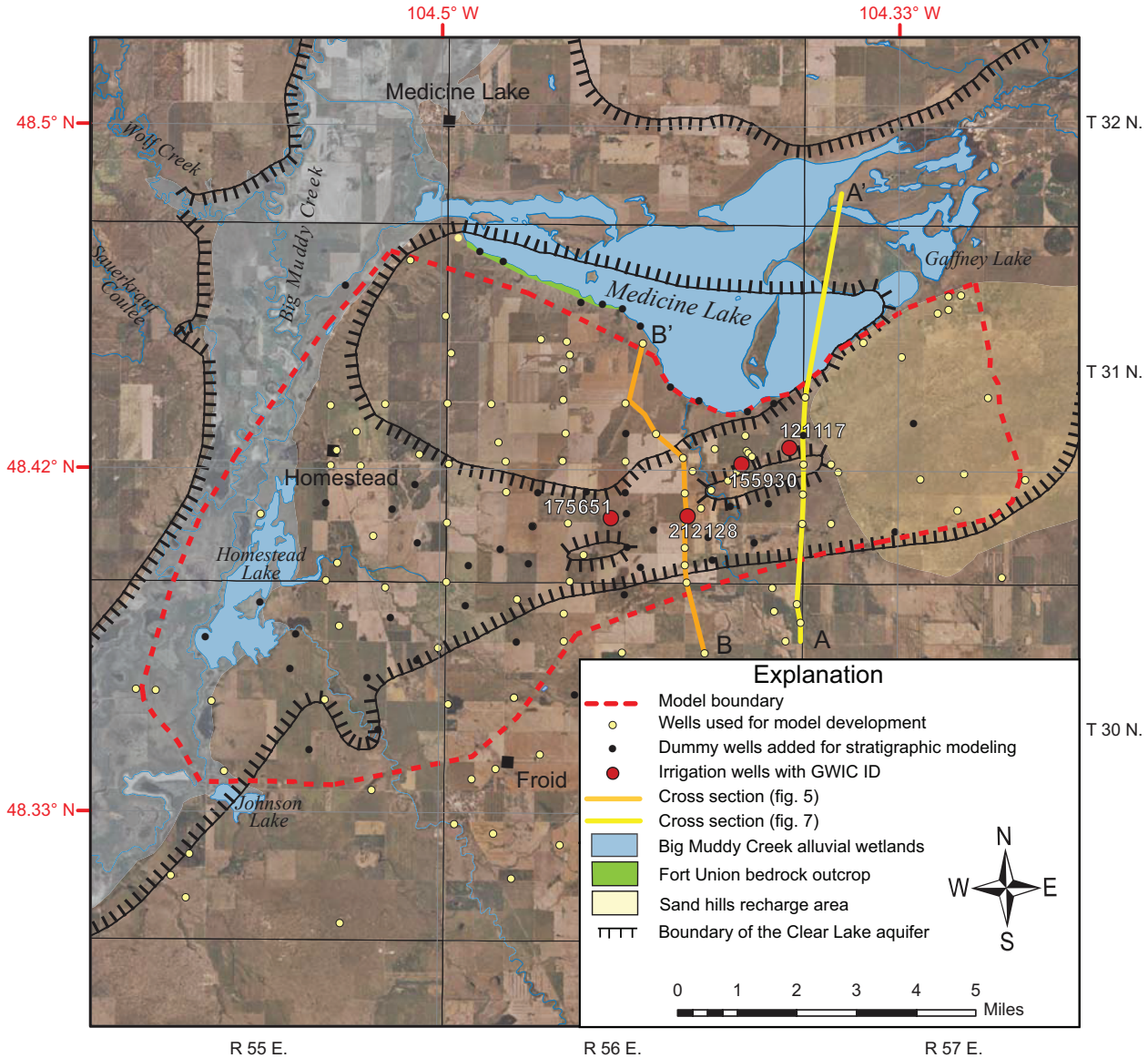

Figure 4. The model area extends from the sand hills in the east to the Big Muddy Creek alluvium in the west. The four existing irrigation wells are shown with their GWIC identification numbers.

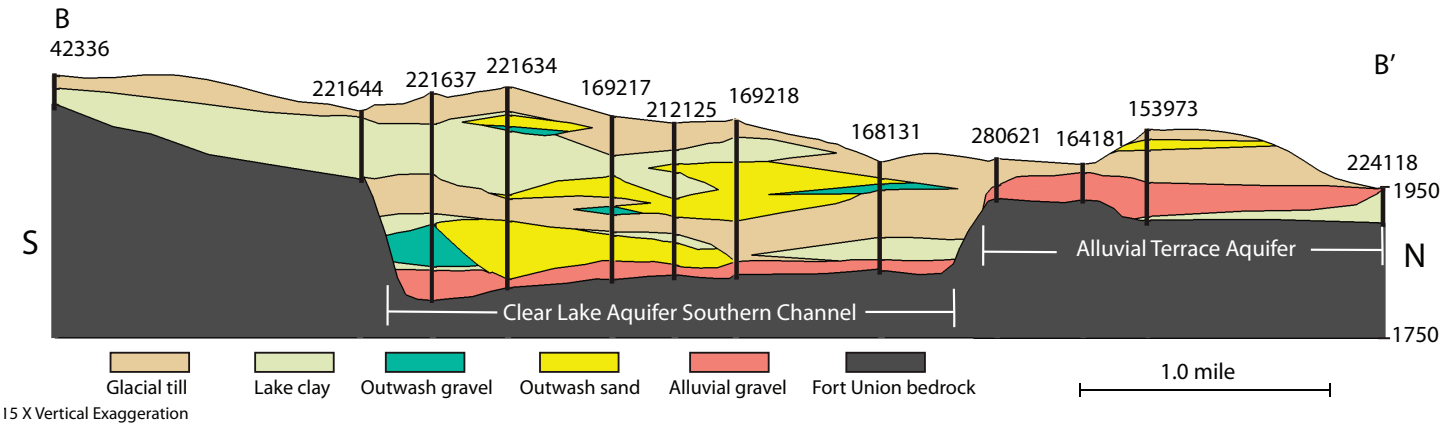

Figure 5. North–south cross section through the model area shows the separation between the deep alluvial gravel of the Clear Lake aquifer and the gravel of the alluvial terrace aquifer. (Cross section location shown in figure 4.) The Clear Lake aquifer consists of the deep alluvial gravel and the outwash sand and gravel.

the spring and fall. Although land-use practices such as intensive grain farming can increase infiltration (Luckey and Becker, 1999) when compared to undisturbed native grassland, differences in annual recharge resulting from land-use changes were not considered in this project.

In conjunction with farming, irrigation development has changed the area hydrogeologic system. Four irrigation wells currently operate in the model area with a capacity to irrigate 720 acres (fig. 4); most of the farmland is not irrigated. Table 1 displays two estimates of the 2015 irrigation water use. The first estimate is based on water usage calculated from total hours of electrical service; this likely overestimates pumping duration because electricity at the well head can be consumed for other purposes. We derived an alternative estimate based on water-level records at nearby observation wells. Changes in water level indicate periods of pump operation and a more reliable estimate of water use. The percentage of the permitted allocation used in 2015, the last column of table 1, was calculated with this method. See Reiten and Chandler (in review) for details on irrigation development and water use.

Changes to the surface-water systems in and near the model area affect the hydrology. Surface water in the groundwater discharge area along Big Muddy Creek is controlled by head gates, diversion channels, and small earthen dams on tributary drainages. The Medicine Lake National Wildlife Refuge controls the surface water entering and leaving the refuge, and manages flows and water levels to improve wildlife habitat. Surface waters on private holdings in the study area have been impounded for stock water and for irrigation. There have been some attempts along the Big Muddy to drain marshy areas and to channelize the flows, but these have no effect on the Clear Lake aquifer where the aquifer is being used for irrigation

Table 1. Water use during 2015 at the four existing irrigation wells in the model area.

GWIC ID Number	Pumping Rate (gpm)	Electric Usage[1] (acre-ft)	WL Response Usage[2] (acre-ft)	Allocation[3] (acre-ft)	Percentage of Allocation Used in 2015
175651	795	230	219	400	55%
121117	800	135	134	338	40%
155930	750	58	53	380	14%
212128	665	65	62	270	23%
Total	3,010	488	469	1388	34%

[1]Yearly volume calculated using hours of electrical service for pumping duration.

[2]Yearly volume calculated using pumping duration determined from water-level responses to pumping recorded in nearby observation wells.

[3]Water rights allocation, permitted yearly volume.

because they are miles downgradient from the area of interest. The wetlands rely on discharge from shallow aquifers, but connection to the deep Clear Lake aquifer, assumed in previous works, is not well supported by the available data.

CONCEPTUAL MODEL

A hydrogeologic conceptual model represents the interactions between the geology and groundwater in the process of receiving, storing, and releasing water. This conceptual model describes the subsurface geology, the hydrologic properties of the aquifer materials and confining units, the groundwater flow system, and sources and sinks (inflows and outflows) of groundwater.

Hydrogeologic Framework

The ancestral Missouri River flowed northeast, eroding a valley into the Fort Union Formation bedrock south of Medicine Lake. Since then, the valley has been cut and buried by multiple glacial events, leaving no surface expression of a once dominant feature. The subsurface is now a meshwork of outwash sand and gravel, lake clays, and tills that have filled the valley. The complex stratigraphy documented in the well logs shows the system to be highly variable with large changes in lithology and aquifer conditions over short horizontal distances. The ancient Missouri River alluvial gravel may be the most continuous unconsolidated deposit in the aquifer system where it often hosts the deepest portion of the Clear Lake aquifer.

Previous studies have identified areas in the aquifer system where outwash sand and gravel overlie, or have been deposited directly on, alluvial sand and gravel deposits (Donovan, 1992). In these areas where the sand and gravel deposits are hydrologically connected, the aquifer thickness is greatly increased, recharge can be local, and the water quality and quantity are sufficient for irrigation development. Identification of these connected areas and the location of hydrogeologic boundaries is necessary to properly evaluate and manage for sustainable use (Russell and others, 2004).

Analyses of water-level responses to pumping stresses helped to identify connections between aquifer segments and to identify boundaries in buried channel aquifer systems. Water-level responses to pumping were used to identify a large area between Medicine Lake and the buried valley aquifer where the upper alluvial terrace deposits are not hydrologically connected to the deeper alluvial deposits of the Clear Lake aquifer (fig. 5). The water levels in wells completed in alluvial terrace aquifer are lower than water levels in the deeper buried valley aquifer wells. The water levels in the upper terrace gravels do not respond to groundwater pumping from the deep portions of the Clear Lake aquifer (Reiten and Chandler, in review).

Hydrogeologic Boundaries

The focus area segment of the Clear Lake aquifer trends east to west and is constrained by bedrock along its north and south boundaries. The Fort Union Formation bedrock in this area is predominately consolidated to semi-consolidated mudstone. Based on literature values, the hydraulic conductivity of the bedrock is two to eight orders of magnitude lower than the aquifer sand and gravel and therefore acts as a barrier to groundwater flow (Anderson and Woessner, 1992). Several bedrock ridges within the buried valley have been identified from well log records (wells 221646, 43120) and from aquifer tests (Reiten and Chandler, in review). These ridges form low-permeability boundaries within the buried valley aquifer. Similar bedrock ridges form longitudinal hydraulic barriers in buried valley aquifers in North Dakota (Shaver and Pusc, 1992).

Although the mudstones and cemented sandstones of the Fort Union bedrock are relatively impermeable compared to the Clear Lake aquifer, thin layers of soft sandstone and coal within the formation form low-yield aquifers. The hydraulic heads measured in Fort Union Formation wells south of the model area show a steep gradient northward toward the buried valley aquifer. The erosion that formed the ancestral Missouri River valley likely exposed Fort Union Formation coalbeds and sandstone layers that have the potential to contribute groundwater to the buried valley aquifer. Completion information and water-level measurements used to determine groundwater flow potential and direction are available online from the Groundwater Information Center database, GWIC (http://mbmg-gwic.mtech.edu).

Material Properties of the Aquifer

The unconsolidated materials forming the Clear Lake aquifer in the model area result from deposition,

erosion, and reworking by numerous geologic events. This results in highly heterogeneous aquifer materials with variable hydraulic properties. In areas where the aquifer supports high-yield production wells, one or more layers of coarse gravel lie near the bottom of the aquifer. These deep gravel deposits typically fine upwards and often contain minor detrital coal and clay layers. Many well logs document upper gravel and sand layers that do not yield sufficient water for irrigation production. However, these shallow layers provide groundwater storage and transmit recharge to deeper deposits. Glacial till primarily acts as an aquitard, but it can be permeable where it is weathered and fractured (Cummings and others, 2012). Thin sand and gravel lenses commonly found in till also locally increase the conductivity and storage of water (Kessler and others, 2013).

Aquifer tests at wells completed in the Clear Lake aquifer alluvial gravel produce K estimates ranging from 70 to 460 ft/day with a geometric mean of 190 ft/day. Tests at wells completed in outwash gravels yield a greater range of values, from 60 ft/day to 6,300 ft/day with a geometric mean of 960 ft/day (table A1, appendix A). In addition to these test results, literature values of hydraulic properties used to guide the model development are listed in table 2.

The irrigation wells within the model domain predominately produce from deep gravels, but aquifer test results indicate leakage from the shallow sand and gravel layers during extended pumping. Additional information on the aquifer properties was gained by analyzing water-level fluctuations recorded at observation wells during the 2015 irrigation season. The drawdown data from irrigation use were analyzed as aquifer tests, producing hydraulic conductivity values from 100 to 450 ft/day (Reiten and Chandler, in review). These values are in agreement with historical aquifer tests conducted on wells completed in the alluvial gravels.

The vertical hydraulic conductivity (K_v) of sedimentary deposits is usually much less than the horizontal hydraulic conductivity (K_H). A study of fluvial and lacustrine deposits found the K_H to be 2 to 10 times larger than the K_v (Freeze and Cherry, 1979). The model K_v values were set to 1/3 of the K_H values initially and adjusted during calibration.

Storage coefficients calculated from aquifer tests (Reiten and Chandler, in review) and those reported in the literature (table 2) were used to constrain the storage values in the transient groundwater flow model. Storage coefficients are derived from drawdown data collected at observation wells. Because of this requirement, storage coefficients could be generated for about ⅓ of the outwash gravel and ½ alluvial gravel aquifer tests. Storage coefficients for the outwash gravel range from 0.0003 to 0.05 with an arithmetic mean of 0.015. This indicates that the outwash gravel of the Clear Lake aquifer is under unconfined to leaky confined conditions. The alluvial gravel aquifer tests generate storage coefficient values from 0.0001 to 0.003 with an arithmetic mean of 0.0009. These data indicate that the alluvial gravel is under confined to leaky confined conditions.

Groundwater Flow System

Potentiometric surfaces constructed from historical water-level data indicate a general northeast to southwest groundwater flow in the greater Clear Lake aquifer (Reiten and Chandler, in review). Water-level data collected in April and May of 2015 show a groundwater divide in the portion of the aquifer southwest of Medicine Lake. Water levels at sites difficult to access

Table 2. Reported hydraulic property ranges for sediment types in the model area.

Material	K_H (ft/day)	K_v (ft/day)	S_S (ft^{-1})	S_Y
Till and Clay	1.0×10^{-6} to 0.1	3.0×10^{-4} to 0.03	1.0×10^{-8} to 1.0×10^{-4}	1.0×10^{-6} to 1.0×10^{-2}
Sand	10 to 100	3.0 to 30	1.0×10^{-8} to 1.0×10^{-4}	1.0×10^{-3} to 0.15
Sand and Gravel	50 to 1,000	5.0 to 100	1.0×10^{-8} to 1.0×10^{-5}	1.0×10^{-3} to 0.20
Sedimentary Bedrock	1.0×10^{-3} to 15	1.0×10^{-4} to 5	1.0×10^{-8} to 1.0×10^{-6}	1.0×10^{-6} to 1.0×10^{-2}

Note. Ranges modified from Anderson and Woessner, 1992a; Weight and Sonderegger, 2001; Fetter, 2001. Sedimentary bedrock includes sandstone, coal, and shale.

and /or measure were estimated using previous levels and area-wide water-level trends. The dominant flow direction is to the west, but in the northeast portion of the model area, flow is northward towards a channel of the Clear Lake aquifer under Medicine Lake (fig. 6, in pocket in back).

Although some groundwater from the alluvial terrace aquifer (fig. 5) discharges to Medicine Lake, data indicate no connection between the lake and the deep aquifer south of Medicine Lake. Heads in the aquifer are higher than the lake, and several wells near the lake are free-flowing artesian (wells 169219, 169220). Using the gradients mapped in the deep aquifer, heads at these two wells would be 2 to 4 ft higher than the lake level if directly connected. However, the heads at the flowing wells are over 40 ft higher than the lake level. These observed artesian conditions can only occur if there is a barrier preventing direct connection between the aquifer and the lake.

Additional evidence for a barrier between the aquifer and Medicine Lake is found in aquifer response to pumping and in water quality. Aquifer tests conducted at irrigation wells near the south side of Medicine Lake indicated barrier boundaries (Reiten and Chandler, in review). Pumping from the closest irrigation well to the lakeshore, Nelson 1 (well 121117), produces more drawdown than pumping from other irrigation wells in the area, indicating a hydraulic boundary near Nelson 1. In areas where lower salinity groundwater enters Medicine Lake, visible evidence of freshening can be seen along shorelines by the presence of bulrushes and other aquatic plants. There is also no apparent aquifer discharge to the lake in our study area.

North–south cross sections constructed using borehole data show the stratigraphic relationships that result in a barrier to flow between the lake and the deep aquifer (figs. 7A,7B). Figure 7A shows the generalized stratigraphic correlations. Figure 7B is further simplified to illustrate that shallow and deep permeable deposits are separated by low-permeability confining beds. Figure 7B also illustrates the continuous nature of the bedrock and till that effectively separates the aquifer system from Medicine Lake. The water level in the Clear Lake aquifer southern channel is above ground at well 169219, but the water level in the northern channel at well 280643 is approximately lake level.

Several monitoring wells (280621, 169212, and169213) on the south side of Medicine Lake also show no detectable water-level response to irrigation pumping. The lower sand and gravel of the deep aquifer appear to be isolated from the upper alluvial terrace aquifer (fig. 5). Extensive layers of clay and glacial till documented in the area act as confining beds separating the upper alluvial terrace from the deep Clear Lake aquifer.

Sources and Sinks

Model area recharge comes as direct infiltration of precipitation and as inflow from adjacent aquifers. As observed in other similar hydrogeologic settings (Seyoum and Eckstein, 2014), inter-aquifer recharge likely provides groundwater from shallow unconsolidated deposits and deeper bedrock aquifers surrounding this buried valley aquifer. These connections to adjacent formations greatly expand the recharge area, and tend to dampen water-level fluctuations resulting from climatic changes.

Groundwater levels in the overall study area respond to large precipitation events and to snowmelt in the spring and fall. Hydrographs show the largest gains in March and early April (Reiten and Chandler, in review). An unusual summer storm resulted in 3 in of rainfall on June 5th, 2015. Some wells north of the model area showed 2 to 3 in of water-level increase within several hours, with water levels remaining elevated for over 2 weeks. Although large precipitation events can provide aquifer recharge, water from most summer rain events is typically consumed by evapotranspiration.

Sinks include groundwater discharge to springs and wetlands as well as groundwater outflow to downgradient parts of the aquifer. The upward seepage to the wetlands along Big Muddy Creek is mostly lost to the atmosphere through evapotranspiration. Donovan (1988) estimated that more than 3 ft of water is evaporated or transpired annually from these area wetlands. There are also some seeps and springs that flow northwards towards Medicine Lake from the model area. These flows are thought to be sourced from the upper terrace alluvial aquifer. Small stock-water ponds constructed downstream from the springs have water levels higher than the lake, and the lower salinity water supports more vegetation than the lake. Groundwater also seeps from the exposed Fort Union bedrock

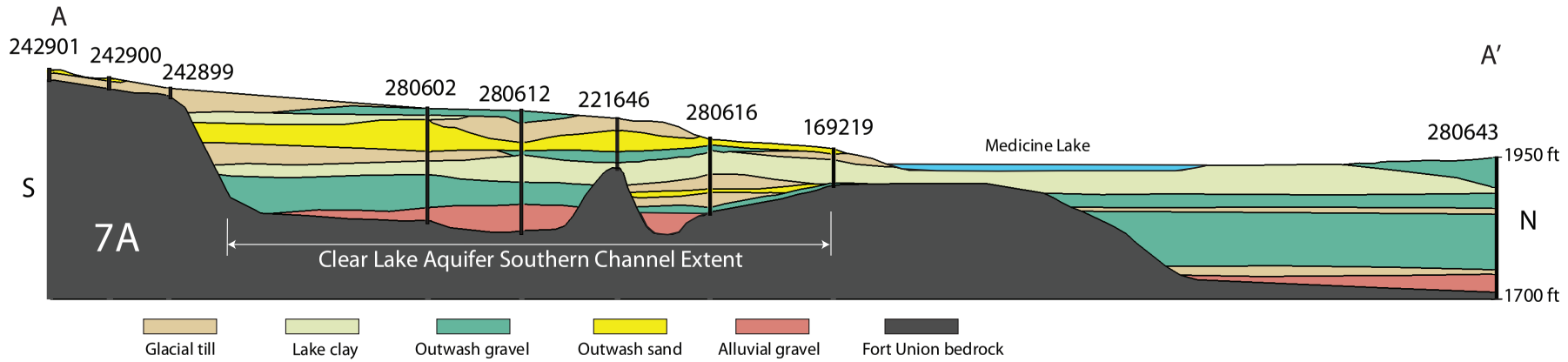

Figure 7. (A) South–north cross section shows the modeled stratigraphy constructed from well log information. The GWIC ID numbers are shown above the wells (cross section A –A' location, fig. 4).

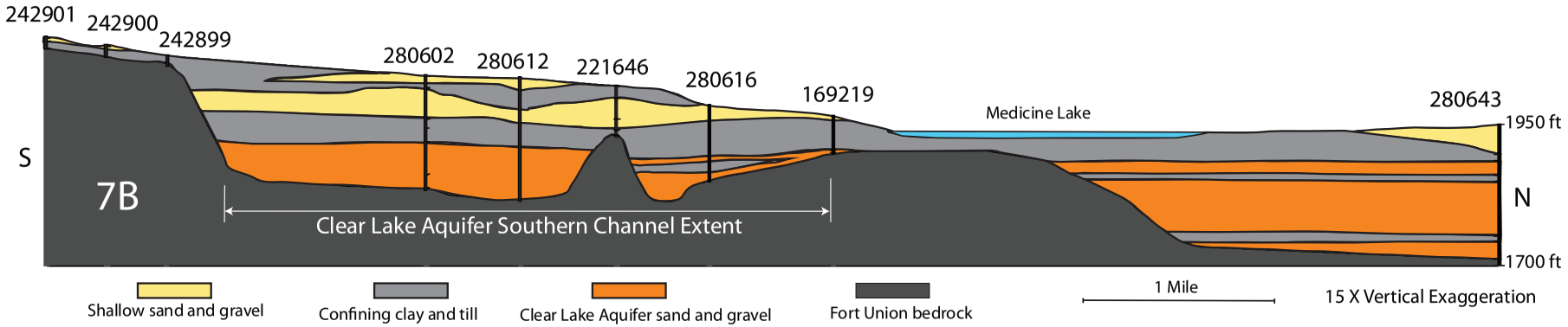

Figure 7. (B) A simplification of figure 7A groups the like materials into confining layers and upper and lower aquifers. Layers of till and clay act as confining layers and where continuous with the Fort Union bedrock, likely form a groundwater flow barrier between the southern channel of the Clear Lake aquifer and Medicine Lake.

at the southwest shore of Medicine Lake. Although the visible spring and seep waters flow towards the lake, there is no observable mixing zone along the southern lakeshore, indicating a low seepage volume.

GROUNDWATER BUDGET

A groundwater budget quantifies the groundwater flow into and out of an area using estimated and measured fluxes. Groundwater flow modeling based on approximate fluxes is often used to quantify part of the water budget, or changes to the water budget due to simulated variations in the sources and sinks. The primary purpose of this model is to simulate water-level changes resulting from increased irrigation water use. The groundwater budget estimate presented below includes reasonable ranges of sources and sinks to compare to model-generated budgets during calibration. It is not intended to be used in conjunction with the model to quantify a part of the area water budget.

There are no measurable surface flows in or out of the South Medicine Lake model area, and therefore the groundwater budget is highly dependent on estimated recharge and evapotranspiration. The acreages of land used for these estimates were determined from satellite images. In reality, the acreages of wetlands varies annually, and is dependent on climatic conditions. Wetlands and ponds decrease in size during droughts, and expand during wet periods. The acreage estimates and ranges of recharge or evapotranspiration used for the groundwater budget calculations are listed in table 3.

Groundwater also enters and leaves the model area as flux from distant segments of the Clear Lake aquifer and other aquifers. Water-level records indicate hydraulic gradients into and out of the model area, but there is little information about the aquifer thickness along the model boundaries. The flux calculations are likewise based on estimations. Therefore the groundwater budget presents a range of reasonable values for comparison, but it is not used as a calibration target. The model-generated flow budgets presented in the model summary section were used to assess change related to the simulated increased groundwater development, and not to provide a precise accounting of groundwater flux.

GROUNDWATER FLOW MODEL CONSTRUCTION

Computer Code

MODFLOW 2005 (Harbaugh, 2005) was used as the numerical model code within the GMS 8.3 (AQUAVEO™) graphical user interface. The steady-state and transient simulations made use of the Hyrogeologic-Unit Flow (HUF; Anderman and Hill, 2000) package and the Pre-Conditioned Conjugate Gradient (PCG2) solver.

Model Grid

The grid dimensions are 80,000 ft by 48,000 ft with cell size of 400 ft by 400 ft. The model consists of six layers that vary in thickness across the domain.

Table 3. Estimated flows for the South Medicine Lake model area.

Flow In	Description	Range of Estimated Flow (acre-ft/yr)
Recharge	Sand hills area, (1–6 in/yr over 11,450 acres)	950–8,680
Bedrock Flux	Inflow along southern boundary, (K=1–5 ft/day, b=20 ft)	200–1,000
Sand Dunes southeast Underflow	Underflow in at the southeast boundary, (K=50–450 ft/day, b=20 ft)	360–3,280
Total In Range		1,510–12,060
Flow Out		
Springs and Seeps	Loss as flow and ET (1–3 ft/yr over 800 acres)	800–2,400
Wetland ET	Loss as ET (1–3 ft/yr over 1,980 acres)	1,980–5,940
Sand Hills North Underflow	Underflow out at the northeast boundary (K=50–450 ft/day, b=10 ft)	390–1,740
Big Muddy Alluvium underflow	Underflow in at the southwest boundary (K=50–450 ft/day, b=20 ft)	30–220
Irrigation Use	Pumping at the four existing wells (no use to full allocation)	0–1,500
Total Out Range		3,200–11,800

Note. The hydraulic conductivity (K) estimates are for a range of materials included in the aquifer. The aquifer thicknesses (b) were estimated and likely vary depending on location.

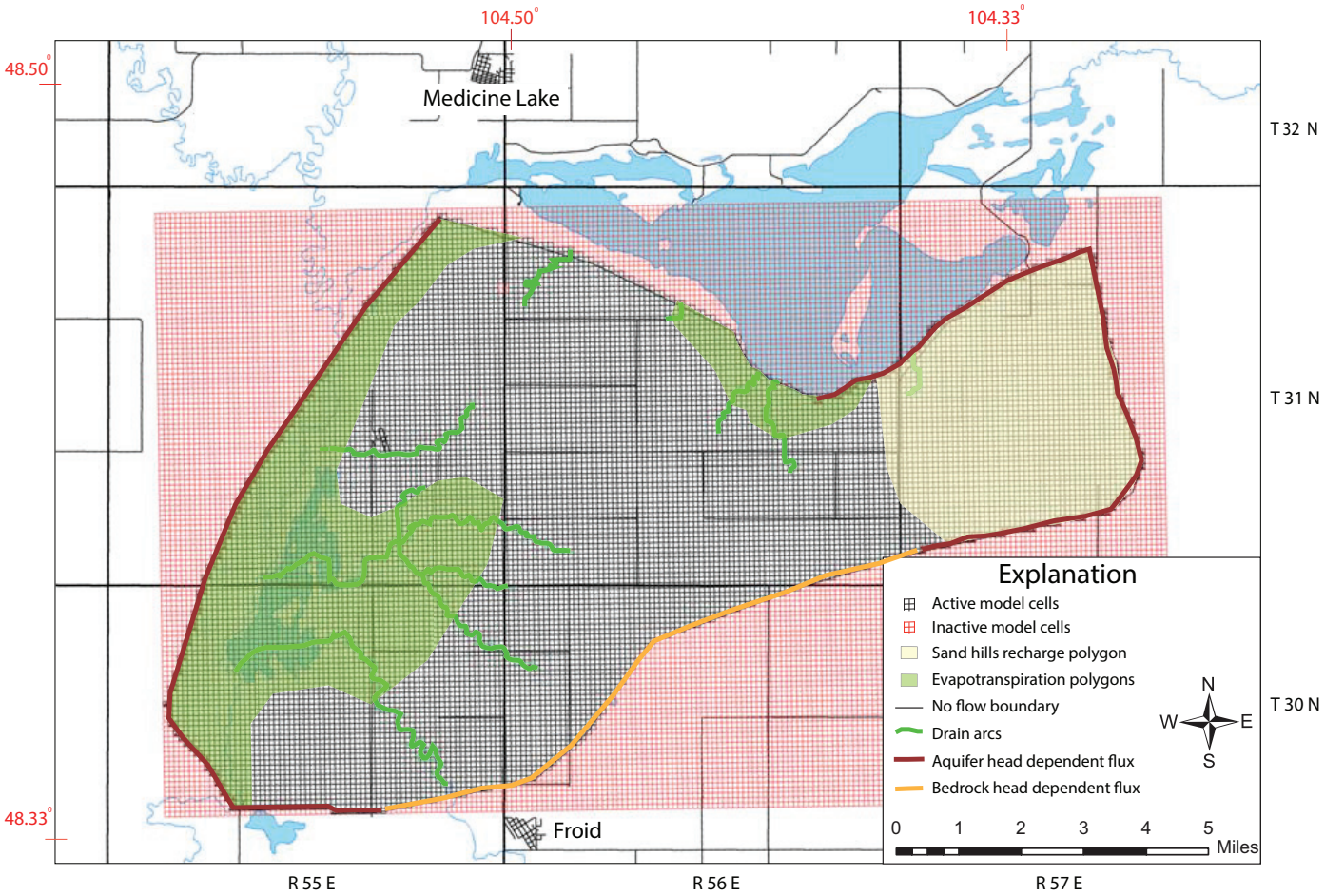

Figure 8. The model grid representing an area 80,000 ft by 48,000 ft was set to have 200 columns, 120 rows, and six layers. A boundary polygon was used to define the active cells in the grid.

The grid was rotated 14.5 degrees north of east and a boundary polygon was used to select the 77,042 active model cells (fig. 8).

Hydraulic properties were designated using the HUF package. This package assigns hydraulic properties to each cell by the material type, as opposed to having a layer represent a continuous geologic unit. This is appropriate because the buried valley stream and glacial deposits are highly variable and discontinuous.

Dry cells in groundwater flow models can increase instability and prevent convergence. The top of the model was set at 10 ft above the average water level in 2015, rather than at the land surface (fig. A1, appendix A) to reduce the number of dry cells. Fort Union Formation contacts from borehole data were used to define the model bottom (fig. A2, appendix A). Points defining the model bottom were set at elevations at least 50 ft below the Fort Union Formation top, thereby establishing a bottom layer with uniform material properties.

The model grid is a compromise between representing aquifer heterogeneity and achieving reasonable computational efficiency. Grid refinement at the pumping centers was attempted, but greatly increased the model run times and model instability.

Hydrogeologic Units

The complex series of deposits filling the buried ancestral Missouri River Valley were simplified prior to modeling the subsurface geology. Similar materials were lumped into one of four hydrogeologic units (HGUs) defined for model development:

1. Till and Clay: All layers described as glacial till, clay-bound gravel, clay, or lake clay.
2. Sand: All layers described as sand, silty sand, coarse sand, and fine sand.
3. Sand and Gravel: All layers described as gravel, alluvial or outwash gravel, sand and gravel, silty gravel, coal layers in gravel, or coal gravel.

4. Fort Union Bedrock: Layers at the bottom of the borehole described as shale, claystone, coal in a shale sequence, or gray or green tight clay.

All logged bedrock contacts were assumed to be the top of the Fort Union Formation. Hydraulic property ranges for each hydrogeologic unit are listed in table 2.

Stratigraphic Modeling

Interpolations of the aquifer stratigraphy were constructed from borehole cross sections using 115 wells in the study area. Where well data were sparse, dummy boreholes were constructed from documented stratigraphy at nearby wells and included in the cross sections to guide the interpolations.

The well logs document many layers of sediment. Simplification of the stratigraphy was accomplished by assigning contact elevations for materials reported in the well records. Similar materials were lumped into hydrogeologic units, ignoring thin layers of inconsistent material. For example, a 2-ft layer of silty sand within a 20-ft thickness of clay or till was excluded and the entire thickness was grouped as clay and till (fig. 9).

The contacts between materials in each borehole were assigned horizon identification numbers to guide cross-section construction. In GMS, the horizon numbers increase upwards from the bottom of the borehole to the top surface contact. We sequentially numbered the repeating layers of sand and gravel, sand, clay, and till (fig. 10) with higher numbers representing the youngest sediment layers. Where sand and gravel was reported at the same elevation as a sand layer, the sand was placed above the sand and gravel to honor the fining upward sequence commonly documented in unconsolidated materials. Not all layers are present in each borehole because lenses of sand and gravel are discontinuous across the study area.

Once the borehole contacts were assigned, borehole cross sections were created throughout the model area (fig. 11, plan view; fig. A3, appendix A). The "auto-fill cross section" function in GMS was used where adjacent boreholes had similar lithology. This process was not automated in most cases due to the highly heterogeneous stratigraphy. The top and bottom surfaces of the stratigraphic model were generated with a TIN (Triangular Irregular Network) function. The borehole contacts and cross-section contacts were interpolated to solids. This automated process was subsequently checked and improved as needed. The solids diagram shown in figure 12 represents the aquifer materials directly overlying the Fort Union bedrock. Additional images of the aquifer system are presented as figures A4–A11, appendix A.

Several GMS features were used to generate the MODFLOW model from the conceptual model. The solids were converted to hydrogeologic units (referred to as HGUs in the HUF package) using the "Solids to HUF" function in GMS. These solids were assigned to grid cells using the "Solids to MODFLOW" command and "grid overlay with K_{eq}" option was selected. This process assigns cell hydrologic properties by the solid material intersected by that cell. The "grid overlay with K_{eq}" function softens abrupt changes in cell properties by assigning cells in the transition zones modified materials properties reflecting the properties of all materials intersected by that cell (fig. 13).

Boundary Conditions

Boundary conditions are mathematical constraints applied to the model domain representing physical features of the conceptual model (Reilly and Harbaugh, 2004). The represented features include sources (water inflow to the system), sinks (water outflow from the system), and flow barriers (restrictions to groundwater flow within and bounding the system).

Sources

The main source of water to the model is groundwater inflow applied at head-dependent flux boundaries. The General Head Boundary (GHB1) package in MODFLOW simulates this source of water. Head elevations were assigned at GHB cells to reflect average water levels. A linear interpolation was applied, assigning heads to cells between known elevation points. The general head boundary was preferred to a specified flow boundary condition because heads are relatively well documented, but there is little knowledge of the flow (Anderson and Woessner, 1992). Although the bedrock forms a valley in the model area, it is covered by sand and gravel or weathered till with the exception of a small outcrop along the south side of Medicine Lake. The unconsolidated materials covering the bedrock along the valley sides are often

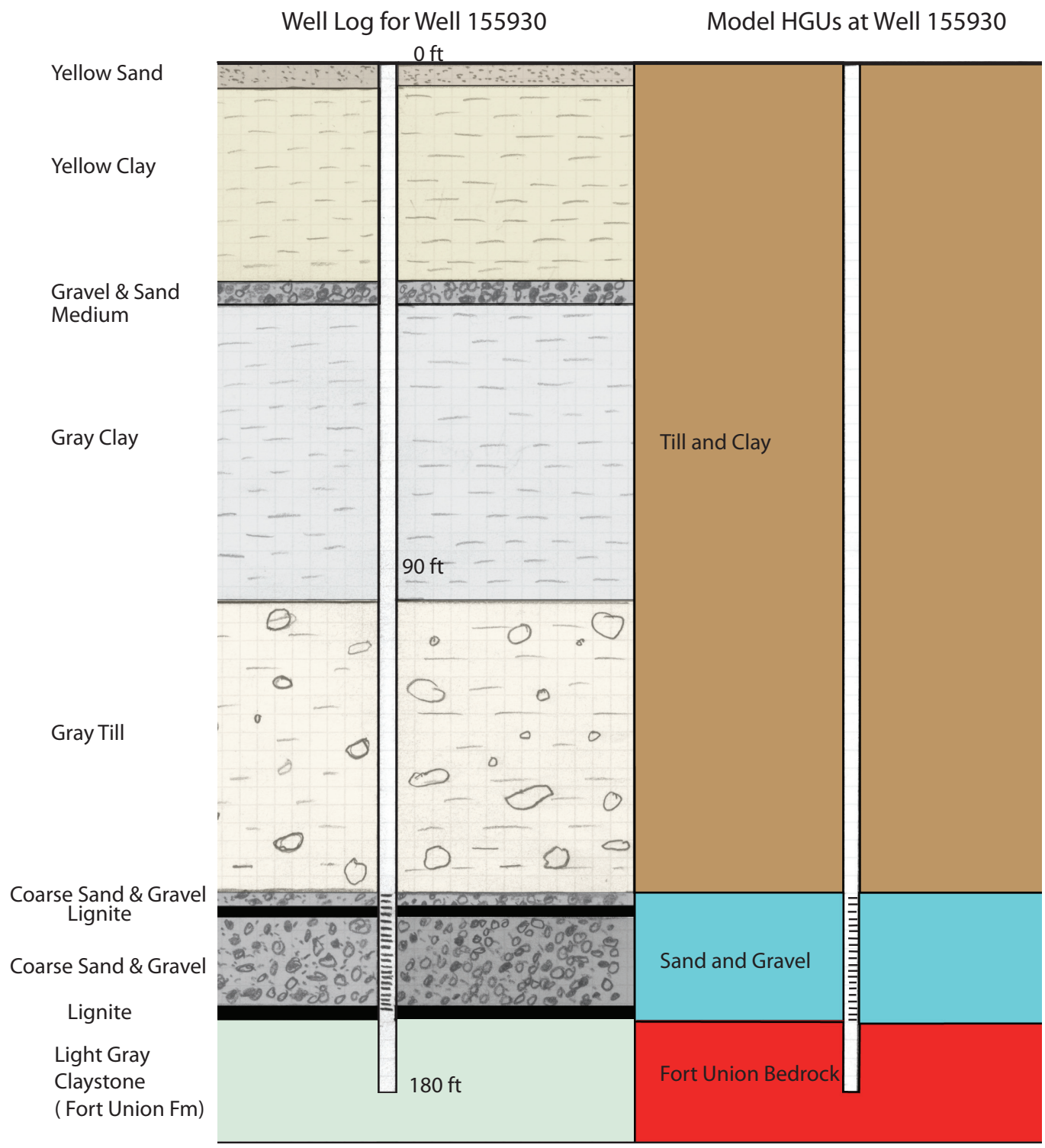

Figure 9. The well log stratigraphy has been simplified in the model by combining materials of similar hydraulic properties into hydrogeologic units.

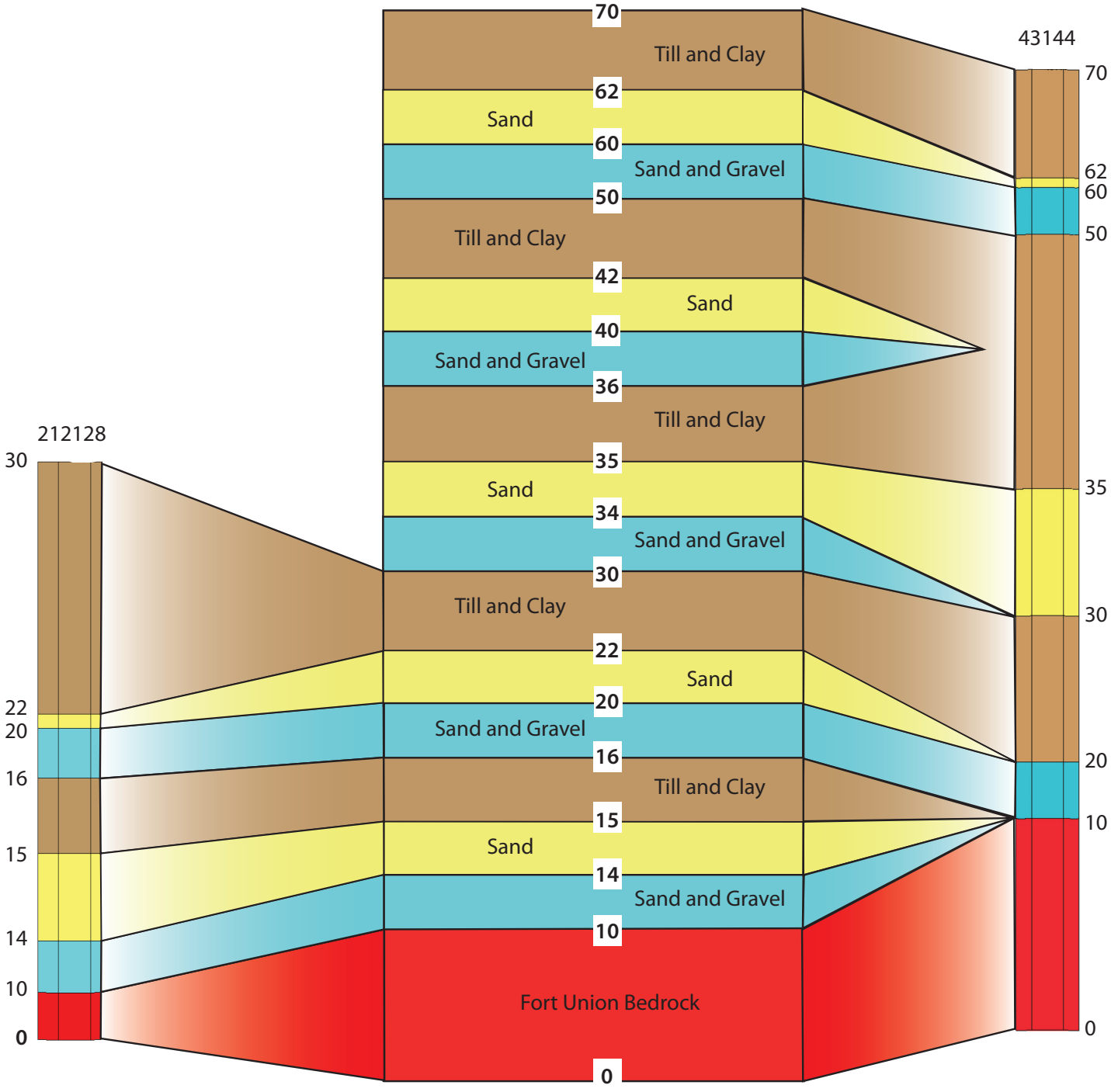

Figure 10. The contacts between materials were assigned horizon numbers for correlation of like materials using the schematic (center) to number GMS borehole contacts (well 212128 left, well 43144 right).

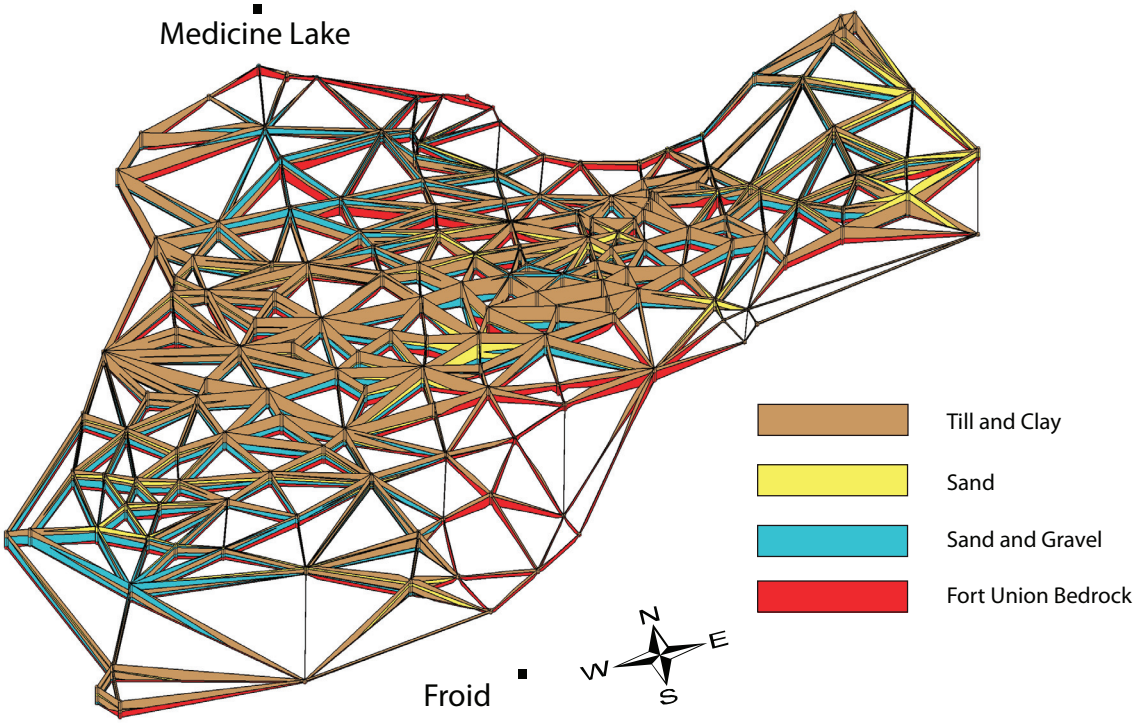

Figure 11. Cross sections were constructed between boreholes and used to guide stratigraphy modeling.

too thin to form high-yield aquifers, but can supply recharge waters to the buried valley aquifer. Heads indicate groundwater flow into the model area from the buried valley aquifer and bedrock aquifers along the southeast edge of the model, and groundwater flow out of the north and west edges (fig. 6). The locations of the head-dependent flux boundaries are shown in figure 8, and the conductance values assigned to the boundary arcs are displayed in figures A12 and A13, appendix A.

Recharge in the sand hills area is also a source of water in the model area. Recharge was applied with the MODFLOW RCH package to model layer 1 by establishing two recharge polygons. The recharge area in the sand dunes (fig. 8) was assigned an initial rate of approximately 5% of annual precipitation. Recharge rates were modified during model calibration. A majority of the model domain receives no recharge because the confined aquifer is more than 100 ft below the surface and is overlain by till and clay.

Sinks

Water leaves the model domain as outflow to adjacent areas of the Clear Lake aquifer, as Big Muddy Creek wetland ET and seeps, and through irrigation pumping. Head-dependent flux boundaries along the northeastern, western, and southwestern boundaries represent groundwater flow out of the domain (fig. 8).

Evapotranspiration is a major sink in the model area. The evapotranspiration package (ETS1) in MODFLOW removes water from layer 1 of the model at polygons representing wetlands (fig. 8). Segmented curves were assigned to the ET polygons representing extinction depths (fig. A14, appendix A).

Groundwater discharge to small creeks or wet coulees in the model area is simulated with drains. Little is known about the rate of discharge at these sites, but aerial images show ponded water and green vegetation. The Drain package (DRN1) in MODFLOW was assigned to cells in layer 1 along arcs (fig. 8). The drain conductance values and arc locations are displayed in figure A15, appendix A. Initial drain conductance was set to values similar to the hydraulic conductivity of the surficial glacial till. Drain conductance values and drain elevations were modified during model calibration.

Pumping from irrigation wells is simulated with the well package (WEL1) in MODFLOW. The screen elevation at each existing well was used to assign pumping to the appropriate model layer. The steady-state model does not include pumping from wells because it simulates average pre-irrigation water levels. Estimates of irrigation pumping rates and duration

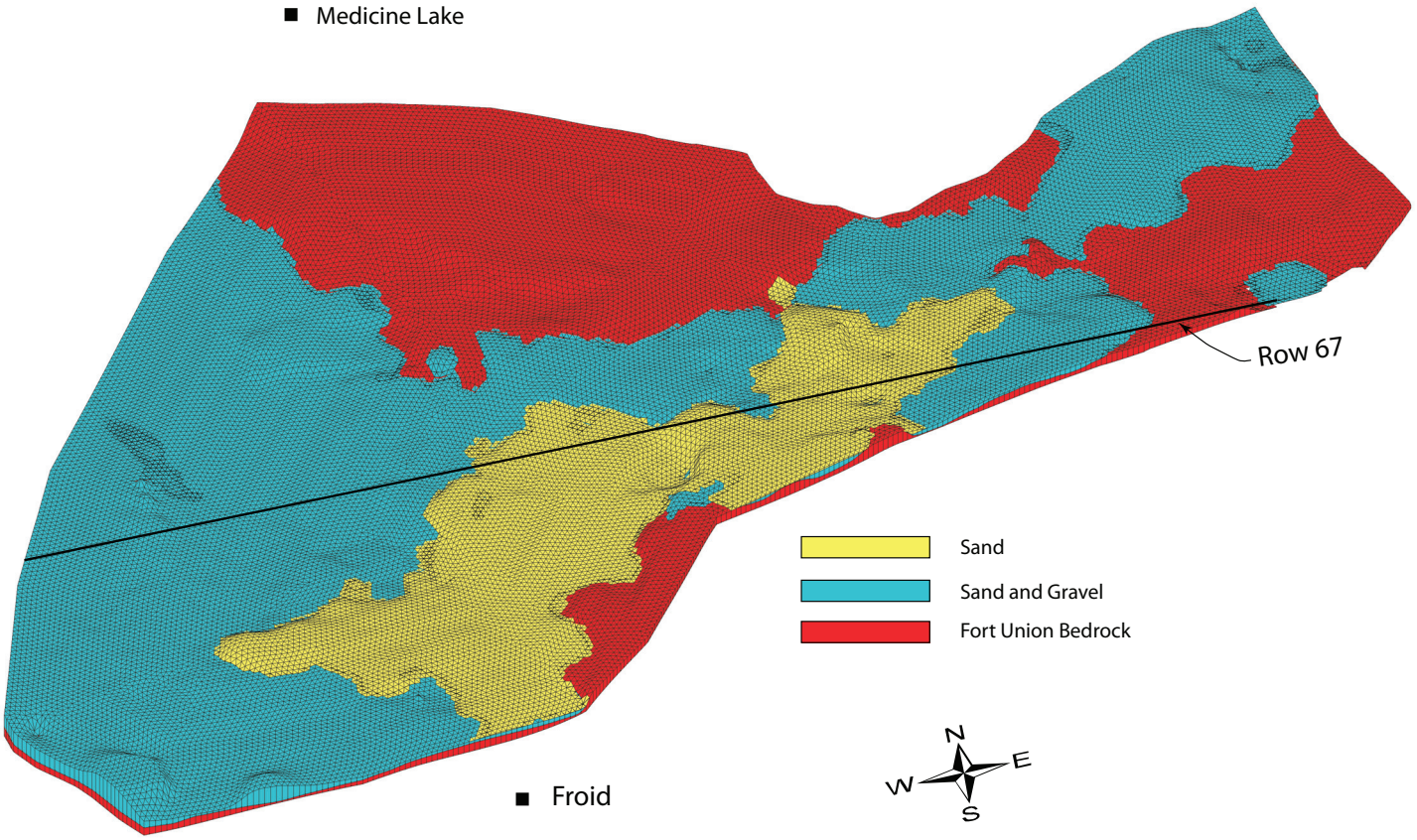

Figure 12. Model solids were interpolated from the borehole cross sections. This oblique view shows the solids representing the deep aquifer materials overlying the Fort Union bedrock. The approximate location of row 67 is indicated for cross sections displayed in figure 13.

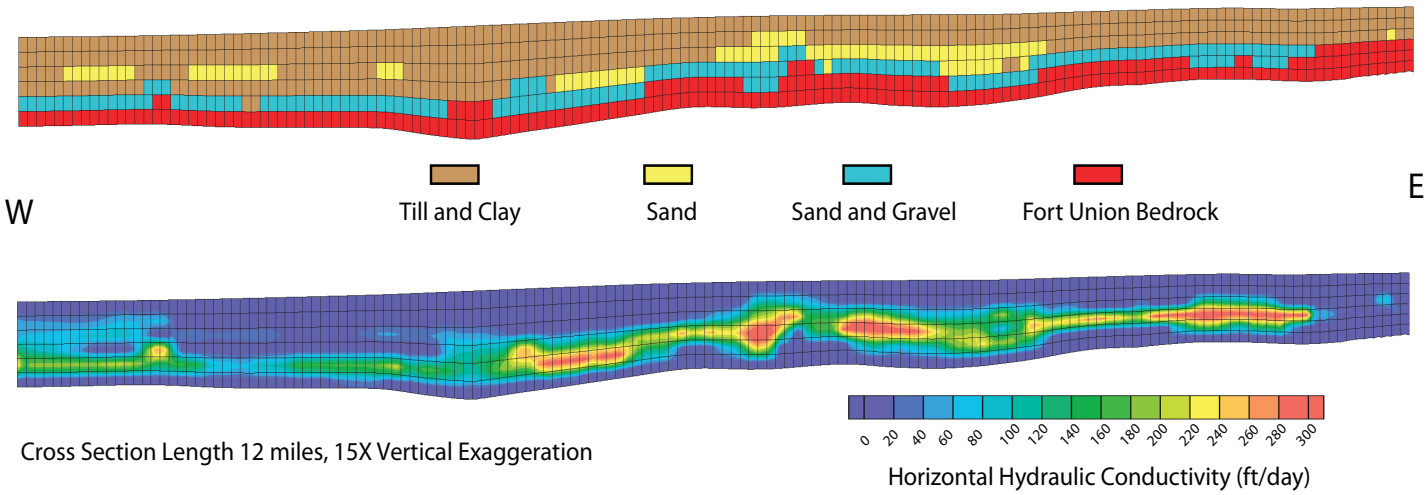

Figure 13. Grid cross section at model row 67 showing the cell materials assignments (top) and the horizontal hydraulic conductivity applied to the cross section using the “grid overlay with K_{eq}” option (bottom).

(table 1) provided detailed input for the time-variable pumping stresses in transient simulations.

Flow Barriers

By default the MODFLOW grid sides and bottom are no-flow boundaries unless assigned otherwise. The north and south sides of the aquifer were initially set as no-flow boundaries for most of the boundary arc length. These were replaced with General Head boundaries where head gradients indicated a groundwater flux from the bedrock. Layer 6 represents Fort Union Formation bedrock, with low hydraulic conductivity and storage. The hydraulic conductivity of the bedrock HGU and the clay and till HGU are set at two or more orders of magnitude lower than the sand and gravel HGU, and therefore restrict lateral and vertical flow (table 2).

Modifications for Transient Simulations

The steady-state model was the basis for development of the 1-yr transient model. The transient model has 131 stress periods with daily increments during the irrigation season. Monthly stress periods are implemented for the remainder of the year when there is little aquifer use (table A2, appendix A). The first stress period was designated as "Steady State". Water-level records near the four irrigation wells show sporadic water use during the irrigation season, and modeling these changes in the aquifer stress required a greater number of short stress periods during the irrigation season. Model simulations with multiple time steps assigned to each stress period were tested and found to produce results similar to those of single time step simulations. Additional time steps only increased model run times; each stress period was assigned one time step.

Variable recharge rates were assigned in the transient model simulations (fig. A16, appendix A). The recharge applied during the spring months represents infiltration of melting snow, and the fall recharge represents rain and snow before the ground freezes. The summer months have the greatest average monthly precipitation in the model area (Reiten and Chandler, in review), but individual events are usually small enough that ET consumes the water before it can recharge the aquifer. The curve used to apply recharge to the model was constructed with higher rates in the spring and fall, and little or no recharge in the summer and winter. Actual recharge rates and the timing of recharge is unknown.

ET rates were assigned using polygons and vary during the simulation. ET in the transient model is controlled by transient rates assigned by rate curves (figs. A17–A18, appendix A). The curves were set to represent increasing ET in the spring, high ET in the summer, and a rapid decline of ET in the fall with the onset leaf senescence. ET rates were adjusted during calibration.

CALIBRATION

Steady-State Calibration

Water levels recorded in model area monitoring wells were used for calibration targets assigned at points representing model "observation" points (fig. 14; fig. B1, appendix B). Most of the monitoring wells (21 of 28) were equipped with data loggers recording hourly water-level data. The goal of steady-state model calibration was to demonstrate that the model could generate reasonable head values and not to precisely match a steady-state potentiometric surface. Average pre-irrigation season water levels recorded at these wells were used for steady-state calibration targets.

The steady-state model was calibrated by varying the Kh and Kv, recharge rates, the GHB conductance values and node elevations, and the drain conductance and node elevations. Cell to cell flow rates were examined to determine areas where the model was restricting flow or discharging unrealistic flows through GHBs. The calibration criteria for the steady-state model included a ±5.0 ft head difference throughout the model domain and a mass balance error less than 1.0% (fig. 14). Figure 15 charts the observed heads vs. computed heads for the calibrated steady-state model.

Transient Model Calibration

The goal of transient model calibration was to match model-generated head fluctuations to the observed water-level fluctuations. This means making the model respond as the aquifer does to known pumping stresses. Data loggers installed in observation wells close to the four irrigation wells recorded pressures every 15 min, providing a detailed record of the water-use timing and duration (fig. B2, appendix B). Hydrographs from monitoring wells more than 1,000 ft from the pumping wells provided the best transient

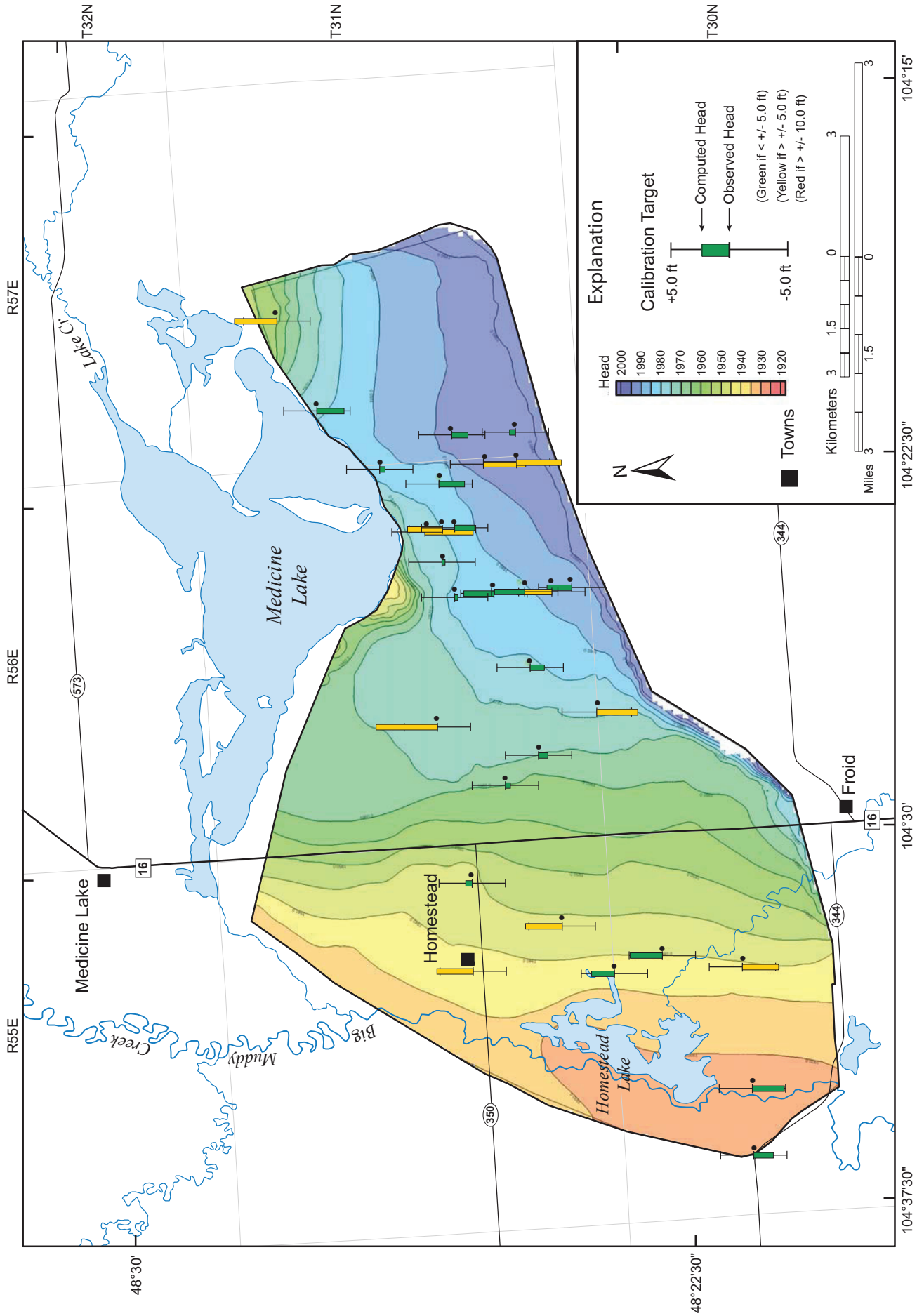

Figure 14. Steady-state model calibration errors at observation points.

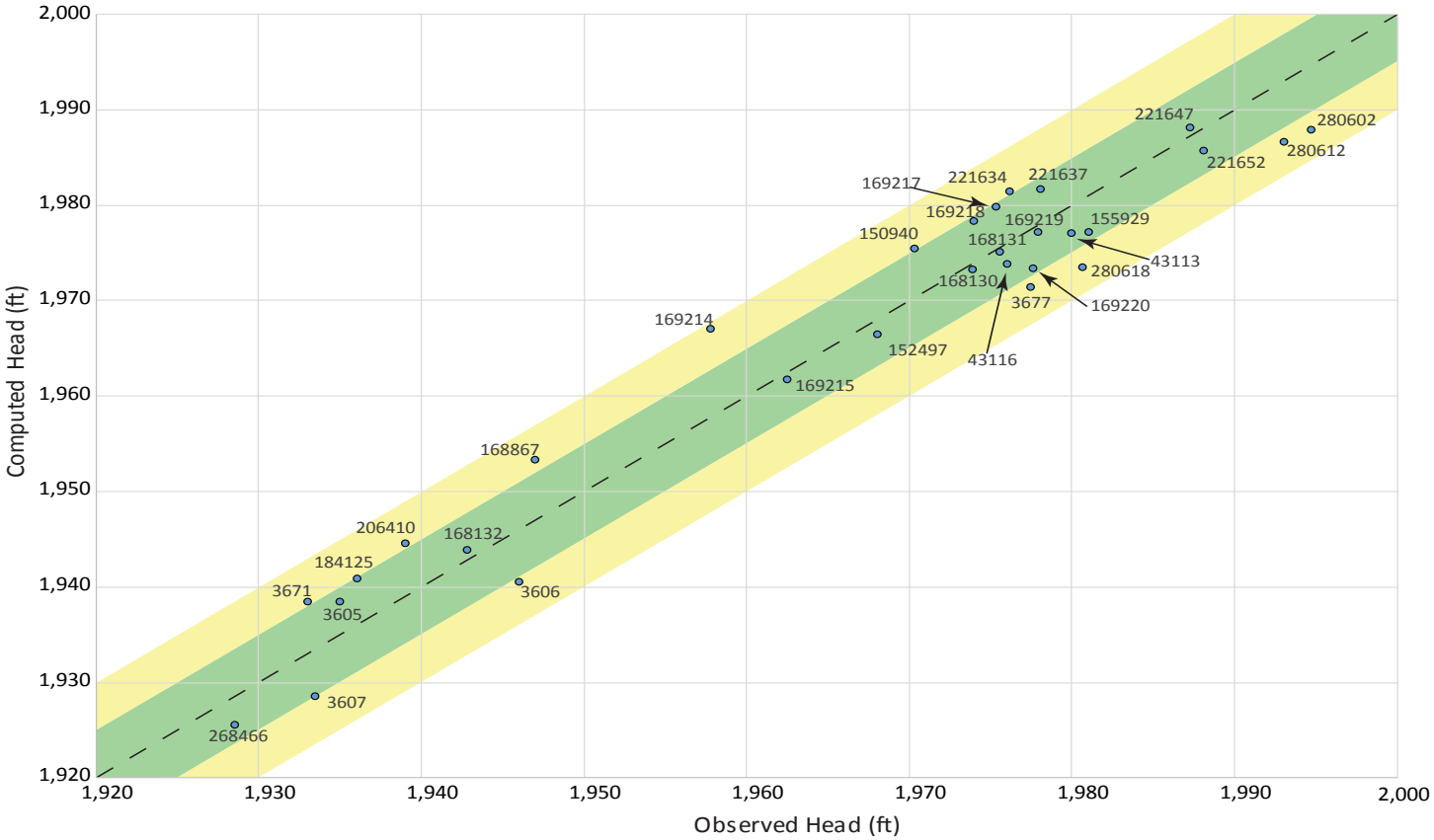

Figure 15. The calibrated steady-state model head values compared to the observed head values shown here with the ±5 ft calibration interval in green, ±10 ft interval in yellow. The color bands correspond to the calibration target colors used in GMS shown in figure 14.

calibration targets. Many of the monitoring wells less than 300 ft from the pumping wells were located in the same model grid cell as the pumping stress, resulting in simulated heads that did not accurately predict observed drawdown. Water-level data for 2015 from each monitoring well provided time-series calibration targets.

Trial and error calibration of the transient model included varying the K_H and K_v, recharge and ET rates, and the GHB conductance values. Hydrographs from observation wells were compared to simulation hydrographs to evaluate the timing of modeled water-level fluctuations. It was difficult to match the drawdown measured in monitoring wells close to the production wells and the response at more distant monitoring wells. This is attributed to the simulated production wells and close observation points being in the same model cells. Head values calculated at the center of each model cell are assigned to the entire cell area, and therefore do not accurately represent the observed water levels close to the production wells (Domencio and Schwartz, 1998). Attempts to reduce the model cell size and increase the number of model layers resulted in very slow or unstable simulations. The water-level changes in distant monitoring wells are better indicators of the actual buried valley aquifer response to the stress of pumping than the water-level changes in close monitoring wells (van der Kamp and Maathuis, 2012). Therefore we focused on matching the response recorded in distant monitoring wells more than on those close to the pumping centers.

The range of aquifer parameters selected for calibration was constrained by aquifer test results for the model area (table A1, appendix A). The materials properties for the calibrated transient model (table 4)

Table 4. Materials properties from the calibrated transition model.

Material	K_H (ft/day)	K_v (ft/day)	S_S (ft^{-1})	S_y
Till and Clay	0.1	0.03	1.0×10^{-7}	1.0×10^{-6}
Sand	150	70	1.0×10^{-6}	1.0×10^{-3}
Sand and Gravel	300	100	1.0×10^{-6}	1.0×10^{-3}
Fort Union Bedrock	4	1.2	1.0×10^{-6}	1.0×10^{-6}

are in good agreement with published values for similar materials (table 2).

Along with adjusting the aquifer properties, the recharge rate applied to the model area was adjusted during transient model calibration (fig. 16). Initially, recharge was applied to the entire model at a constant rate. Recharge was refined to reflect seasonal differences and by applying it only to the sand hills area. Even though most of the precipitation falls in the summer months, highest recharge was applied to the model in the spring and fall when ET losses are reduced (fig. A16, appendix A). The results displayed in figure 16 show simulated heads compared to observed water levels at a location near the center of the model domain. Transient calibration resulted in variable recharge rates totaling up to 0.15 ft/yr (1.8 in/yr), which is approximately 13% of the average annual precipitation at Medicine Lake. Recharge through the sand hills contributes 1,207 acre-ft of water to the model, a value at the low end of the estimated water budget range (table 3).

Simulation of evapotranspiration in the low-lying areas along the Big Muddy and, to a lesser extent, along the south shore of Medicine Lake improved the calibration to head targets in the center of the model domain. A polygon of approximately 11,300 acres represents the potential ET water loss in the Big Muddy area, and a smaller polygon, about 1,160 acres, extends along the south shore of Medicine Lake (fig. 8). Variable ET rates and extinction depths were assigned to these polygons (fig. A17, A18, appendix A). The maximum ET rate curves were generated by proportioning 3.0 ft/yr over the warmer months, with August having the greatest potential ET water loss.

The resulting model ET rates, calculated by dividing the output ET volume by the ET polygon areas, are 0.47–0.50 ft/yr. Much of the ET polygon areas would have heads below the extinction depth for all or part of the year and therefore do not remove ET water from the model during the entire simulation. If the area considered for this calculation is reduced to land that appears as wetlands on aerial images (2,150 acres), the simulated yearly rate is approximately 2.2 ft/yr. This range falls more in line with previously measured and estimated values of 3–5 ft/yr (Donovan, 1988). A hydrograph for a wetland piezometer 5 mi northeast of the model area (157817) showed a 3-ft water-level decline in 2015, which is attributed to ET.

Sensitivity Analysis

Sensitivity of the model output to the aquifer parameters and boundary conditions was tested by varying model inputs and charting changes in the

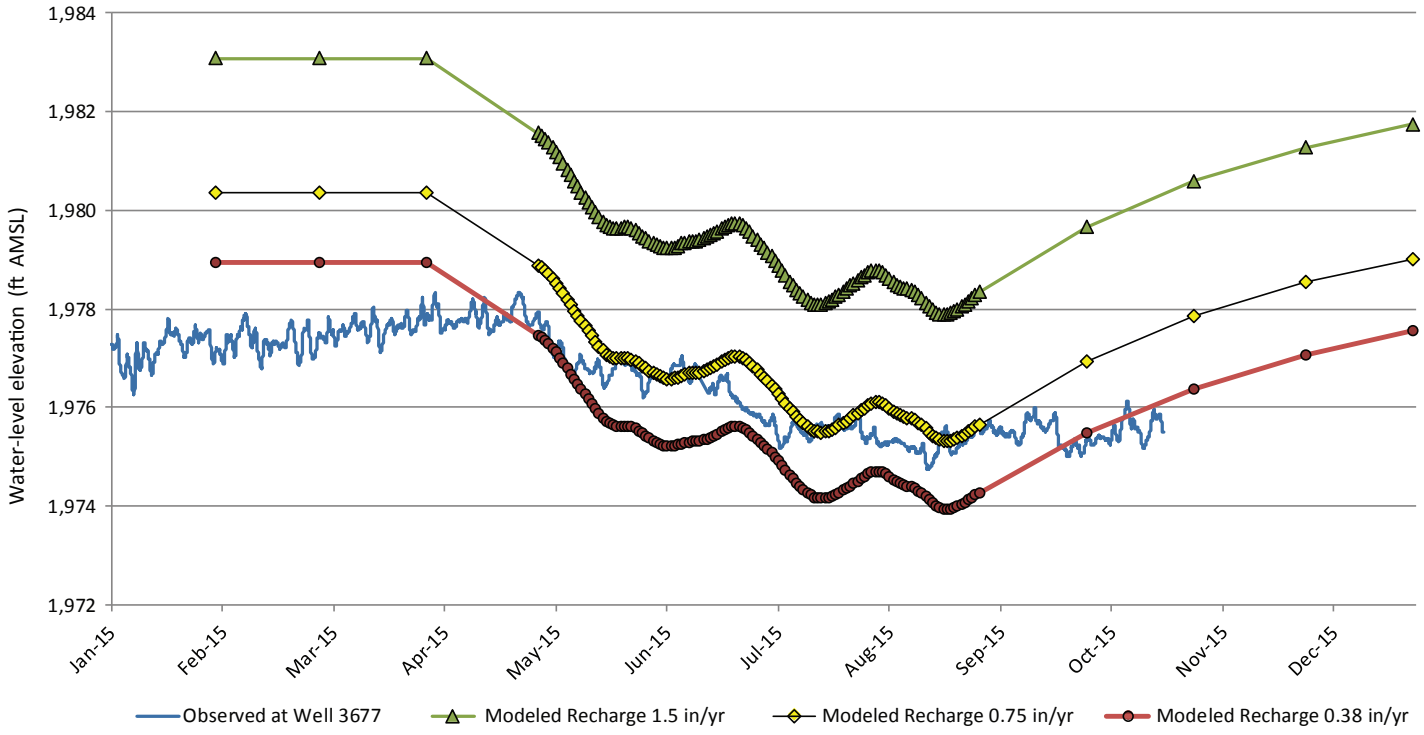

Figure 16. Recharge rates and hydrographs during model calibration. The recharge rates listed as an average for the entire model area, but the sand hills area rate was set four times higher than the main model area during these calibration runs.

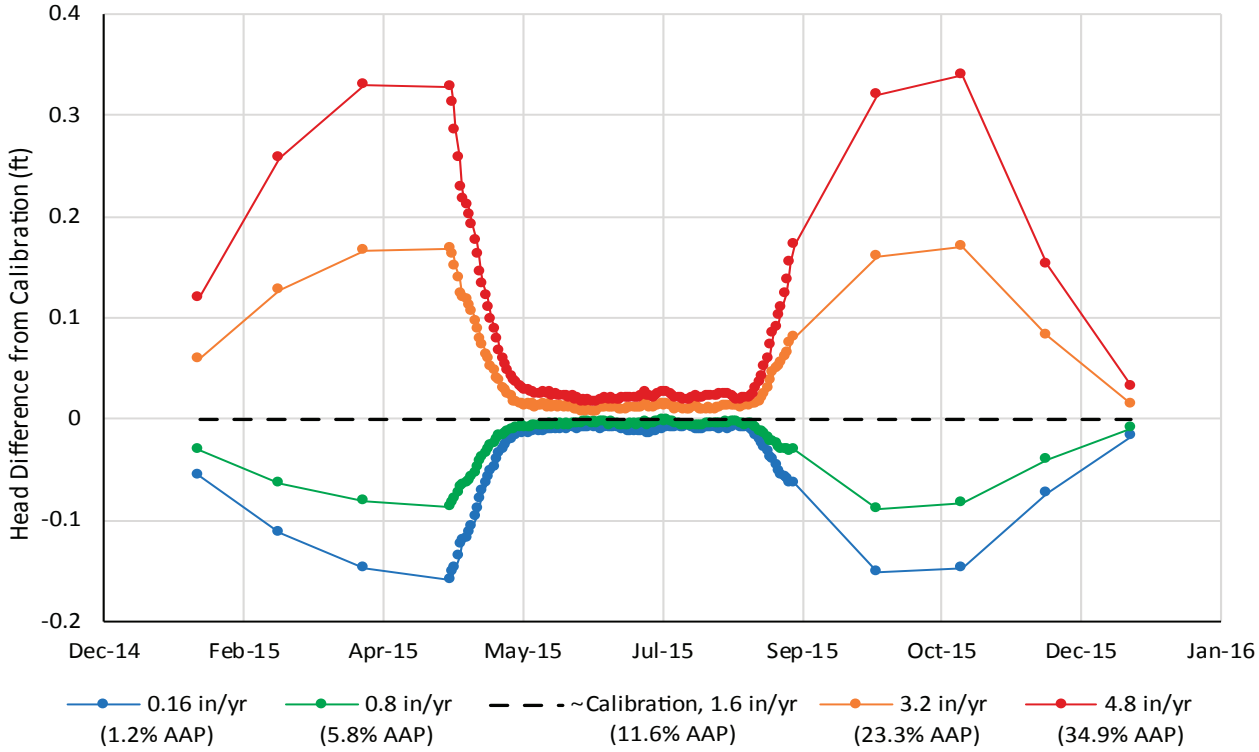

Figure 17. Transient model simulations at well 169215 show head differences resulting from recharge rate changes. The model was more sensitive to high recharge rates. Well 169215 is central in the model domain. AAP, percentages of average annual precipitation.

model outputs. Individual parameters were increased and decreased to evaluate the model sensitivity to such changes.

The model was not sensitive to minor changes in recharge, but showed slightly greater sensitivity to increased rates (fig. 17). This result is not surprising since recharge to the modeled aquifer is thought to come from distant recharge areas and not from direct infiltration in the model area.

Layers four through six of the model use General Head boundaries along the south border of the model to represent inter-aquifer recharge to the Clear Lake aquifer from the Fort Union bedrock. The GHB conductivity values where raised and lowered from the best calibration level by several orders of magnitude, and the model heads in layer four at well 43116 were compared. The model is more sensitive to decreases in conductance than to increases in conductance (fig. 18).

Sensitivity to ET depends on distance from ET polygons and the depth of the model layer. The model cell representing well 169215 (cell 83082, layer 4) produced ±0.5 ft head change when the ET rates were varied from one to over 3 ft per year. The same range of ET rates at a location close to Big Muddy Creek (cell 8239, layer 1) produced approximately three times the change in head, showing more sensitivity to decreased ET (figs. C2, C3, appendix C).

The model heads in both layer 4 at cell 83082 (well 169215) and layer 1 at cell 8239 near Homestead showed little sensitivity to changes in drain conductance (figs. C4 and C5, appendix C).

MODEL SCENARIOS

The transient model was used to simulate five water-use scenarios (table 5). Scenario 1 relies on 2015 water-level data for the transient calibration and includes pumping from four existing irrigation wells (table 6). Scenario 2 provides a logical comparison to this by simulating aquifer conditions without any irrigation pumping. Other simulations increased the water use by more frequent pumping, and by modeling additional wells. Four additional irrigation wells were added to the model and given a hypothetical allocation of 271 acre-ft/yr each. The addition of these four wells roughly doubled the irrigation development in the model area (table 6). The hypothetical well sites were selected at locations with farmed fields and where the

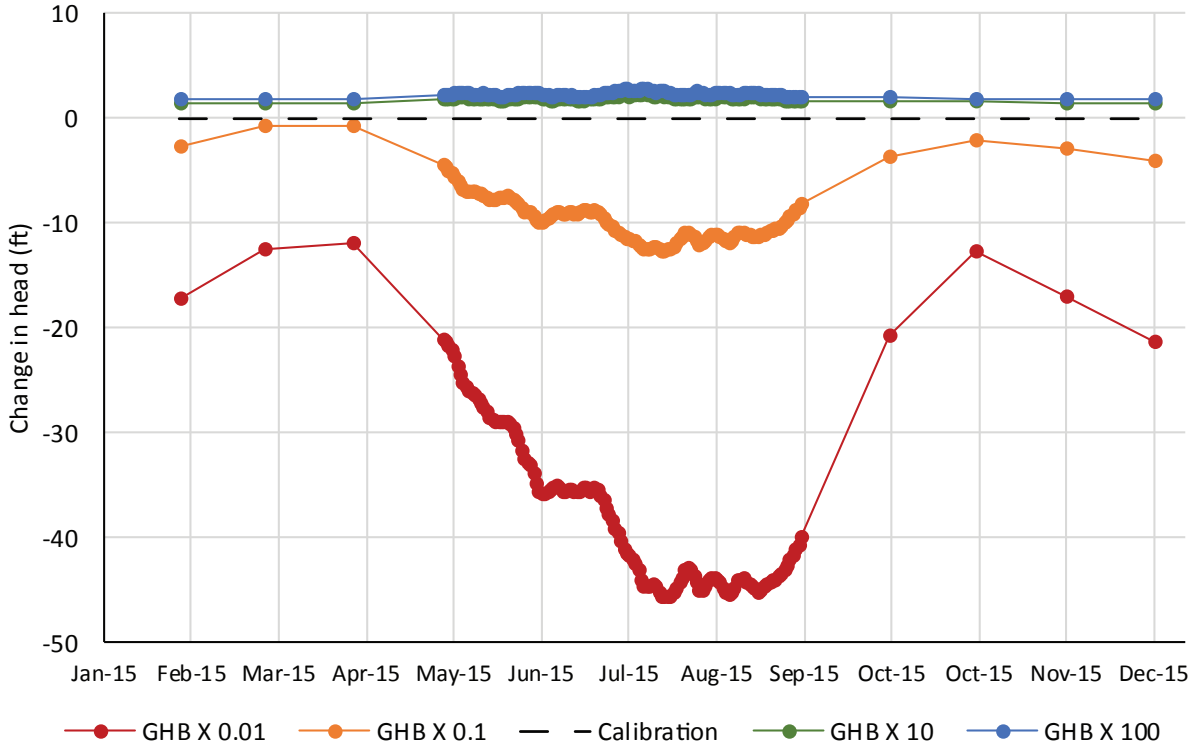

Figure 18. Simulations varying the deep GHB's conductance values showed the model was more sensitive to decreases in the conductance than increases. Simulations increasing the conductance by 10 and 100 times generated heads similar to those produced by the calibrated model.

water quality would most likely be suitable for irrigation (fig. 19).

Scenario 2, without pumping stresses, provided a "control" head data set to compare the water-use scenarios. The head distribution from each scenario was subtracted from the "no irrigation use" solution to calculate the head difference across the domain after every stress period. This process, which expresses head change as water-level difference, isolates drawdown related to pumping from fluctuations produced by boundary conditions. The water-level differences at each cell show the head change over time (fig. 20), and, when contoured over the domain for a given stress period, illustrate the aerial extent of drawdown (fig. 21).

Water-level differences at cells in model layer four were evaluated to assess changes from increased water use during the simulated irrigation season (fig.19; fig. D1, appendix D). Four locations near the pumping wells demonstrate potential well interference and combined drawdown (figs. D2–D5, appendix D). Charts constructed at four locations in the Big Muddy Creek alluvial valley assess potential effects at the wetlands (figs. D6–D9, appendix D).

Table 5. Model scenarios.

Scenario	Scenario Description
1: Four Well 2015 Volume	Water-use volume measured in 2015 (calibration).
2: No Irrigation Use	The irrigation wells inactive during the no-pumping scenario.
3: Four Well Max Allocation Volume	Pumping increased to use the full volume allocated on the existing water rights.
4: Eight Well 2015 Volume	Four new wells added with pumping rates similar to the four existing wells in 2015.
5: Eight Well Max Allocation Volume	Four new wells added and all wells pumping the full allocation volume.

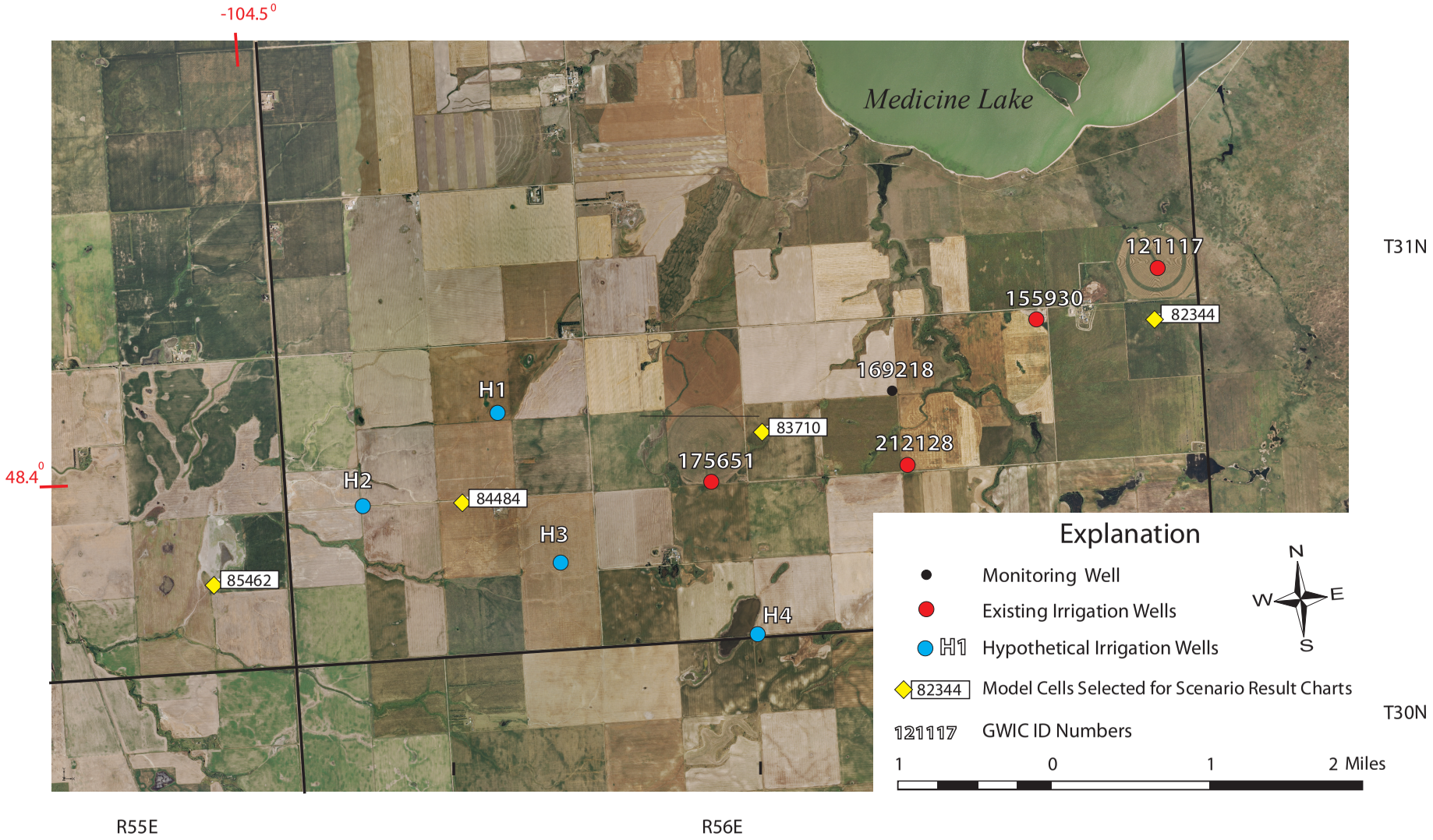

Figure 19. Locations of existing irrigation wells and four irrigation wells added to the model for scenarios 4 and 5. Locations of the model cells selected for data output are shown with the cell numbers.

Table 6. Scenario pumping rates and volumes.

			Scenario 1	Scenario 2	Scenario 3	Scenario 4	Scenario 5
Well Name	GWIC ID	Pumping Rate (gpm)	Volume Pumped (acre-ft/yr)	Volume Pumped (acre-ft/yr)	Volume Pumped (acre-ft/yr)	Volume Pumped (acre-ft/yr)	Volume Pumped (acre-ft/yr)
Nelson 1	121117	800	134	0	365	134	365
Nelson 2	155930	750	61	0	411	61	412
Nelson 3	212128	665	69	0	292	69	292
Bolstad	175651	795	219	0	432	219	432
H1	NA	750	0	0	0	140	271
H2	NA	700	0	0	0	165	271
H3	NA	800	0	0	0	150	271
H4	NA	650	0	0	0	166	271
		Scenario Total	483	0	1500	1104	2585

Note. H1–H4 designate hypothetical wells.

Scenario 1: Four well 2015 volume pumping (483 acre-ft)

Model calibration was achieved by matching the simulation hydrographs to the observed water-level fluctuations (fig. 20). The model heads at well 169218 were about 4 ft higher than the observed heads, and the model showed greater water-level recovery after the irrigation season (fig. 20). Overall, the simulated response has a similar pattern to the observed heads. While it would be optimal to have the model heads more closely match the observed heads, the similarity in timing and magnitude to observed drawdown suggests that the model responds to pumping stresses similarly to the aquifer. This indicates that the model simulates the aquifer's response to increased pumping, but may be off by several feet in water-level elevation.

Scenario 1 applies the pumping schedule recorded at the four existing irrigation wells during the 2015 irrigation season. Results show well interference between the existing four irrigation wells (fig. 21). The greatest drawdown is at the easternmostwell, 121117 (Nelson 1), which is the closest irrigation well to the

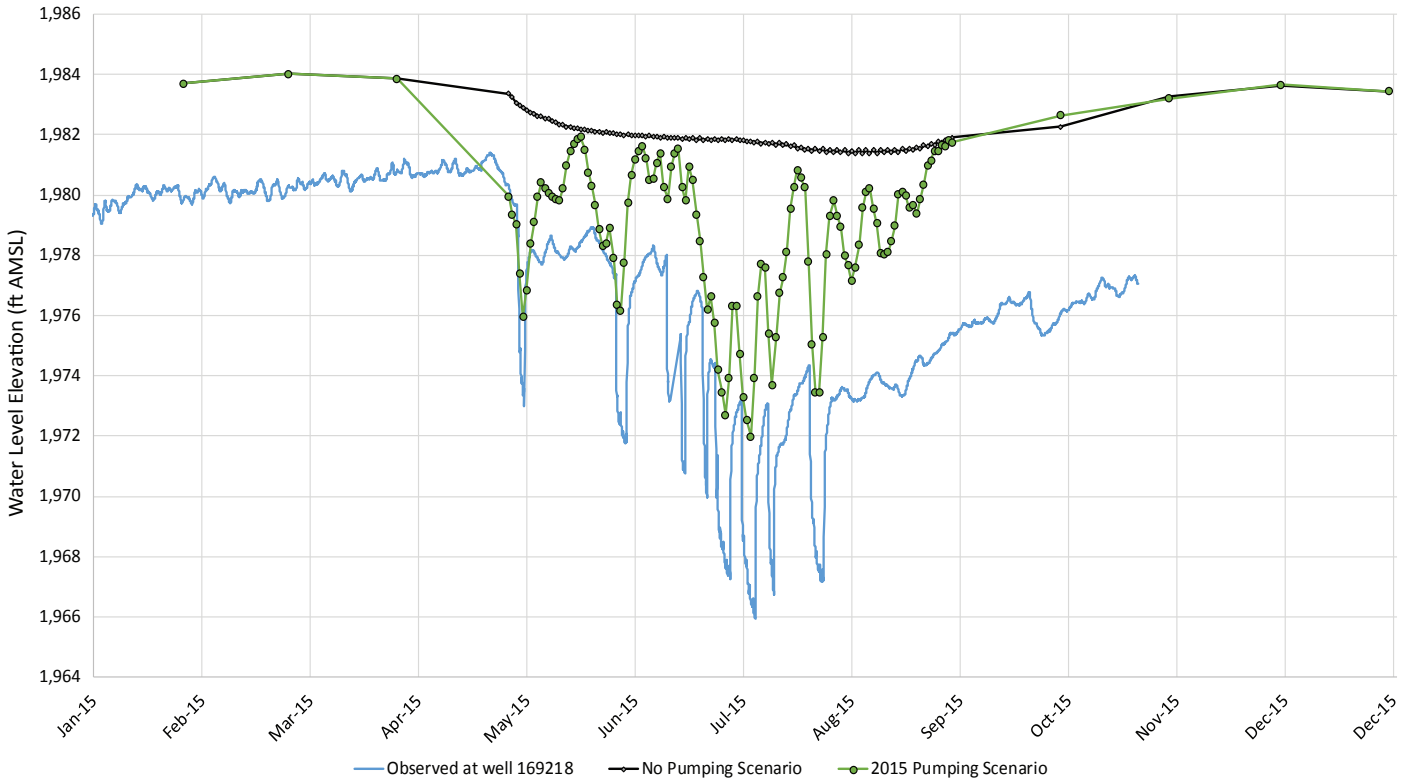

Figure 20. The 2015 pumping scenario model at well 169218 shows water-level fluctuations very similar to the observed fluctuations. The no irrigation use scenario shows water-level declines in the summer months resulting from ET losses and reduced summer recharge. (Well location on figure 19).

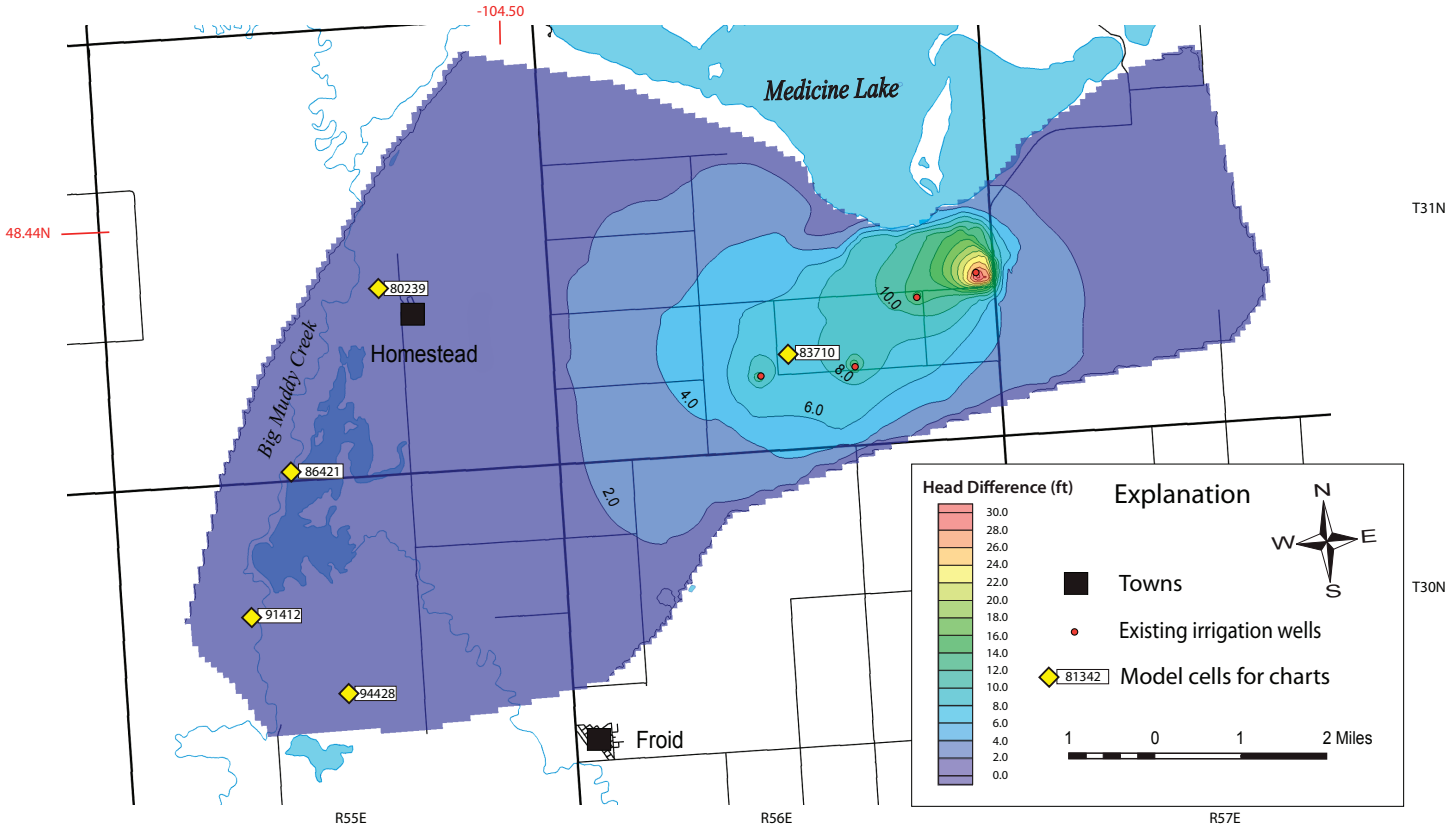

Figure 21. The layer 4 head difference between "no irrigation use" and 2015 volume pumping scenario shows well interference and the increased drawdown due to hydrogeologic boundaries at the easternmost irrigation well. The model predicts up to 0.40 ft of drawdown at cell 80239 near Homestead. Model output is for stress period 77, middle July.

barrier boundary between the aquifer and Medicine Lake. The possibility of well interference becomes obvious when drawdown is observed in monitoring wells located next to unused irrigation wells. If the irrigation wells were pumped simultaneously, the drawdown cones would quickly intersect one another. For example, the monitoring well near the irrigation well, 155930 (Nelson 2), shows drawdown when the Nelson 1 (well 121117) irrigation well is pumping and the Nelson 2 is not being pumped. The water-level fluctuations recorded in the model area monitoring wells result from the complex interaction of the four existing irrigation wells (location, fig. 19).

The model-simulated head changes along Big Muddy Creek are greatest during July (stress period 77). The maximum predicted head change in the aquifer, which is over 100 ft below the surface and separated from the wetlands by multiple confining layers of till and clay, is up to 0.40 ft at cell 80239 near Homestead. The interaction between the deep Clear Lake aquifer and the shallow alluvial system is unknown in this area, although aquifer discharge to the wetlands and streams has been assumed in previous studies (Donovan, 1992; Schuele, 1998).

Scenario 2: No irrigation use

Pumping was turned off at the four existing irrigation wells during the "no irrigation use" scenario. All other transient model conditions were left unchanged. These results were used to calculate time-series head differences between the non-pumping condition and the other scenarios. The water-level changes in Scenario 2 (fig. 20) result from simulated seasonal changes in ET and recharge. The ET and recharge boundary conditions were kept the same for all scenarios. Therefore, rather than simulating conditions prior to irrigation development, the "no irrigation use" scenario generates a control data set for comparing pumping scenarios.

Scenario 3: Four well full allocation volume pumping (1,500 acre-ft)

The four existing irrigation wells pump approximately the full allocation volume (table 1) in scenario 3. The simulated volume, 1,500 acre-ft, exceeds the allocated volume of 1,388 acre-ft by 7 percent due to a small mismatch between the model pumping on–off schedules and the daily stress periods. Pumping in this scenario increased 210 percent over the 2015 recorded

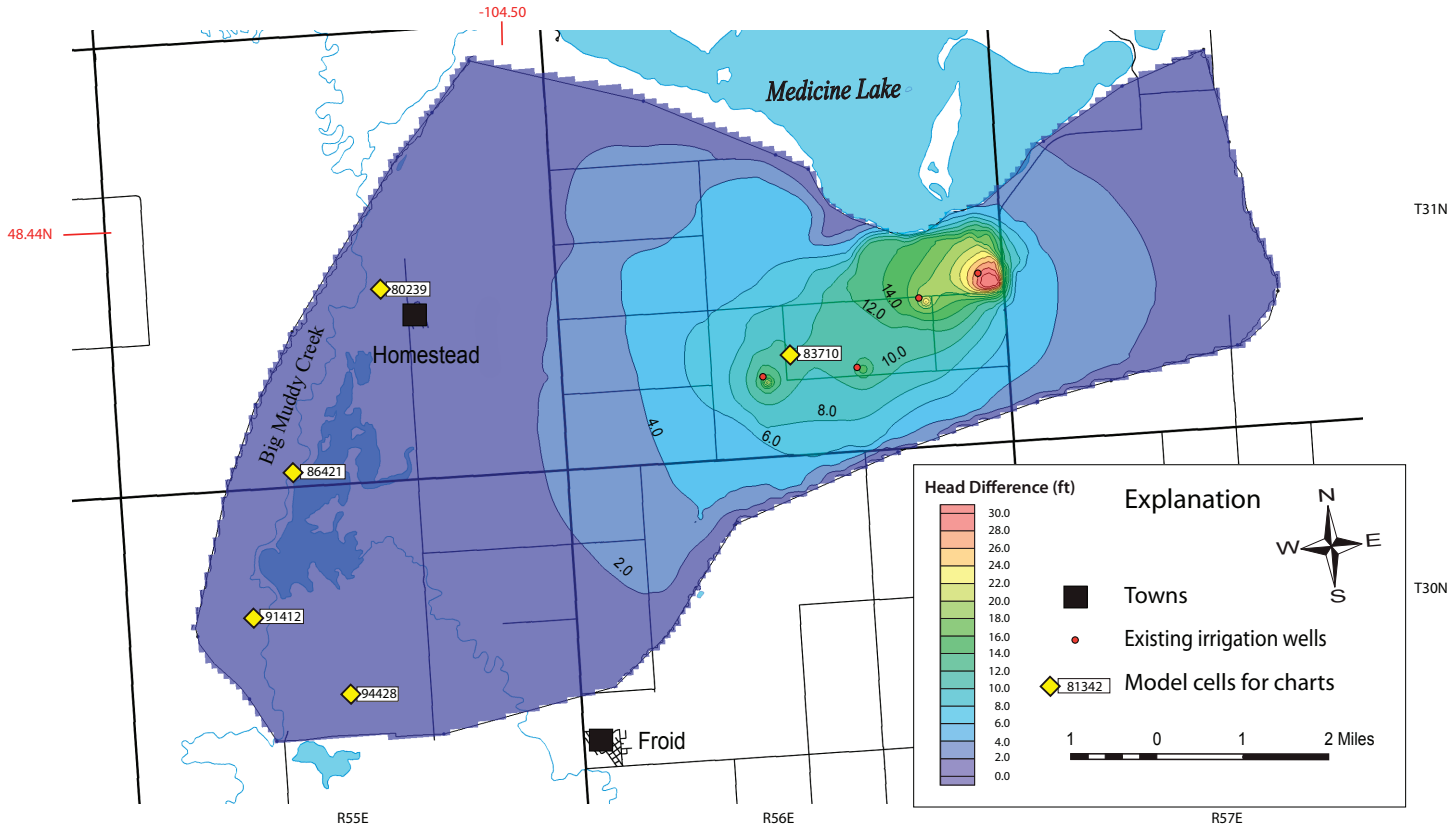

Figure 22. The head differences between the “no irrigation use” scenario and a scenario where the four existing irrigation wells pump maximum allocation volumes shows increased well interference. The model predicts an increased zone of influence and drawdown up to 0.45 ft at cell 80239 near Homestead. Model output is for the period with greatest drawdown, in mid-July.

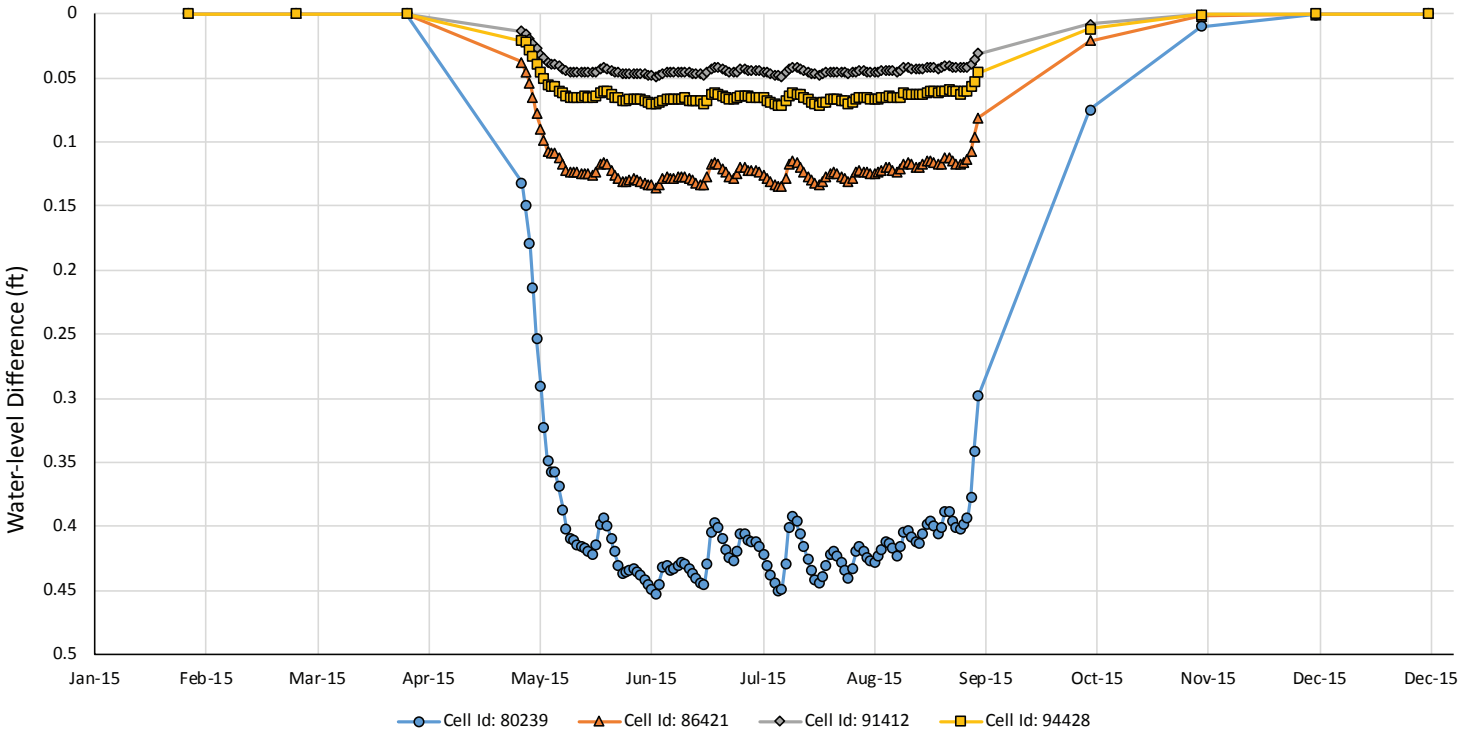

Figure 23. The water-level differences at four model cells along Big Muddy Creek predict up to 0.45 ft water-level change when the four existing wells pump the full allocation volume, scenario 3. The cell locations are shown in figure 22.

volume. The four irrigation wells pump nearly continuously during this simulation to withdraw the full allocation. Historical water-use records indicate that irrigators in the study area have never used this volume, even during dry years.

Scenario 3 causes a greater aquifer drawdown with the extended irrigation pumping (fig. 22). Although the volume pumped in this scenario was more than tripled, the simulated water-level change in the aquifer near the wetlands of Big Muddy Creek is less than 0.5 ft (fig. 23).

Scenario 4: Eight well 2015 volume pumping (1,104 acre-ft)

The fourth scenario simulated realistic irrigation development by doubling the number of irrigation wells in the focus area. Four hypothetical wells were placed in an area with ample farmland and high-quality groundwater, thus suitable for irrigation expansion. The pumping schedule was set to resemble that measured in 2015. The hypothetical well pumping rates (set at 650, 700, 750, and 800 gpm) kept production similar to the existing irrigation wells (table 6). The total volume pumped from the new wells was approximately 620 acre-ft.

The additional irrigation wells expanded the area of pumping drawdown (fig. 24). The expansion was predominately westward as expected, since the hypothetical wells are west of the existing wells. This scenario predicts approximately 1.4 ft of water-level change in the aquifer near Homestead during the peak use period in July (fig. 25).

Scenario 5: Eight well full allocation volume pumping (2,585 acre-ft)

The fifth scenario simulates eight wells pumping a hypothetical full allocation volume of 2,585 acre-ft during the irrigation season. Pumping from the four existing wells equals their permitted allocation. The four new wells pumped approximately 270 acre-ft each. The wells need to pump nearly continuously to extract this volume.

This scenario produced the greatest drawdown of the four pumping scenarios tested (fig. 26). The drawdown at four selected cells along the Big Muddy shows that there would be approximately a 2-ft decline in the water levels near Homestead (cell 80239).

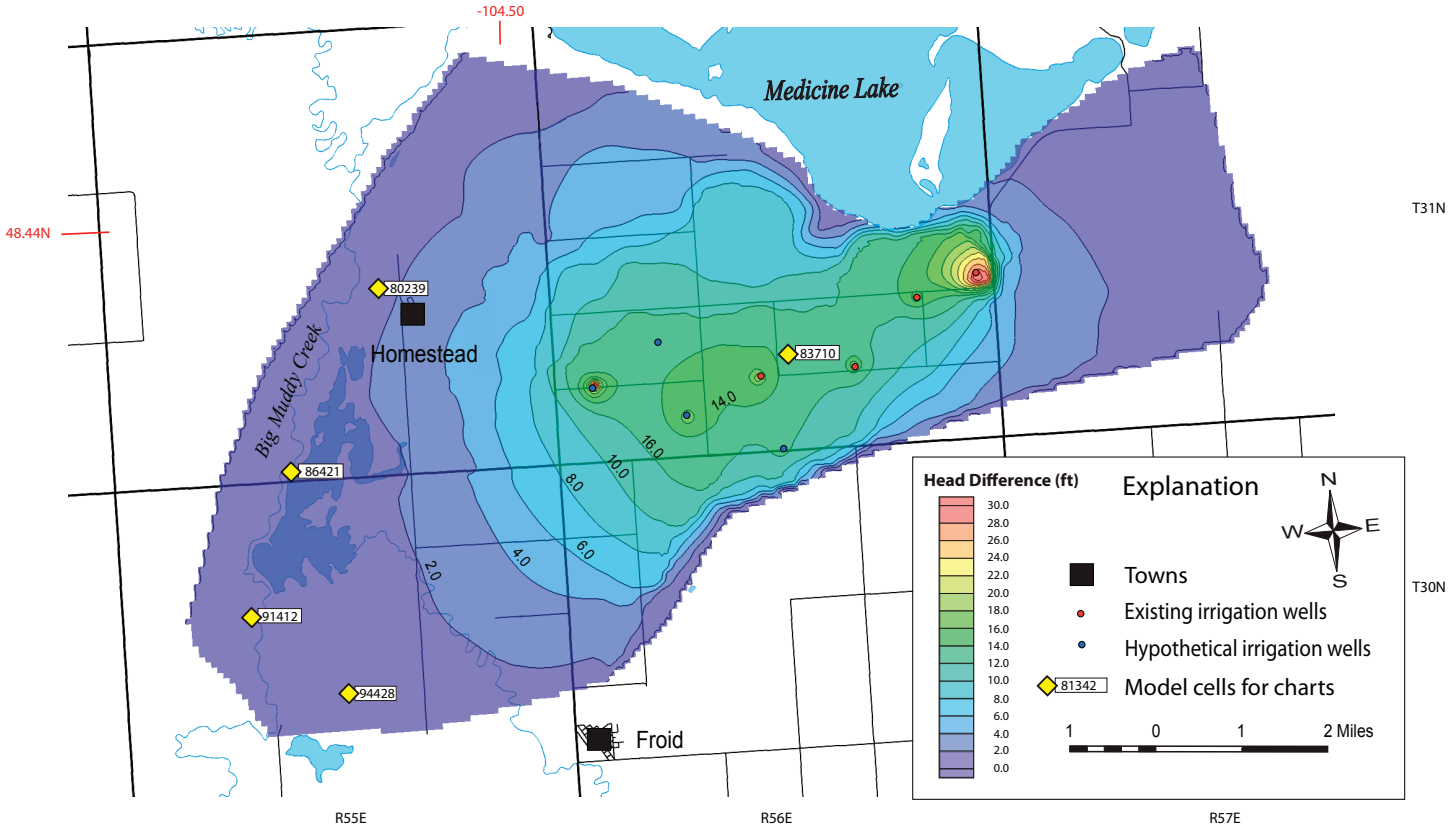

Figure 24. The layer 4 head difference between "no irrigation use" and scenario 4 simulates less than 2 ft of drawdown at cell 80239 near Homestead. Model output is for the period with greatest drawdown, in mid-July.

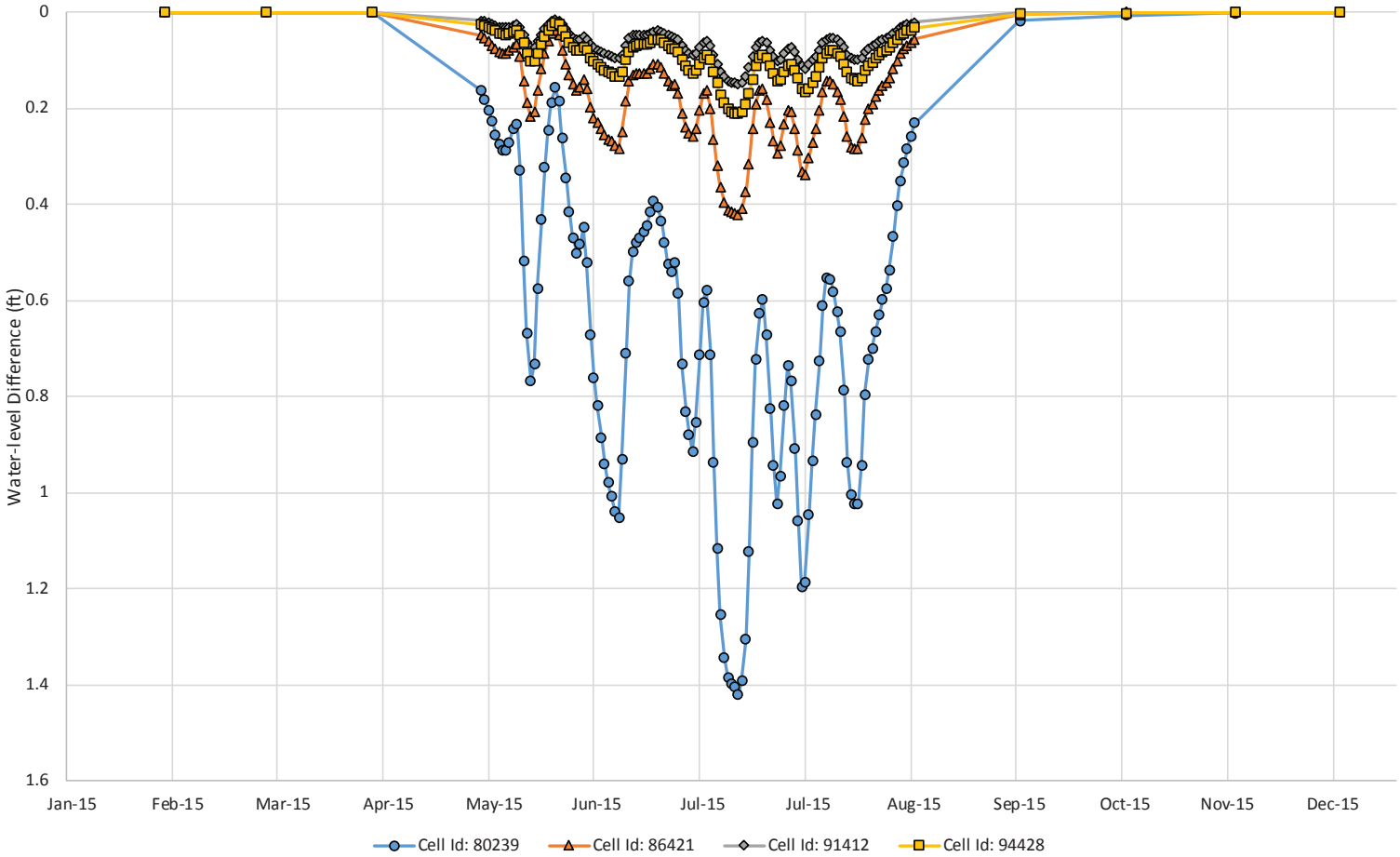

Figure 25. The water-level differences at four model cells along Big Muddy Creek predict up to 1.4 ft change in aquifer water levels with eight wells pumping at rates similar to 2015, scenario 4. The cell locations are shown in figure 24.

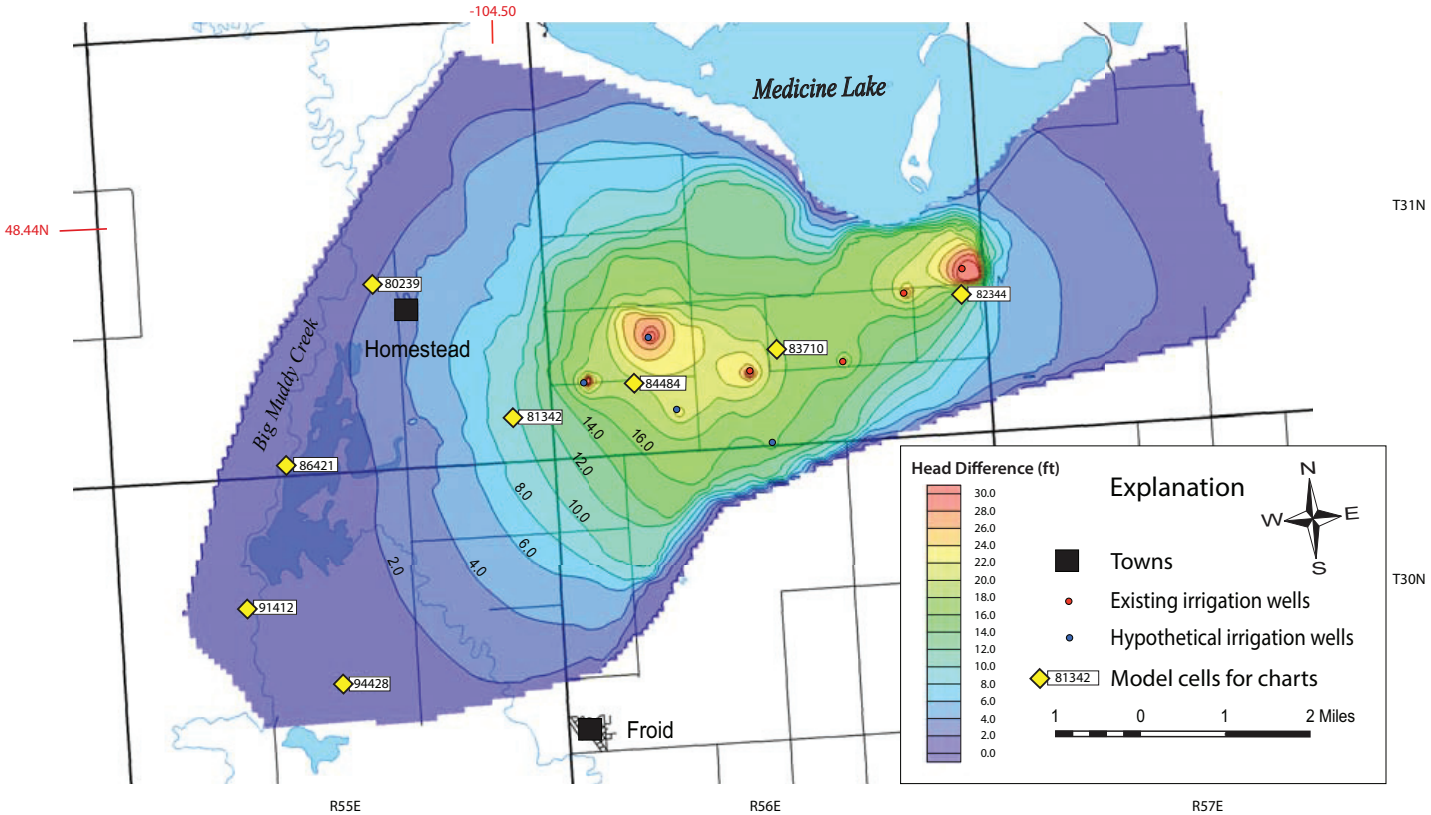

Figure 26. The layer 4 head difference between “no irrigation use” and scenario 5 predicts 2 ft of drawdown at cell 80239 near Homestead. This model output is for the period with greatest drawdown, in mid-July.

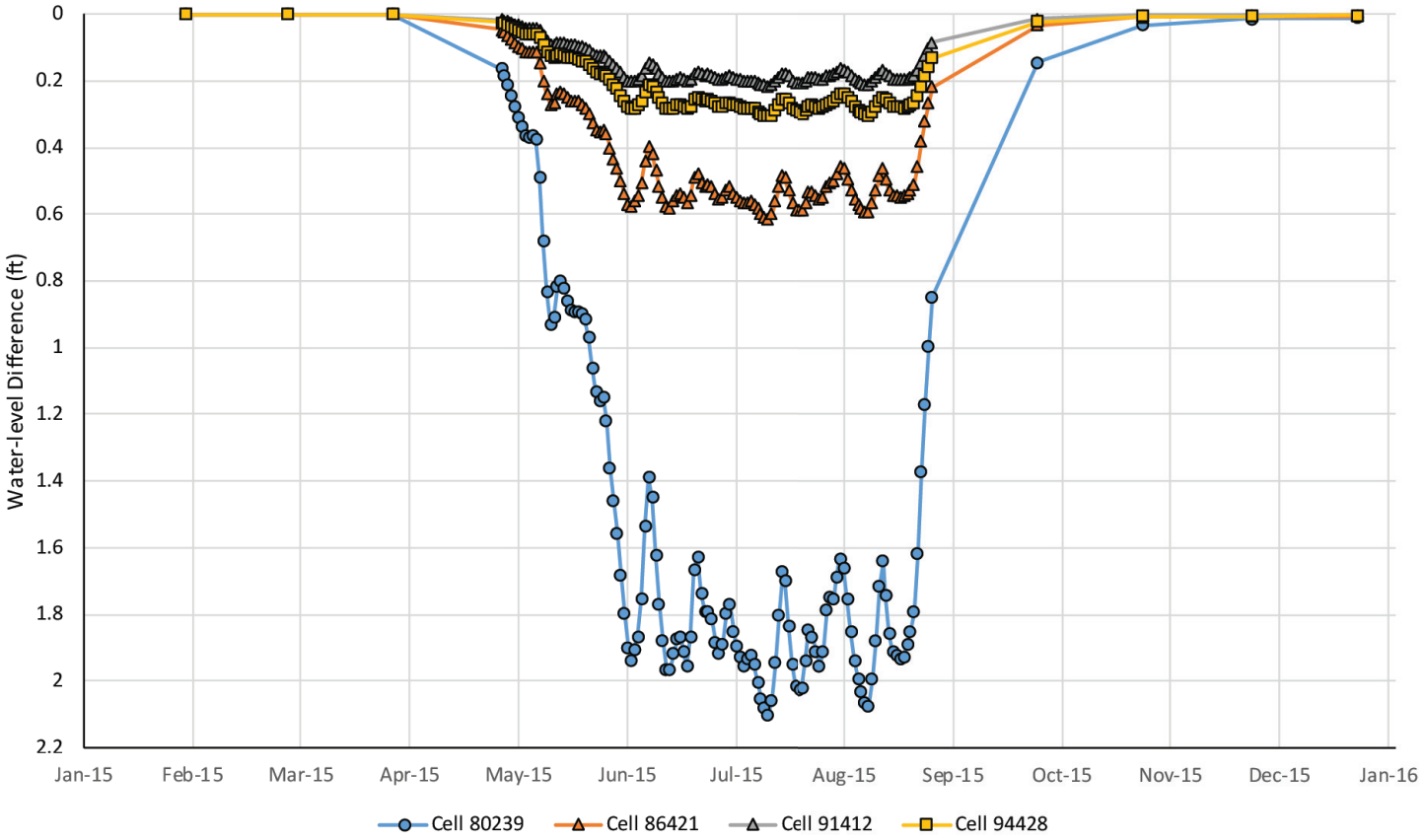

Figure 27. The water-level differences at four model cells along Big Muddy Creek predict up to 2 ft change in aquifer water levels for scenario 5. The cell locations are shown in figure 26.

The other cells monitored showed less decline (fig. 27). The locations of the cells selected for water-level charts are shown in figure 26.

MODEL SUMMARY AND CONCLUSIONS

Model Summary

Scenario Comparisons

Scenario 1 simulated the aquifer water levels observed during the 2015 irrigation season, a 1-yr transient calibration. Scenario 2 was simulated to generate a "no irrigation use" comparison data set used to evaluate the predictive scenarios.

The pumping frequency and number of irrigation wells were increased in the predictive scenarios. With the four existing irrigation wells pumping the full allocated volume in scenario 3, water levels in the aquifer remained depressed throughout the irrigation season. This results from nearly continuous pumping to extract the full allocation. At cell 84484 in the middle of the model, scenario 3 predicted 5 ft of drawdown, similar to the maximum drawdown simulated during 2015 volume pumping (scenario 1, fig. 28). Scenario 3 produced a little over 0.4 ft of drawdown in the aquifer under the Big Muddy Creek alluvial valley at Homestead (fig. 29).

As expected, the model predicted increased drawdown with twice as many irrigation wells simulated in scenarios 4 and 5. The eight wells pumping at 2015 use levels in scenario 4 tripled the maximum drawdown seen in scenario 1 (four wells pumping at the 2015 rates). The eight well - full allocation pumping in scenario 5 caused four times the maximum drawdown from the existing four wells in scenario 3 (fig. 28). The eight well-full allocation scenario resulted in about 2 ft of aquifer drawdown near Homestead (fig. 29). Additional comparisons at other model locations are presented in appendix D.

Model Flow Budgets

In addition to simulating pumping-induced changes in the water table, model results quantify changes in the flow budget due to variations in well locations and withdrawal rates. The total budget volumes for each scenario (table 7) fall at the upper end of the range estimated independently for this flow system (table

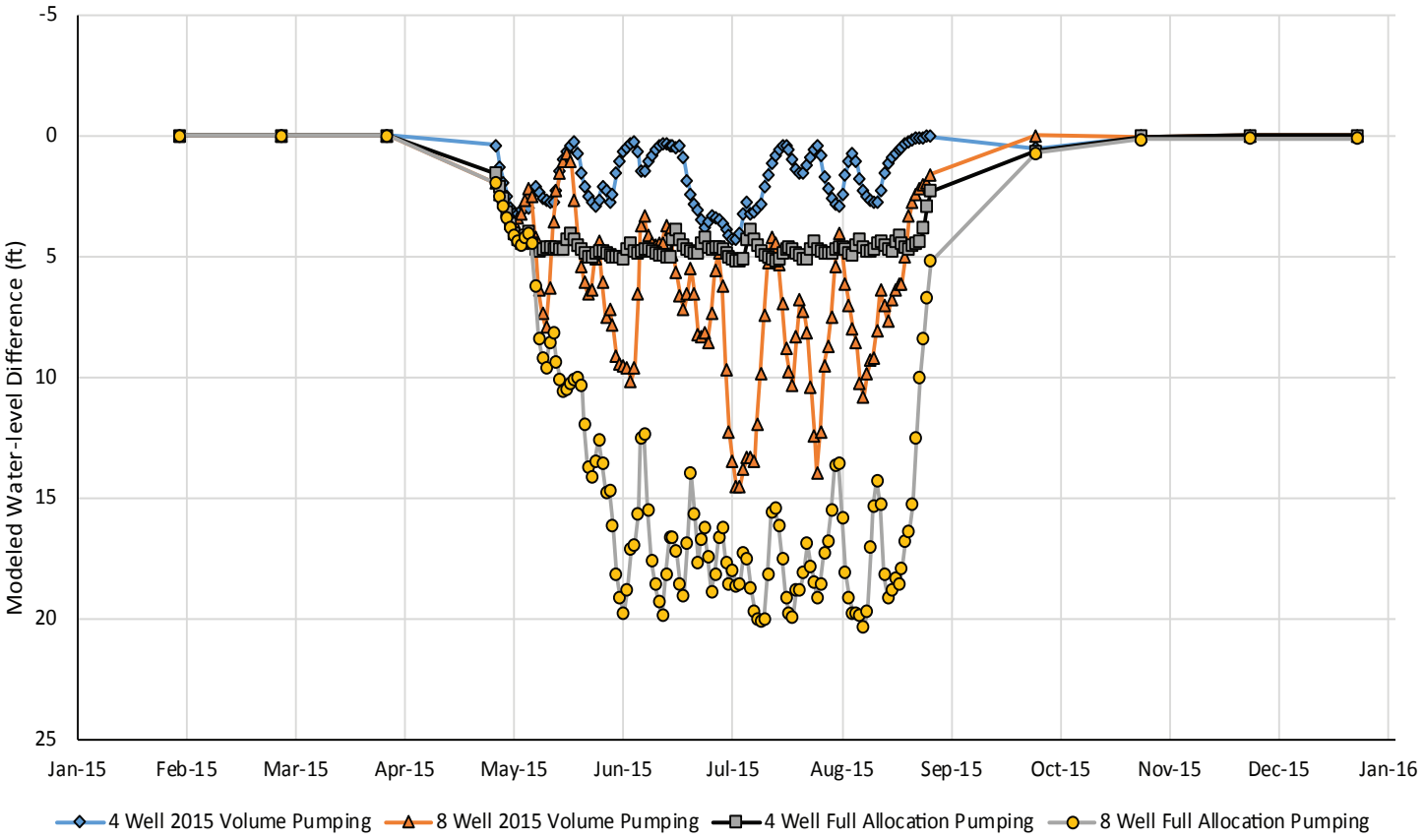

Figure 28. Time-series water-level differences between no irrigation and four pumping scenarios calculated at cell 84484 in the middle of the model. Cell locations are shown in figure 26.

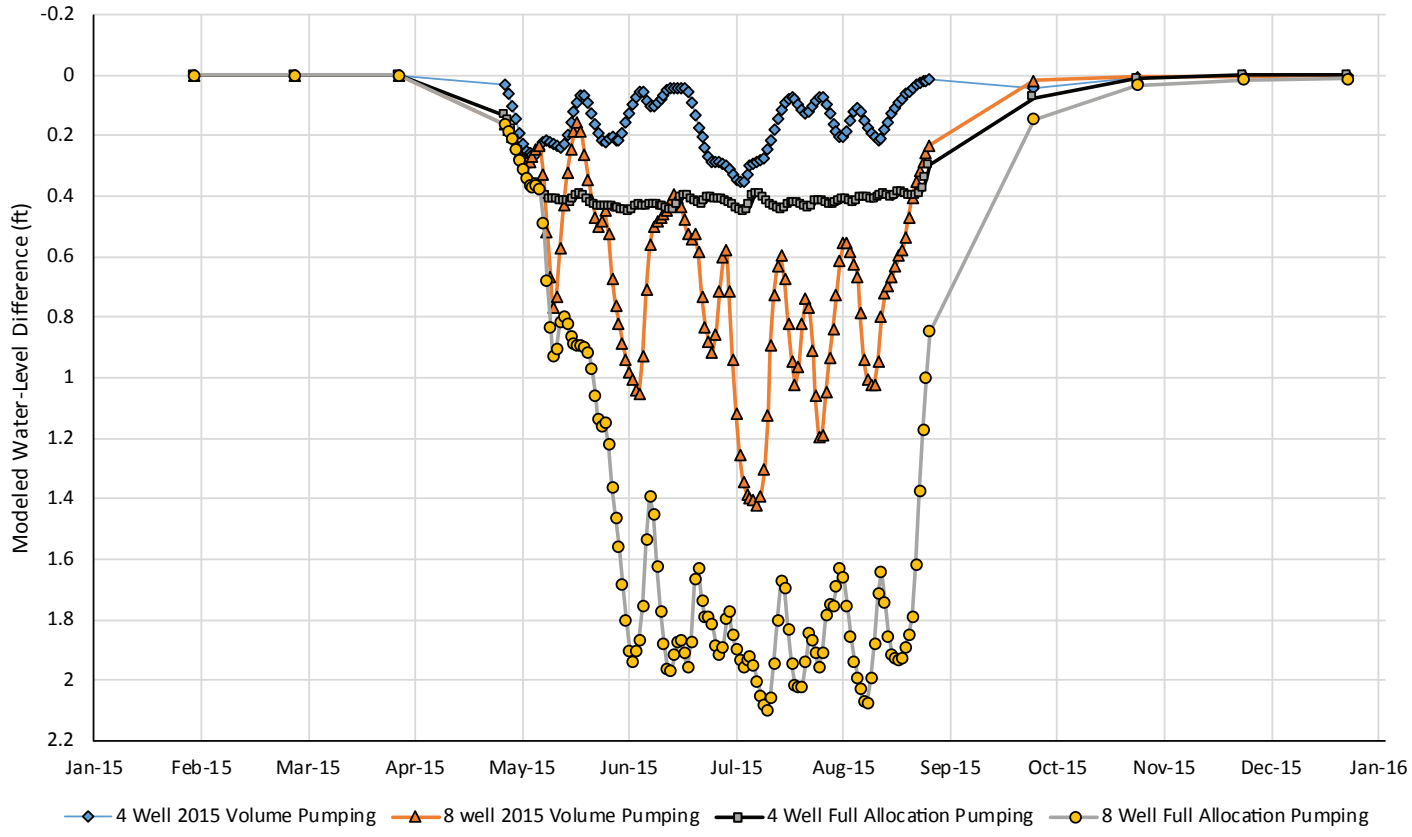

Figure 29. Time-series water-level differences between no irrigation and four pumping scenarios calculated at cell 80239 near Homestead. Cell locations are shown in figure 26.

Table 7. Model Flow Budget summaries.

Model Scenario	1: Four Well 2015 Level Pumping (acre-ft)			2: No Irrigation Pumping		
	In	Out	Difference (In-Out)	In	Out	Difference (In-Out)
Storage	152	147	5	57	52	5
GHBs	10,961	4,935	6,026	10,633	5,014	5,619
Recharge	1,207	0	1207	1,207	0	1,207
Wells	0	483	-483	0	0	0
Drains	0	570	-570	0	589	-589
ET	0	6,191	-6,191	0	6,245	-6,245
Total	12,320	12,327	-7	11,897	11,899	-2
Percent Discrepancy			0.05%			-0.02%

Model Scenario	3: Four Well Maximum Allocation Pumping (acre-ft)			4: Eight Well 2015 Level Pumping (acre-ft)		
	In	Out	Difference (In-Out)	In	Out	Difference (In-Out)
Storage	155	150	5	228	222	6
GHBs	11,674	4,778	6,897	11,338	4,832	6,506
Recharge	1,207	0	1,207	1,207	0	1,207
Wells	0	1,500	-1,500	0	1,104	-1,104
Drains	0	543	-543	0	547	-547
ET	0	6,106	-6,106	0	6,103	-6,103
Total	13,037	13,077	-40	12,773	12,808	-35
Percent Discrepancy			-0.31%			-0.28%

Model Scenario	5: Eight Well Maximum Allocation Pumping (acre-ft)		
	In	Out	Difference (In-Out)
Storage	256	248	8
GHBs	12,379	4,622	7,756
Recharge	1,207	0	1,207
Wells	0	2,585	-2,585
Drains	0	509	-509
ET	0	5,916	-5,916
Total	13,842	13,882	-40
Percent Discrepancy			-0.29%

3). Figure 30 shows the changes in the water budgets with increasing irrigation water use. The overall mass balance error for each simulation was 0.3% or less in each case.

Recharge in the model flow budgets represents precipitation or snowmelt applied to the model surface whereas, in reality, recharge to the system comes from inflow from a larger area. Recharge was held constant for all of the scenarios.

The GHBs contribute the most water to the model in each scenario, which is reasonable because these boundaries represents flow into the model area from adjacent areas of the Clear Lake aquifer and the Fort Union bedrock. GHBs either contribute or remove water from the model depending on the head difference between model cells and the assigned boundary heads. In these model simulations, increased pumping induced inflow along GHBs representing upgradient sources, and reduced outflow along GHBs representing the alluvium in the Big Muddy Creek Valley (fig. 30). Scenario 5, with the highest pumping volume, predicts that 83% of the pumped water comes from changes in GHB flow.

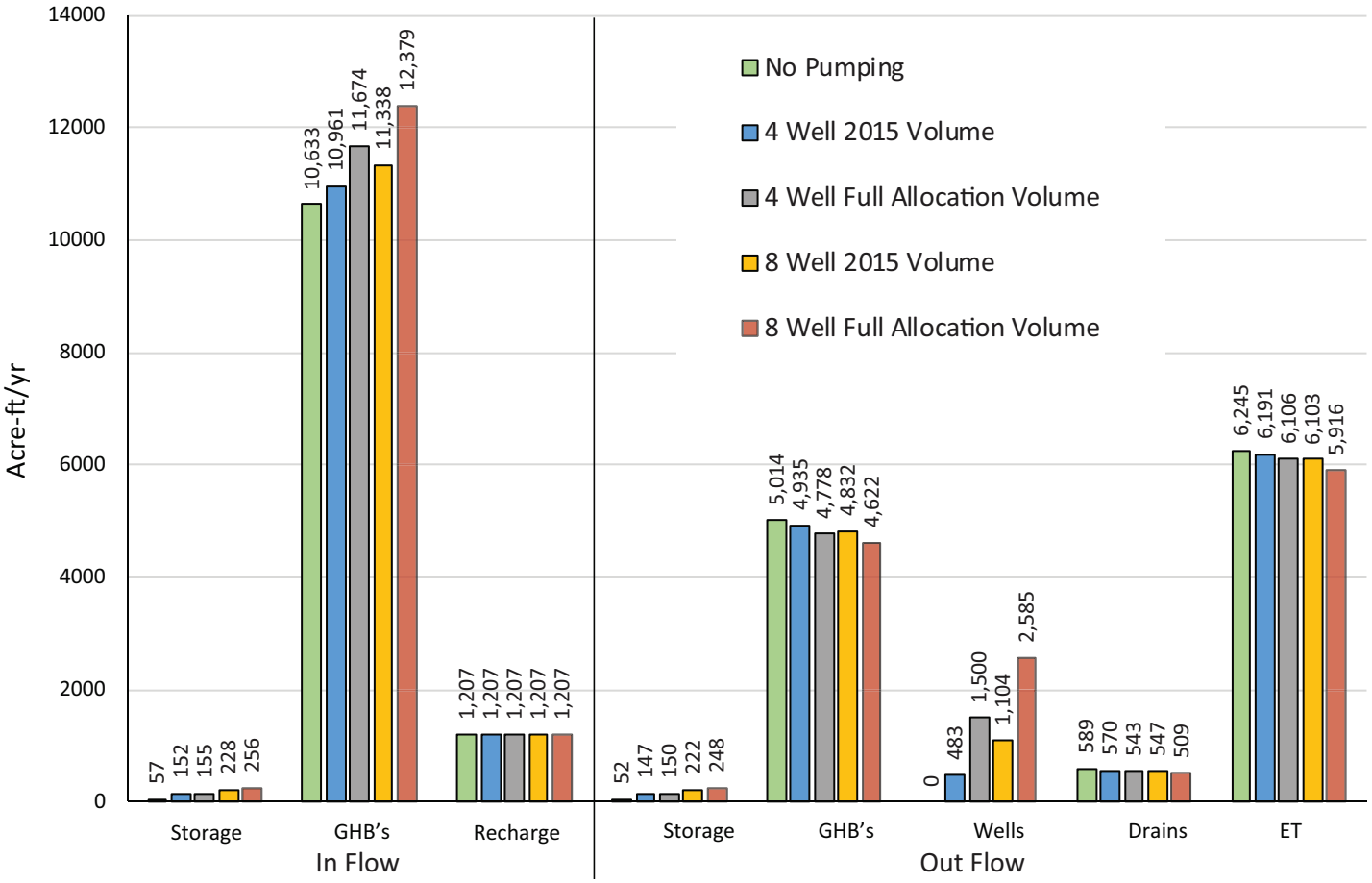

Figure 30. Comparison of model flow budgets (acre-ft/yr) for the five scenarios shows increased head dependent flow into the model and decreased head dependent flow, ET, and drain flow out of the domain as pumping increases.

Figure 30 also shows a reduction in ET and drain flow with increased irrigation pumping. ET was reduced by 329 acre-ft between scenario 2: "no irrigation use" and scenario 5: "eight wells maximum allocation pumping," which accounts for 13% of the pumped volume. ET in the model decreases as the heads in layer 1 decline. Therefore, areas with high water tables would have less water available to phreatophytes or for wetland seeps. This could lead to a reduction in land that is currently subirrigated. The drain flows decreased by 80 acre-ft between these scenarios, accounting for 3% of the maximum pumped volume. Drains represent seepage areas in small drainages and coulees. This reduction could reduce surface-water flows and evaporation from small sloughs and ponds. The increased pumping scenario flow budgets are compared to the calibrated model budget in table D1, in appendix D.

DISCUSSION

Model Development

This modeling effort emphasized a realization of the complex stratigraphy with enough detail to represent the stratigraphic control on the flow system. Sediment layers from various geologic processes, including periods of deposition and erosion, were lumped together based on similar lithologic and hydrogeologic properties. For example, dense layers of lake clays were combined with glacial till based on their similar low hydraulic conductivity and their tendency to act as aquitards. Likewise, the sand and gravel of glacial outwash was grouped with alluvial gravels of the ancestral Missouri River channel deposits. Numerous flow model runs were conducted to find the level of stratigraphic simplification that retained enough detail to behave similarly to the real system. A more detailed representation of the stratigraphy could be accomplished by increasing the number of model layers and decreasing the cell size, but additional cells increases the model run time. The typical run time for the 1-yr transient model was approximately 25 min. Grids with 10 layers and smaller cells provided more stratigraphic detail, but exceeded the available computational power.

The number of active model cells could be reduced by assuming a no-flow boundary where the buried channel aquifer contacts the Fort Union bedrock. However, inter-aquifer flow from the bedrock to the alluvial gravel seems to contribute substantial groundwater, and appears to play an important role in controlling water quality. Water from wells along the southern boundary of the aquifer have poor water quality, indicating influx of high sodium absorption ratio (SAR) water from Fort Union bedrock (Reiten and Chandler, in review).

The drawdown in the model area is strongly influenced by hydrogeologic boundaries. These boundaries include the low transmissivity sediments and semi-consolidated bedrock deposits that restrict groundwater flow to the wells. Although the Clear Lake aquifer is several miles wide in some locations, the most productive wells are along the lateral boundaries. This observation is consistent with buried valley aquifers documented in North Dakota (Kehew and Boettger, 1986). Nelson 1 (121117) has the highest yield of the four existing irrigation wells, but it also shows the greatest drawdown resulting from its proximity to the barrier boundaries (fig. 21).

A 3-D numerical model is well suited to simulate the complex stratigraphy and interactions of multiple pumping wells. Analytical models predict drawdown assuming a homogeneous sheet-like aquifer of an infinite extent. Aquifer tests required for irrigation well permitting indicate barrier boundaries, but do not identify the boundary locations. The stratigraphic modeling helped identify and locate barrier boundaries.

Model Predictions

Concerns about new irrigation development in the South Medicine Lake model area are focused on possible impacts to the surface-water and groundwater resources. The hydrogeologic study and model generated by this project confirm the hydrologic disconnect between the surface water in Medicine Lake and the groundwater of the Clear Lake aquifer in the model area. To the west, the surface water in Big Muddy Creek and the associated wetlands have the potential to receive water from the underlying Clear Lake aquifer, but the extent of the connection between the systems is unknown. There is a lack of stratigraphic information near the Big Muddy Creek wetlands. Well 3605 is the closest well west of the wetlands. The well log, like others in this area, indicates that the wetlands and the creek are separated from the buried valley aquifer by confining layers of clay, sandy clay, and till. Aquifer head changes predicted by some of the scenarios decrease the vertical head gradient, which could reduce the upward flow towards the wetlands. The model predicts greater drawdown in the deep aquifer (layer 4) than in the surface (layer 1) at all four cell locations along Big Muddy Creek Valley (fig. 31).

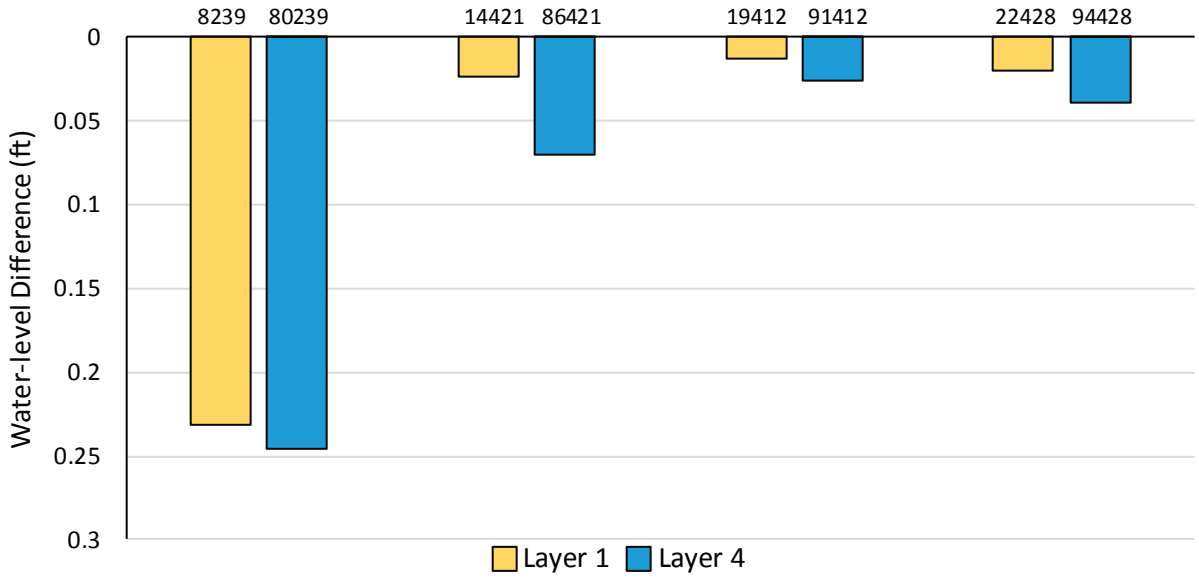

Figure 31. Scenario 1 water-level differences calculated for layer 1 and layer 4 at four locations near the Big Muddy Creek wetlands predicts less drawdown in the surface than in the deep aquifer. The drawdown is for mid-July. Cell numbers are above the chart columns; layer 4 cell locations are shown in figure 26.

Model scenario 1 showed little head change under the Big Muddy Creek wetlands 4 to 5 mi from the closest production well. There has been no observed changes to the wetlands with this level of irrigation development (Reiten and Chandler, in review). The model did confirm measurable well interference, but the interference does not impede or restrict pumping at any of the existing irrigation wells. The 0.2 ft decline (fig. 31, cell 80239) in layer 1 heads near Homestead could potentially reduce ET in subirrigated areas.

Model scenario 3 increased the pumping at the four existing irrigation wells to the full allocated volume for each well, totaling 1,500 acre-ft/yr. Although the water table would remain depressed for the entire season with the continuous pumping, the predicted water-level decline in the aquifer below the closest wetlands near Homestead is less than 0.4 ft. This small head change has the potential to decrease seepage across the confining layers, but the change may be imperceptible at the surface. The water levels in the center of the model are predicted to drop about 5 ft. Continuous pumping would likely increase well interference, but the head decline would not likely impede production.

Model scenario 4 predicted that eight wells pumping at the 2015 water-use volume would also be unlikely to impact wetlands along Big Muddy Creek. In this scenario, the wells would extract approximately 1,100 acre-ft/yr, and produce up to 1.4 ft of decline in the deep aquifer near Homestead (fig. 29). Even though 400 less acre-ft/yr is withdrawn in this scenario than in scenario 3, some of the hypothetical wells are located closer to the Big Muddy Creek wetlands. This produces greater drawdown when these wells are operating. The maximum predicted drawdown is not maintained with the typical pumping schedules observed in this area. Due to the cost of pumping, farmers only use the water they need to supplement precipitation. The need is driven by the crop type and the weather, and therefore varies from year to year for each location. The model predicts less drawdown in the shallow aquifer or confining layers of layer 1 than in the deep aquifer layer 4 (fig. 32). Short-term water-level declines in the deep aquifer would likely

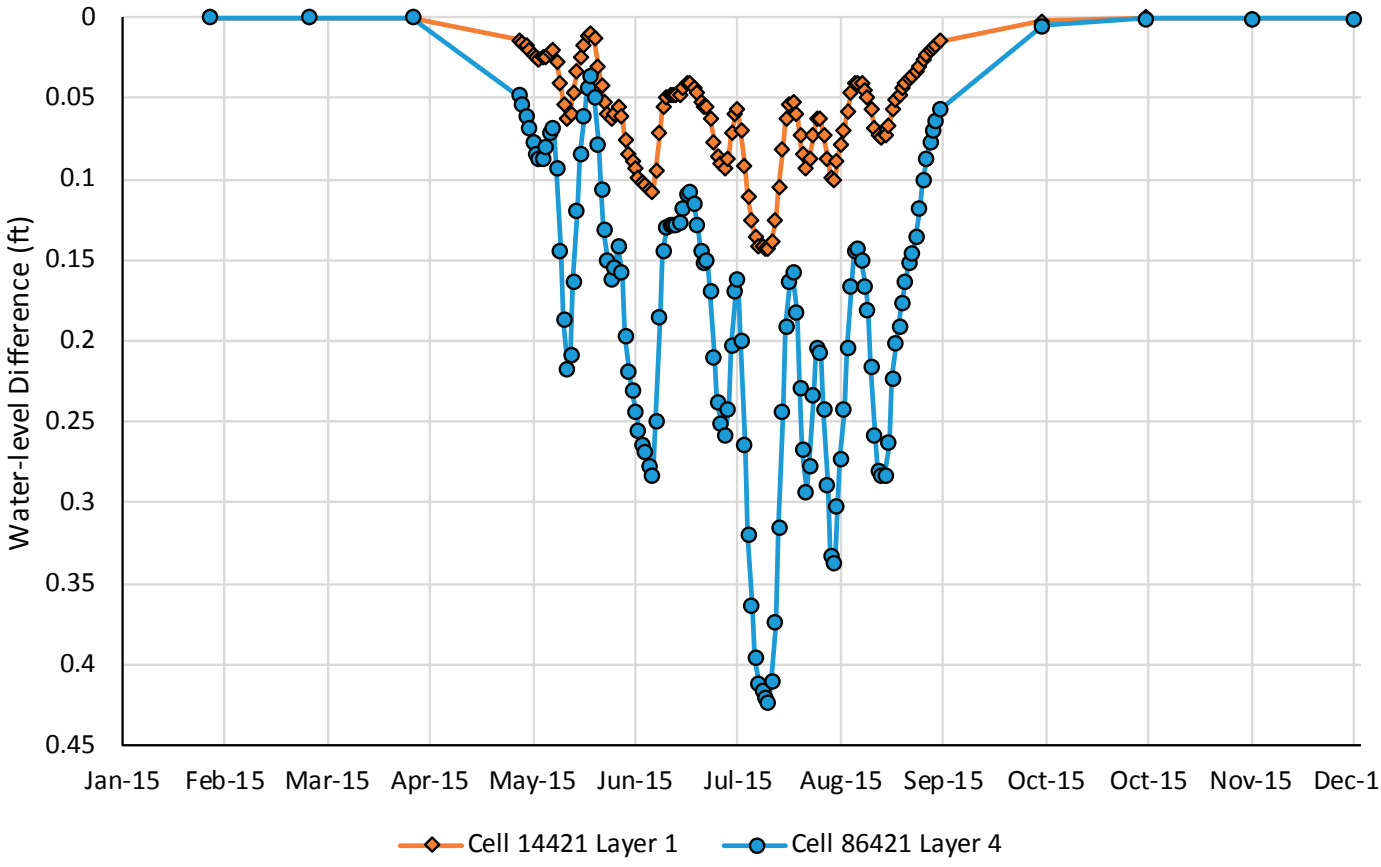

Figure 32. Scenario 4 predicts less drawdown in layer 1, representing the shallow aquifers and wetlands, than layer 4, the deep aquifer at cell 86421 near Big Muddy Creek wetlands. The cell location is shown in figure 26.

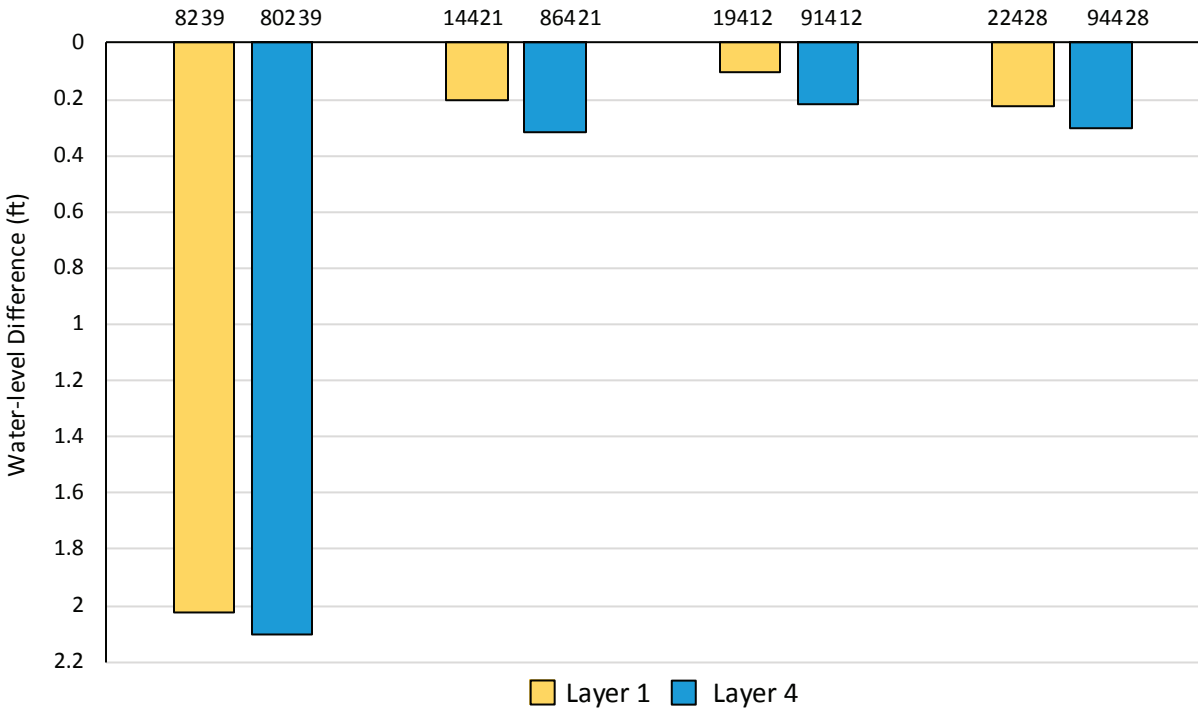

Figure 33. Scenario 5 water-level differences calculated for layer 1 and layer 4 at four locations near the Big Muddy Creek wetlands predicts less drawdown in the surface than in the deep aquifer. The drawdown is for mid-July. Cell numbers are above the chart columns; layer 4 cell locations are shown in figure 26.

be imperceptible at the wetlands.

In scenario 5 all eight wells pumped the full allocation volume, totaling 2,585 acre-ft/yr. The model predicts head declines greater than 2 ft in the Clear Lake aquifer, and slightly less in the shallow aquifers under the Big Muddy Creek alluvial valley near Homestead (fig. 33). This would likely decrease seepage to some wetland areas, and decrease ET water loss. Water levels in the center of the model are predicted to remain about 20 ft lower during the irrigation season. Pumping costs would increase, and well interference may limit use at some wells, especially those close to barrier boundaries (fig. 26). The results of this model simulation indicate that increasing the irrigation volume to 2,600 acre-ft/yr may result in unacceptable drawdown in the aquifer.

The model scenarios also predicts an increase in inflow from model GHBs with additional irrigation water use. This increased flow into the model area represents flow from connections to bedrock aquifers and extensions of the buried valley aquifer. The actual flow into the Big Muddy Creek drainage from north and west of the model area is poorly understood, but lowering the heads in the model area along the Big Muddy Creek Valley would induce flow towards the wetlands from other sources of groundwater outside the model domain.

Assumptions and Limitations

This model was constructed to evaluate the impacts of increased irrigation water use on existing groundwater and surface-water resources by evaluating changes in water levels resulting from new stresses. It was calibrated to timing and magnitude of water-level fluctuations produced by known pumping stresses. It was not designed or calibrated to match or predict absolute water levels at all points in the model domain.

The model underpredicts drawdown at some of the observation wells, and overpredicts aquifer recovery after pumping. These deviations from the observed values most likely result from the model cells representing average aquifer drawdown over the cell area. In reality, the Clear Lake aquifer has large changes in aquifer properties over short distances horizontally and vertically. Drawdown is amplified in tightly confined buried valley systems because of the lateral boundaries and confining layers (van der Kamp and Maathuis, 2012).

The model area has a wealth of borehole informa-

tion that supported stratigraphic interpretation between boreholes. Sediments in some geologic settings are deposited in nearly uniform layers, but the sediments in the Medicine Lake area have been eroded, filled, and reworked by multiple glacial episodes. Large variations in aquifer thickness and material type have been documented in short horizontal distances in this area. The deeper alluvial deposits are quite variable, typical of stream-deposited sediments. While the deposits usually coarsen with depth, the alluvial sand and gravel deposits are commonly interbedded with clay or clay-bound sand and gravel, reducing the overall transmissivity of the aquifer. Simplification of the aquifer stratigraphy was necessary to develop this model and therefore limits model results. The interpolated aquifer thickness and transmissivity generated from stratigraphic modeling can be verified or refined by future drilling and well development.

The assignment of head-dependent flux boundaries models groundwater flow into and out of the model. This cross-boundary groundwater flow provides an important source of water to the Clear Lake aquifer. The east and west GHBs that cross the buried valley aquifer were located miles away from the irrigation pumping centers to reduce boundary impacts. GHBs along the north and south boundary of the model were assigned low conductance values to represent the interaction of the buried valley aquifer with bedrock aquifers. The bedrock aquifers with higher water-level elevations have the potential to add measurable water to the buried valley aquifer. Better records of temporal variation in head in the bedrock aquifer would improve simulations of these boundaries.

The new irrigation well locations and water-use allocations were assigned in areas of possible development, and with use rates similar to existing wells. The scenarios tested assumed development of four wells with similar water-use levels operating simultaneously. If these wells were developed one at a time, the effects on other wells and wetlands could be assessed in a stepwise fashion. Water quality may limit irrigation development in the model area since the quality appears to decline to the west, towards the Big Muddy (Reiten and Chandler, in review).

The sensitivity analysis showed that cells in layer 1, representing the wetlands, were more sensitive to changes in ET rates than cells representing the deep aquifer. There are few wells in the Big Muddy Creek area to provide control points for stratigraphic modeling, to document actual vertical gradients, or to provide continuous water-level data for calibration. The model predicts upward gradients from the Clear Lake aquifer, but the magnitude of the flow vectors indicate the substantial flow in the deep aquifer below the wetlands (fig. 34). More monitoring data from this area would support use of the model to simulate the wetlands, and to evaluate effects of head declines resulting from potential increased irrigation water use.

Recommendations

The model is useful to evaluate aquifer conditions at potential well sites, and to predict effects of new water use on existing water users and wetlands. Wells can easily be added to the model to simulate site-specific increased use, and simulations can be varied to estimate optimal pumping volumes and well locations.

The stratigraphic modeling in the South Medicine Lake focus area can be used to guide new development into areas where the aquifer is productive. Stratigraphic modeling north of the model area was used to guide drilling for new irrigation wells near Dagmar, MT. Cross sections constructed using borehole data were used to estimate the drilling depths and to help locate productive parts of the aquifer. The resulting new irrigation wells were in the permitting process as of 2018.

Models are only as good as the information used in their construction. This model may be updated as new wells are installed and additional water-level data are collected. The predictive power of the model would increase with extension of the calibration period to include multiple years of water-level and use data. Water use was lower than normal in 2016 due to abundant summer precipitation. At the other extreme, 2017 was the second driest year recorded in Sheridan County over the period 1895 to 2018, and the recorded water use was higher than normal (NCEI, 2018). These data provide an opportunity for a 3-yr calibration of the model. Recharge and ET variations resulting from a wet year (2016), and a dry year (2017) could be included to refine model response to climate changes. The extended calibration period would make the model more useful for investigating possible impacts of climate change.

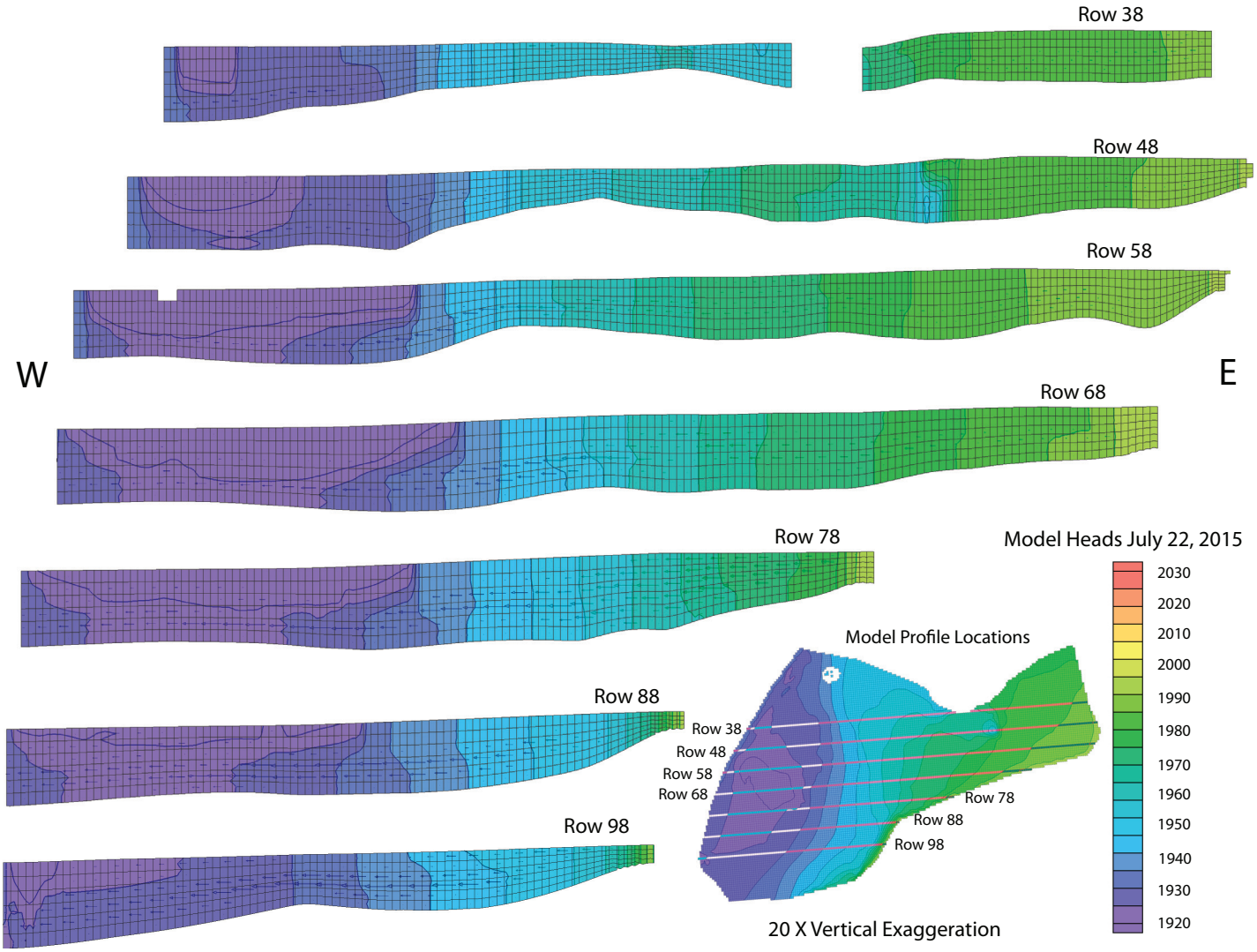

Figure 34. Profiles through the transient model for July 22, 2015 indicate upward gradients towards the surface wetlands. The size scaled flow vectors indicate the dominate flow is under the wetlands in layers 4 and 5. Row 48 shows effects of pumping at well 121117.

The interaction between the deeper Clear Lake aquifer, the shallow alluvial aquifers, and wetlands of the Big Muddy Creek Valley is poorly understood. The discharge from the deeper aquifer to the shallow system was assumed in previous works, and is important to evaluate the possible effects of irrigation development presented in this report. Test drilling, nested monitoring wells, and water-quality sampling could provide the information needed to improve the conceptual model of this area. The poor water quality and clay soils in this area make future irrigation development in the Big Muddy Creek alluvial valley unlikely, but irrigation development outside the valley may change conditions in the wetlands.

ACKNOWLEDGMENTS

This project was only possible with support from the Sheridan County Conservation District, U.S. Fish and Wildlife Service Medicine Lake Refuge, Fort Peck Tribes, Montana DNRC, and members of the groundwater reservation technical advisory committee. They provided project support, years of data collected from previous studies, and connections to the many area landowners and residents for access to wells and surface-water features. Their proactive approach to groundwater management will hopefully serve as a template for other areas in Montana.

Manuscript reviews by Kirk Waren, Ali Gebril, Ginette Abdo, and Madeline Gotkowitz provided constructive suggestions. Editing was provided by Susan Barth, and Simon Bierbach refined maps and figures.

REFERENCES

Anderman, E.R., and Hill, M.C., 2000, MODFLOW-2000, the U.S. Geological Survey modular ground-water model—Documentation of the Hydrogeologic-Unit Flow (HUF) package: U.S. Geological Survey Open-File Report 03-347, 36 p.

Anderson, M.P., and Woessner, W.W., 1992, Applied groundwater modeling, simulation of flow and advective transport: San Diego, Academic Press, Inc.

Cummings, D.I., Russell, H.A.J., and Sharpe, D.R., 2012, Buried-valley aquifers in the Canadian Prairies: Geology, hydrogeology, and origin: Canadian Journal of Earth Science, v. 49, p. 987–1004.

Domencio, P.A., and Schwartz, F.W., 1998, Physical and chemical hydrogeology: Ann Arbor, Wiley, v. 1.

Donovan, J.J., 1988, Ground-water and geologic data for northeastern Montana in the Wolf Point 1 x 2 degree quadrangle: Montana Bureau of Mines and Geology Open-File Report 208, 633 p.

Donovan, J.J., 1992, Geochemical and hydrologic dynamics in evaporative groundwater-dominated lakes of glaciated Montana and North Dakota: Ph.D. dissertation, Penn State College of Earth and Mineral Sciences, 251 p.

Donovan, J.J., and Bergantino, R.N., 1987, Groundwater resources of the Fort Peck Indian Reservation, with emphasis on aquifers of the preglacial Missouri River valley: Montana Bureau of Mines and Geology Open-File Report 178, 40 p.

Fetter, C.W., 2001, Applied hydrogeology: Upper Saddle River, N.J., Prentice-Hall.

Freeze, R.A., and Cherry, J.A., 1979, Groundwater: Engle Cliffs, N.J., Prentice Hall.

Harbaugh, A.W., 2005, MODFLOW-2005, The U.S. Geological Survey modular ground-water model—The ground-water flow process: U.S. Geological Survey Techniques and Methods 6-A16.

Kehew, A.E., and Boettger, W.M., 1986, Depositional environments of buried-valley aquifers in North Dakota: Groundwater, p. 728–784.

Kessler, T.C., Comunian, A., Oriani, F., Renard, P., Nilsson, B., Klint, K.E., and Bjerg, P.L., 2013, Modeling fine-scale geological heterogeneity—Examples of sand lenses in tills: Groundwater, p. 692–705.

Luckey, R.L., and Becker, M.F., 1999, Hydrogeology, water use, and simulation of flow in the High Plains aquifer in northwestern Oklahoma, southeastern Colorado, southwestern Kansas, northeastern New Mexico and northwestern Texas: Water-Resources Investigations Report 99-4104, U.S. Geological Survey.

Reilly, T.E., and Harbaugh, A.W., 2004, Guidelines for evaluating ground-water flow models: U.S. Geological Survey, Scientific Investigations Report 2004-5038, 37 p.

Reiten, J.C., 2002, Sheridan County ground-water management program: Management of water resources from the Clear Lake aquifer: Montana Bureau of Mines and Geology Open File Report 447, 32 p.

Reiten, J.C., and Chandler, K.M., in review, Hydrogeology and water management of the Clear Lake aquifer with emphasis on the South Medicine Lake Management Area: Montana Bureau of Mines and Geology.

Russell, H.A., Hinton, M.J., van der Kamp, G., and Sharpe, D.R., 2004, An overview of the architecture, sedimentology and hydrogeology of buried-valley aquifers in Canada: Natural Resources Canada, p. 26–33.

Schuele, F., 1998, Numerical simulation of Quaternary glacial outwash and alluvial gravel aquifer in the northern Great Plains of Montana and North Dakota: Master's Thesis, West Virginia University.

Seyoum, W.M., and Eckstein, Y., 2014, Hydraulic relationships between buried valley sediments of the glacial drift and adjacent bedrock formations in northeastern Ohio, USA: Hydrogeology Journal, p. 1193–1206.

Shaver, R.B., and Pusc, S.W., 1992, Hydraulic barriers in Pleistocene buried-valley aquifers: Groundwater, v. 30, no. 1, p. 21–28.

Sloan, C.E., 1972, Ground-water hydrology of prairie potholes in North Dakota: United States Government Printing Office.

van der Kamp, G., and Maathuis, H., 2012, The unusual and large drawdown response of buried-valley aquifers to pumping: Groundwater, p. 207–215.

Weight, W.D., and Sonderegger, J.L., 2001, Manual of applied field hydrogeology: New York, McGraw-Hill.

Western Regional Climate Center, 2017, Evaporation Stations.

APPENDIX A

MODEL DETAILS

Table A1. Aquifer test results used to assign hydrologic properties to model materials.

Well	GWIC ID	Transmissivity (ft²/day)	Hydraulic Conductivity (ft/day)	Storage Coefficient
Nelson 1	121117	3,230	110	0.0024
Nelson 2	155930	4,620	210	0.00017
Nelson 3	212128	9,880	450	0.00025
Bolstad	175651	2,940	160	0.0017

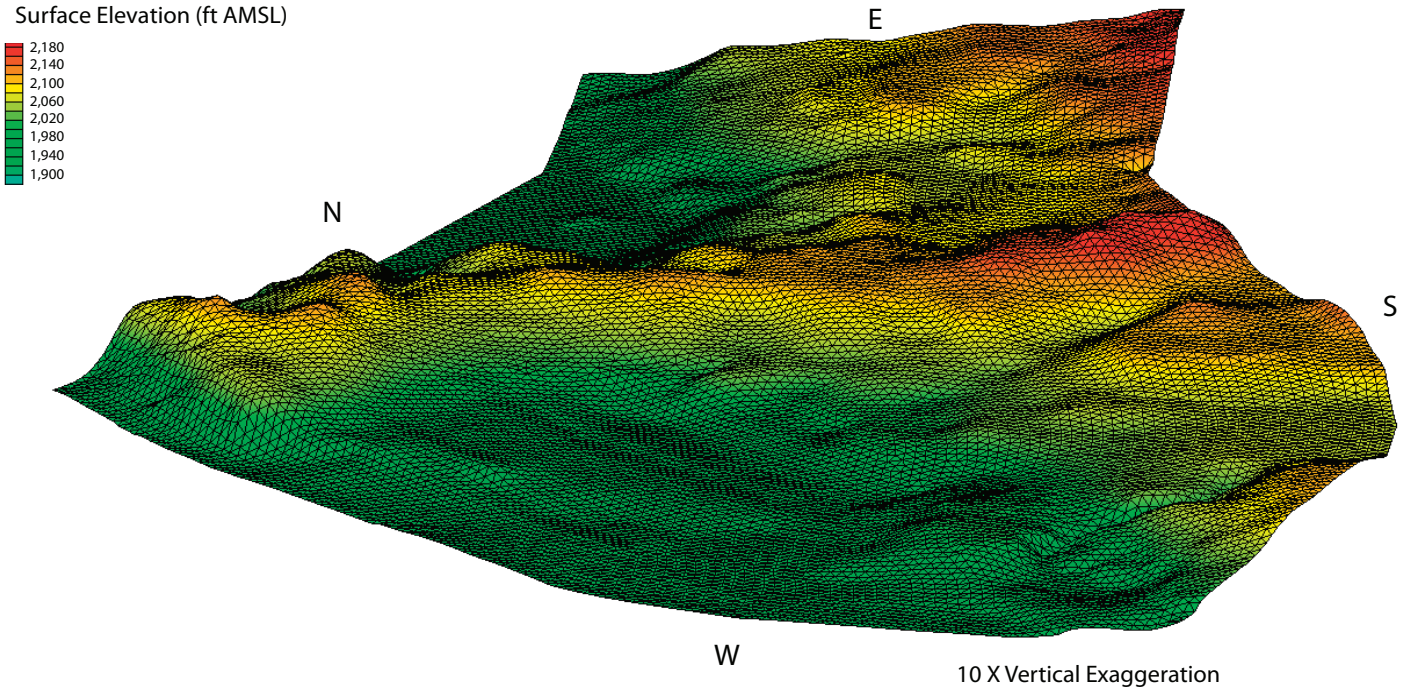

Figure A1. Model area land surface interpolation. This surface was used for the ETS surface for model ET calculations.

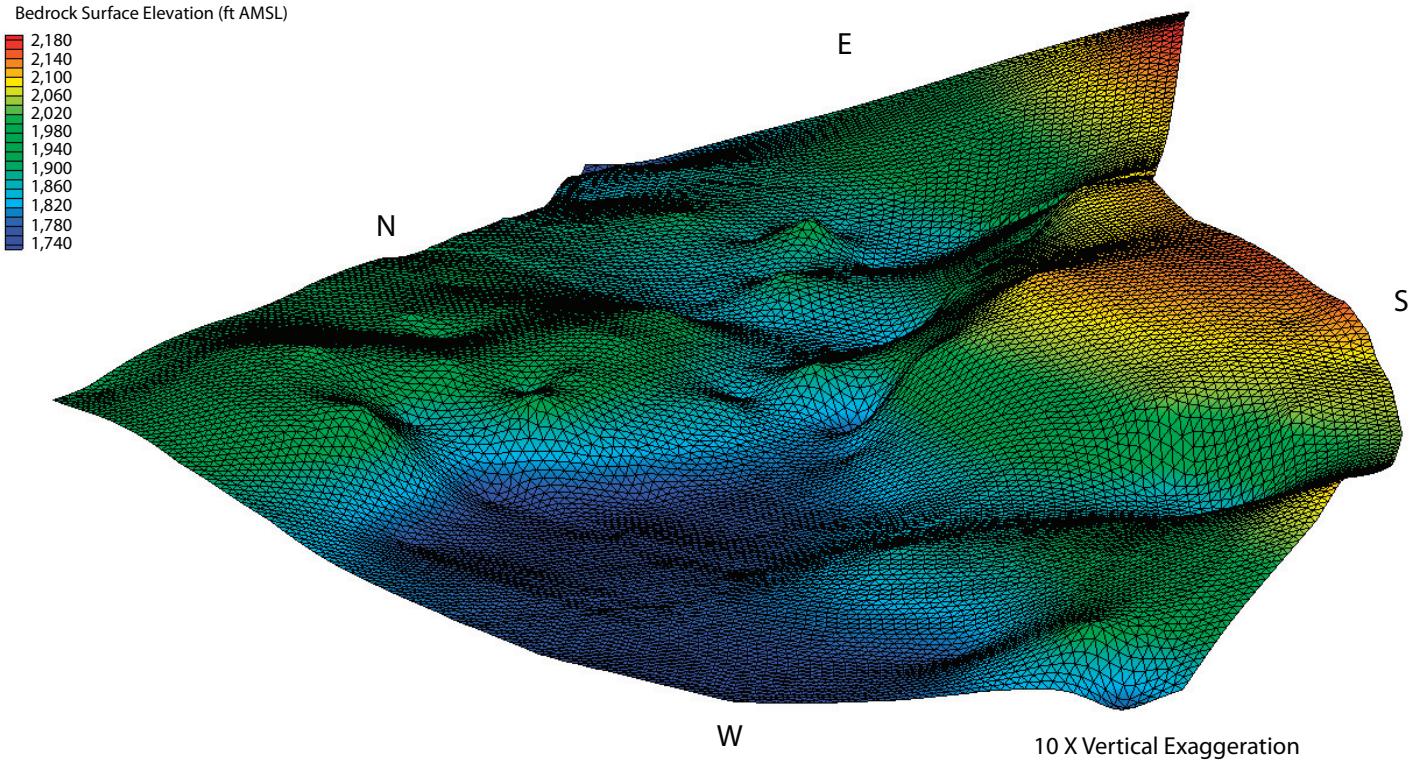

Figure A2. Bedrock Interpolation from borehole contacts.

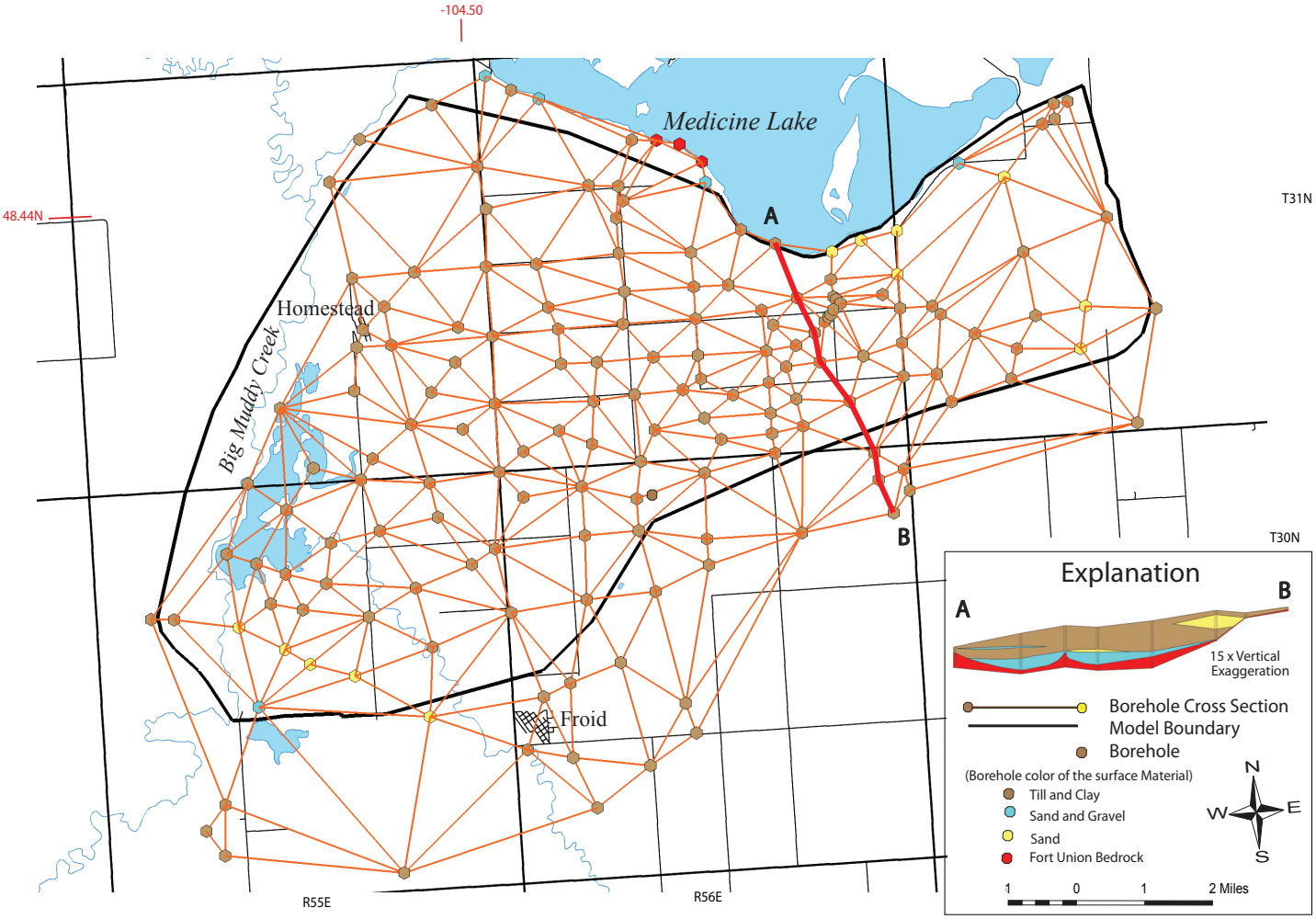

Figure A3. Model boreholes and borehole cross sections used for stratigraphy modeling. Example cross section shown from borehole at A to borehole at B.

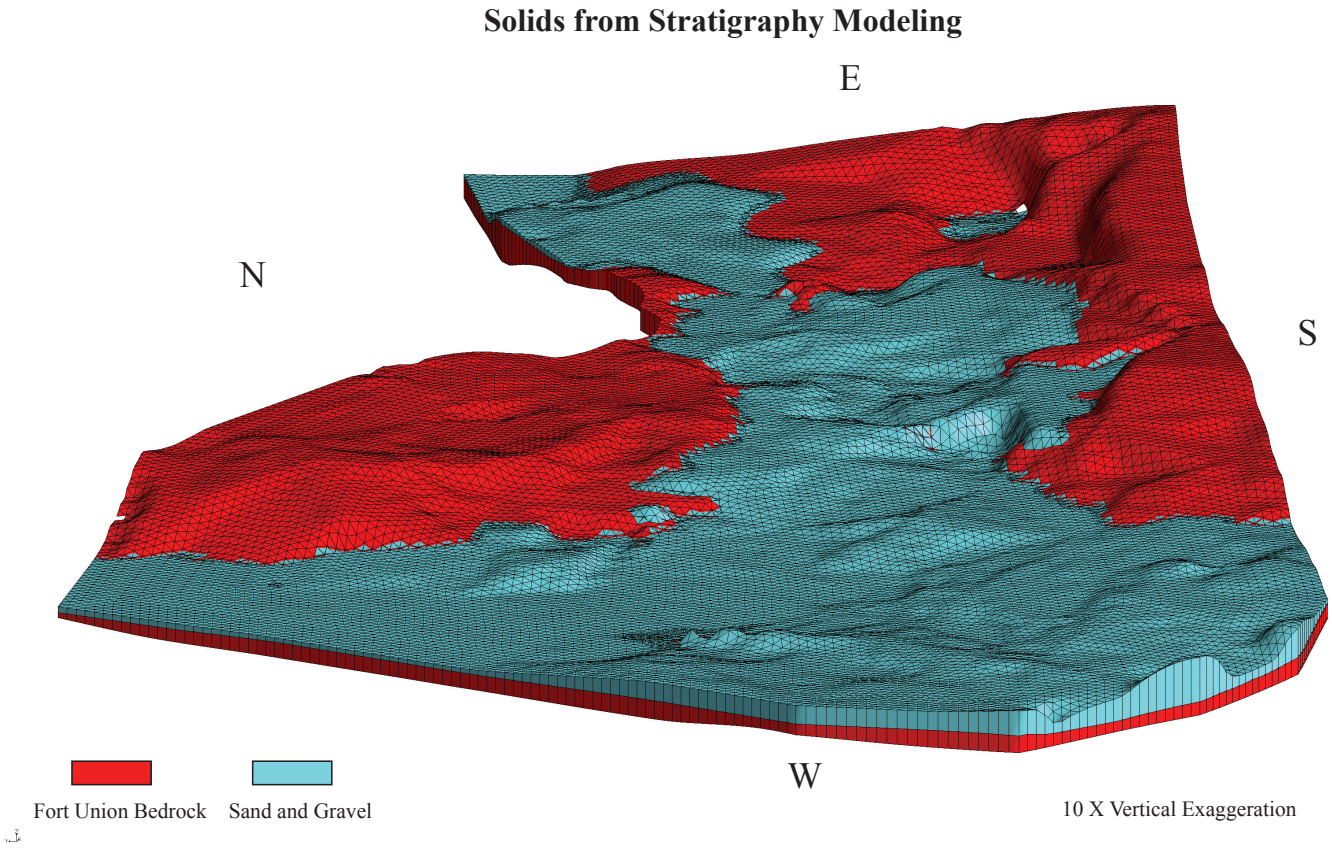

Figure A4. Lower gravel over Fort Union Bedrock.

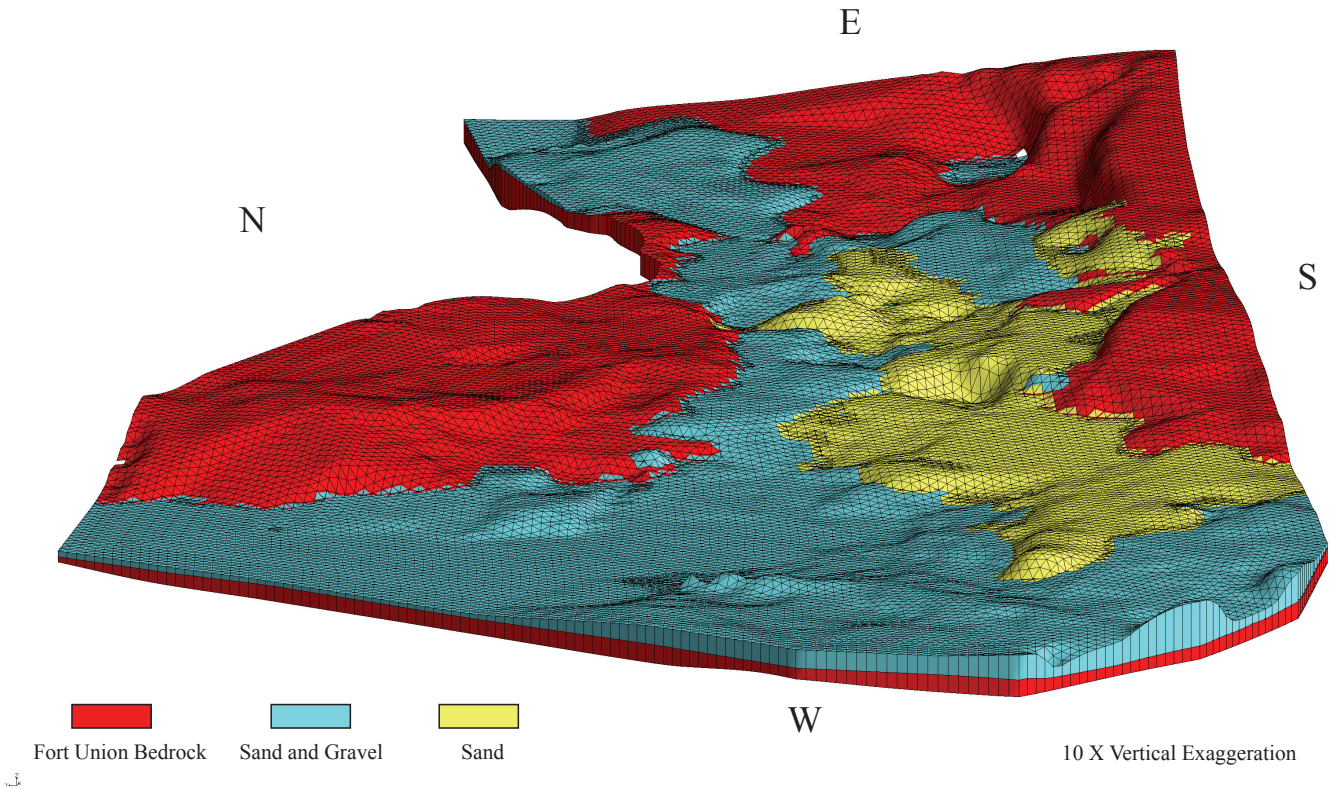

Figure A5. Lower sand and gravel.

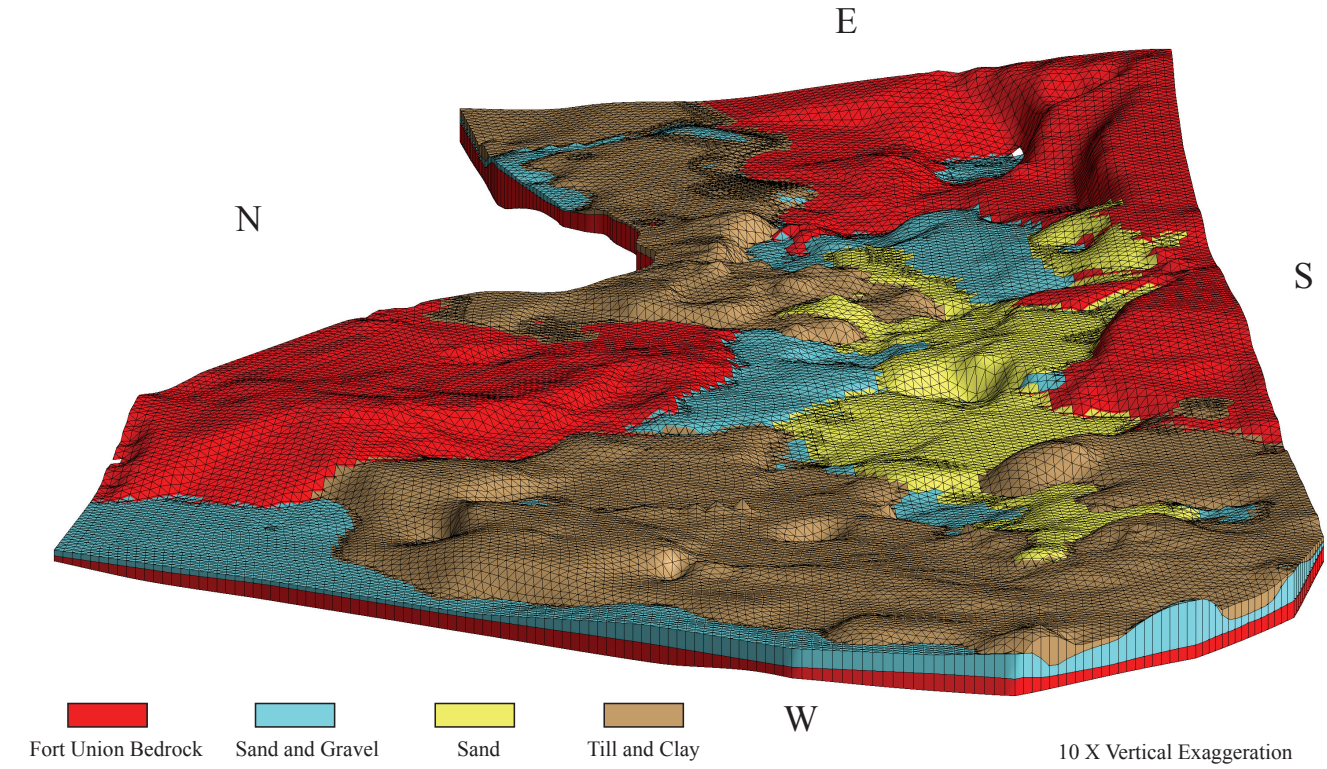

Figure A6. Lower till and clay.

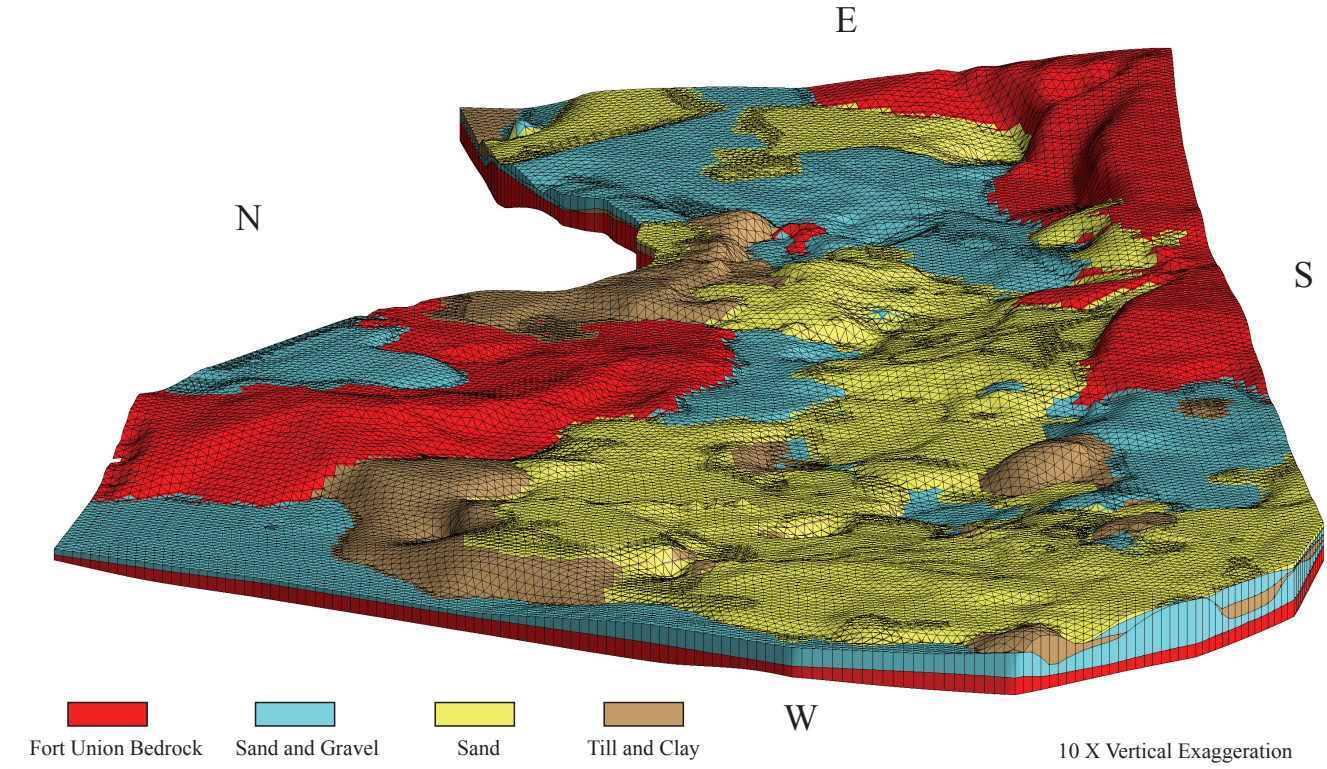

Figure A7. Intermediate sand and gravel.

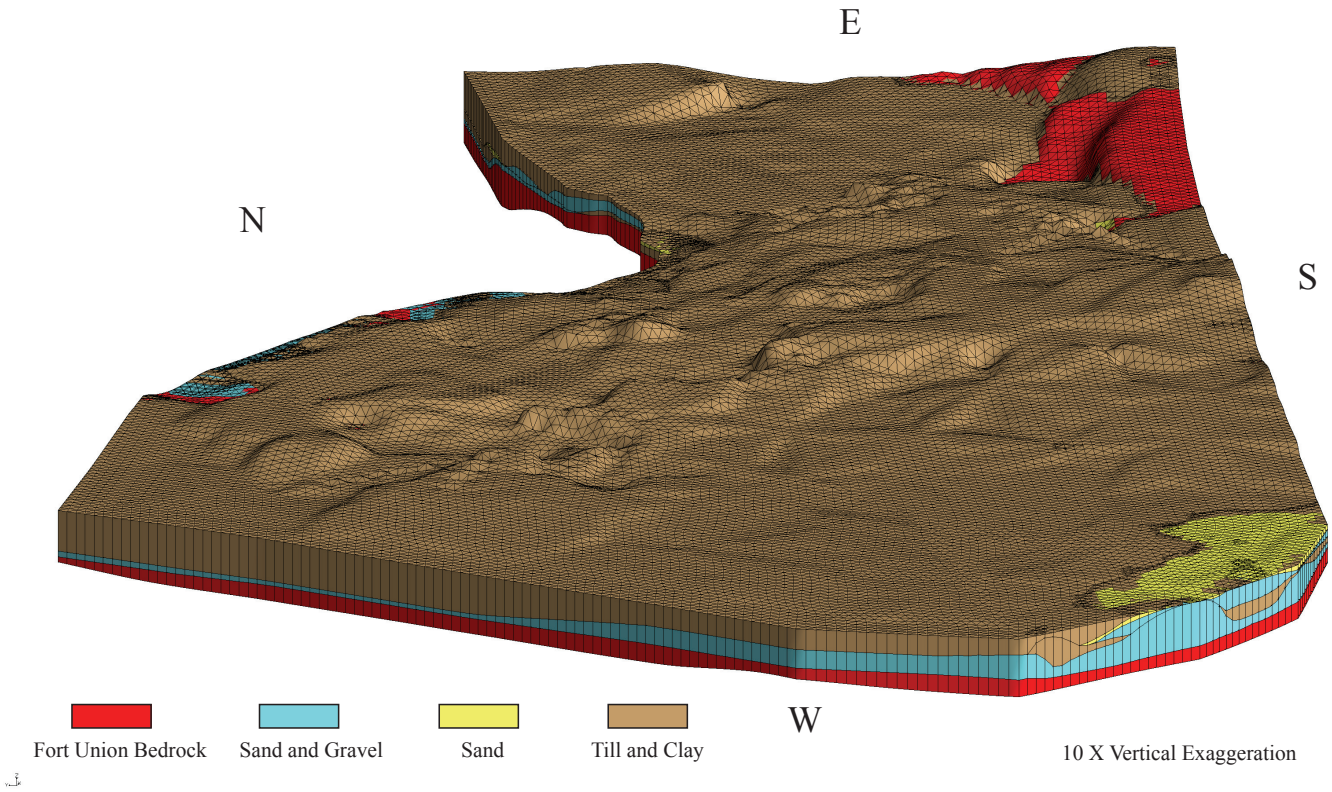

Figure A8. Intermediate till and clay.

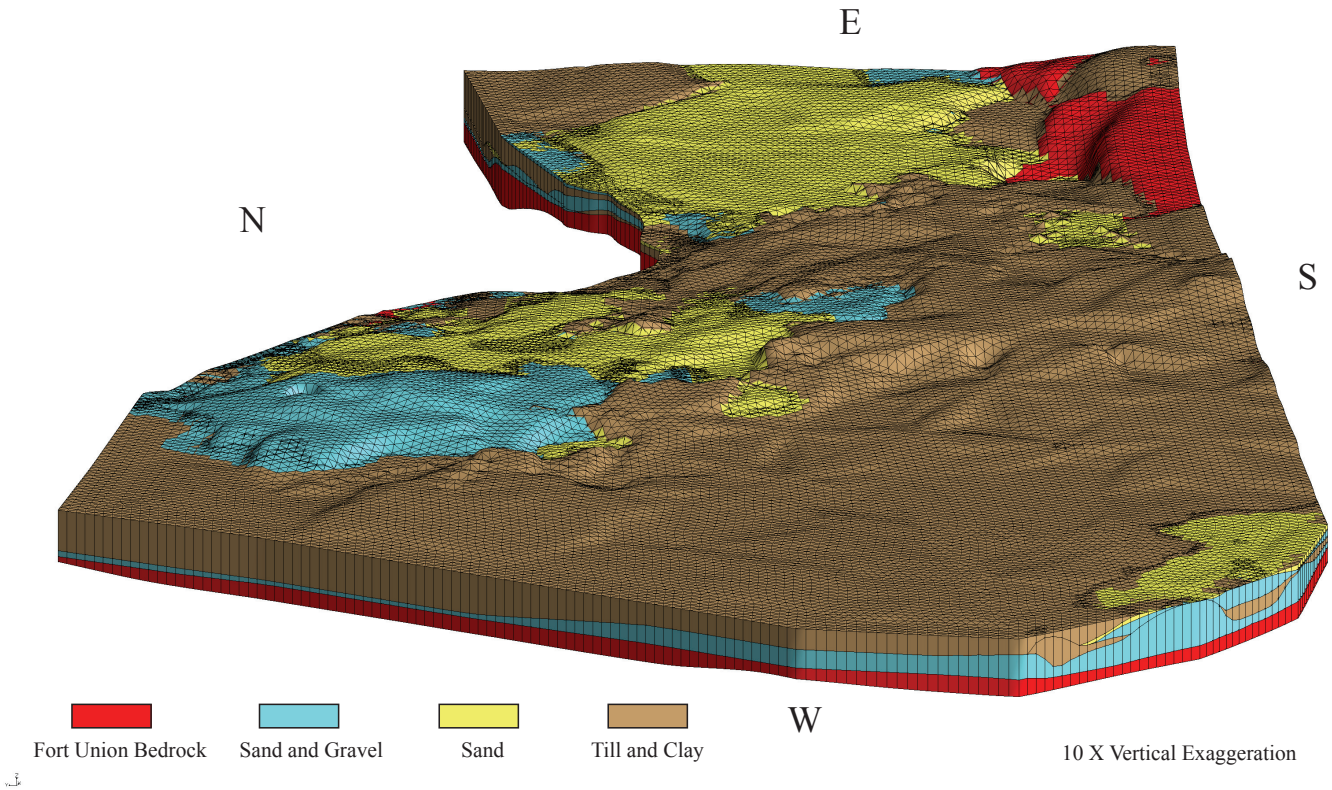

Figure A9. Upper sand and gravel.

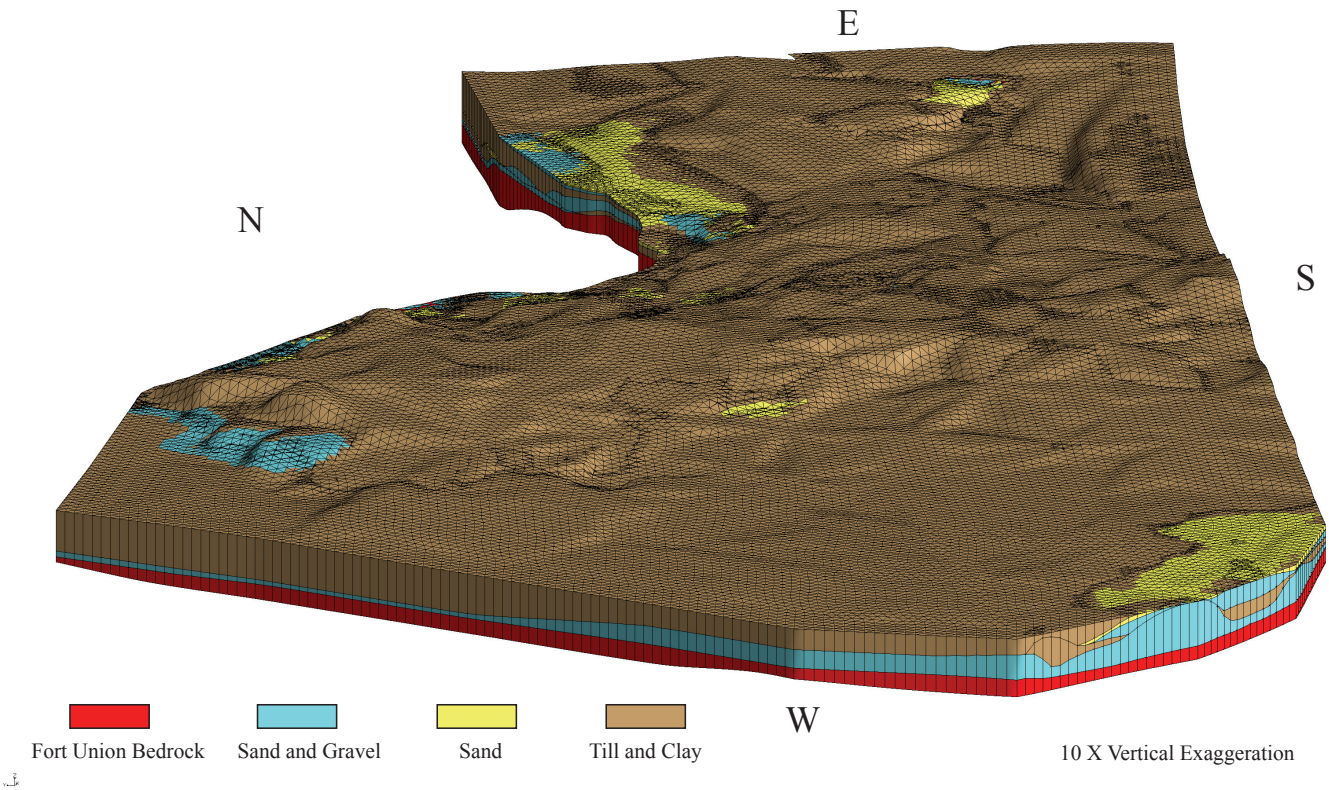

Figure A10. Upper till and clay.

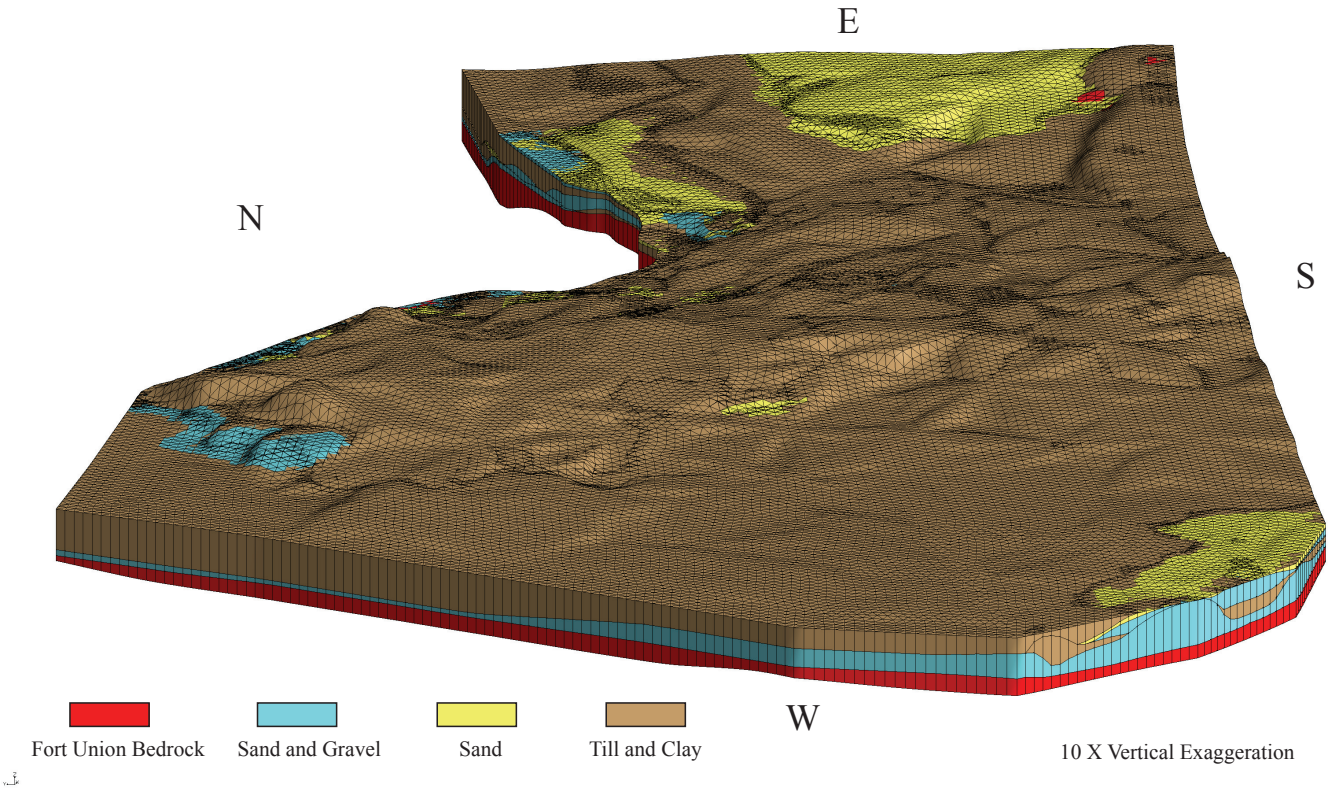

Figure A11. Upper sand in sand hills area.

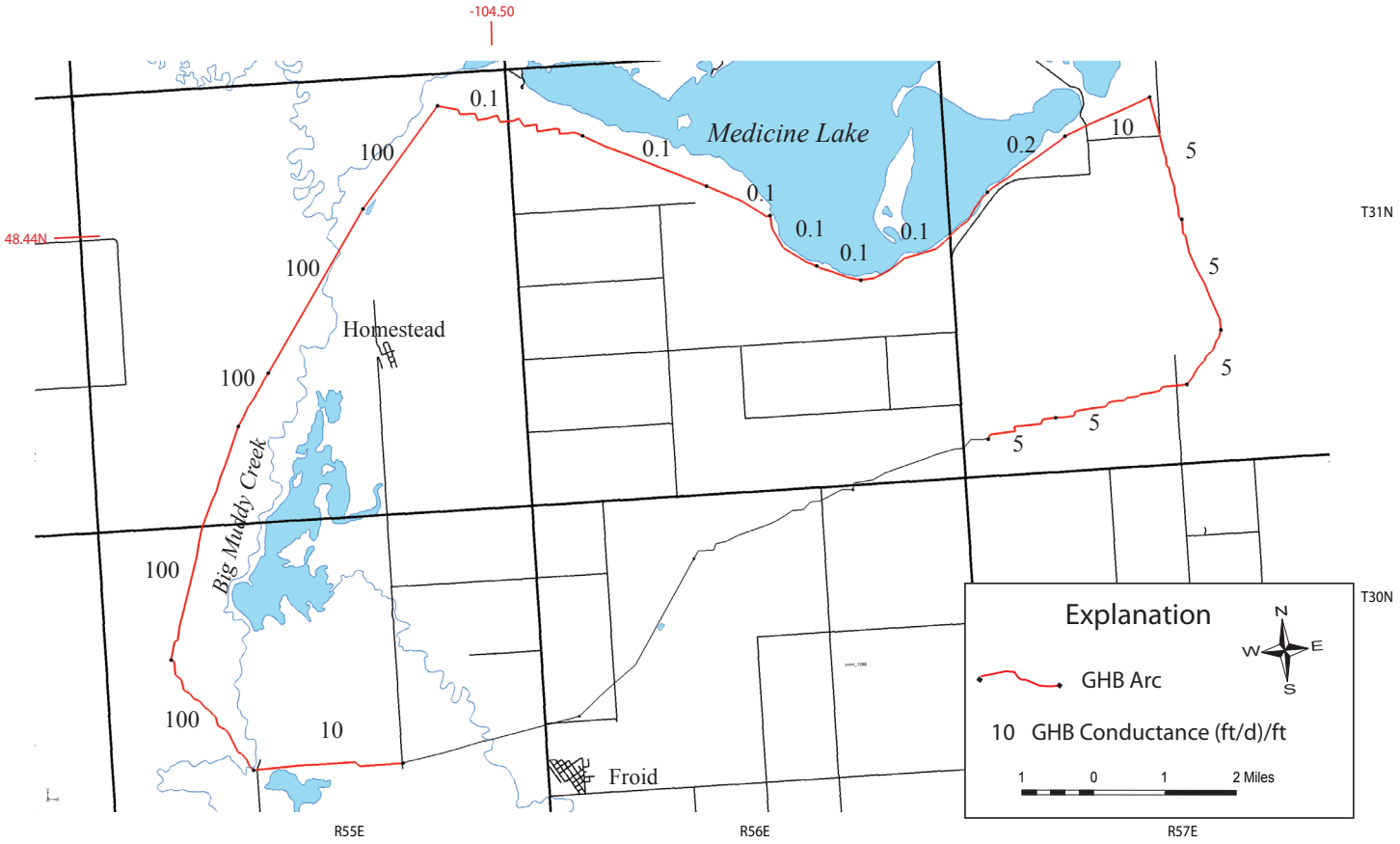

Figure A12. General Head Boundary location and arc conductance, (ft/day)/ft in layers 1–6.

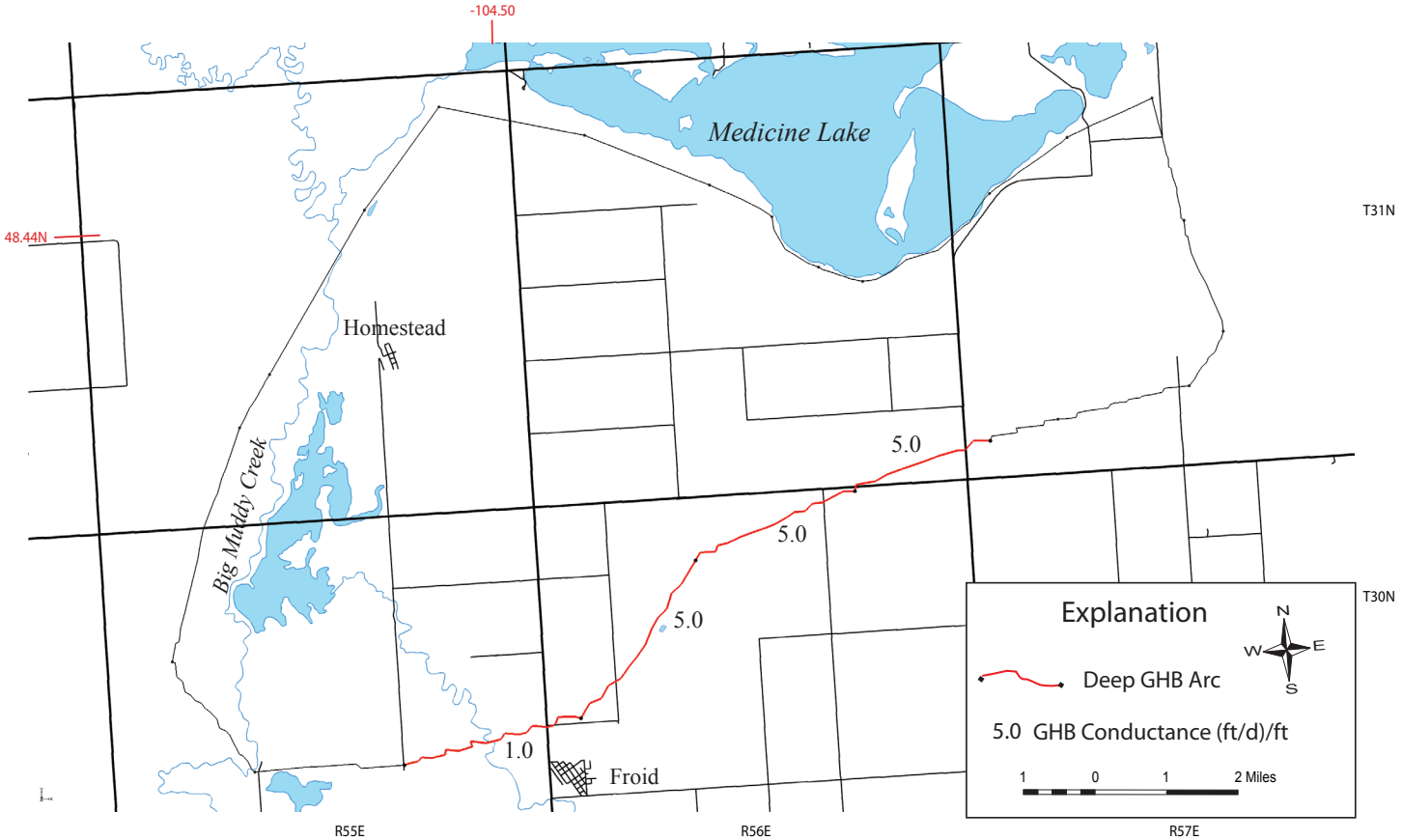

Figure A13. The deep GHB were assigned to layers 4–6 to represent water flow from the Fort Union bedrock along the south boundary of the model.

	PXDP	PETM
1	0.0	1.0
2	0.1	0.5
3	0.4	0.2
4	1.0	0.0
*		

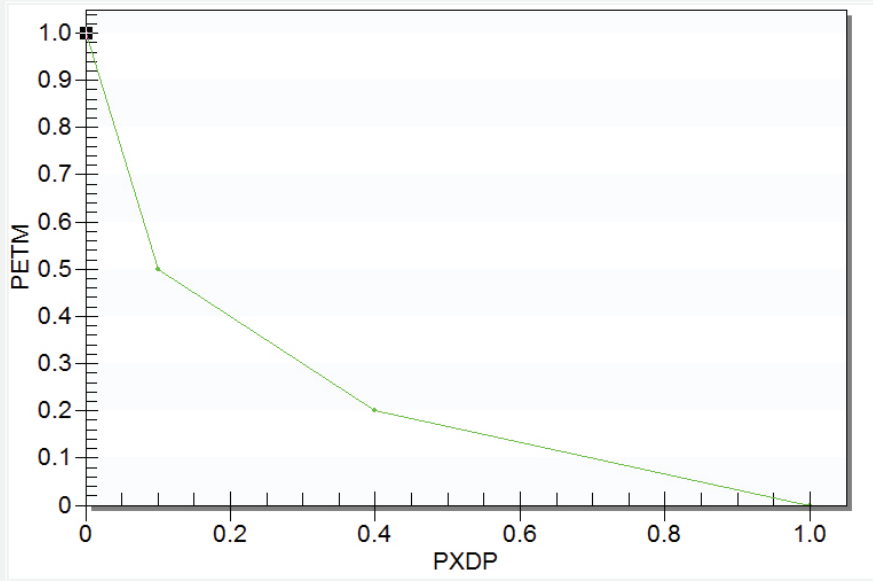

Figure A14. The ETS1 extinction depth curve represents a rapid decline in ET as the head drops below the ET surface.

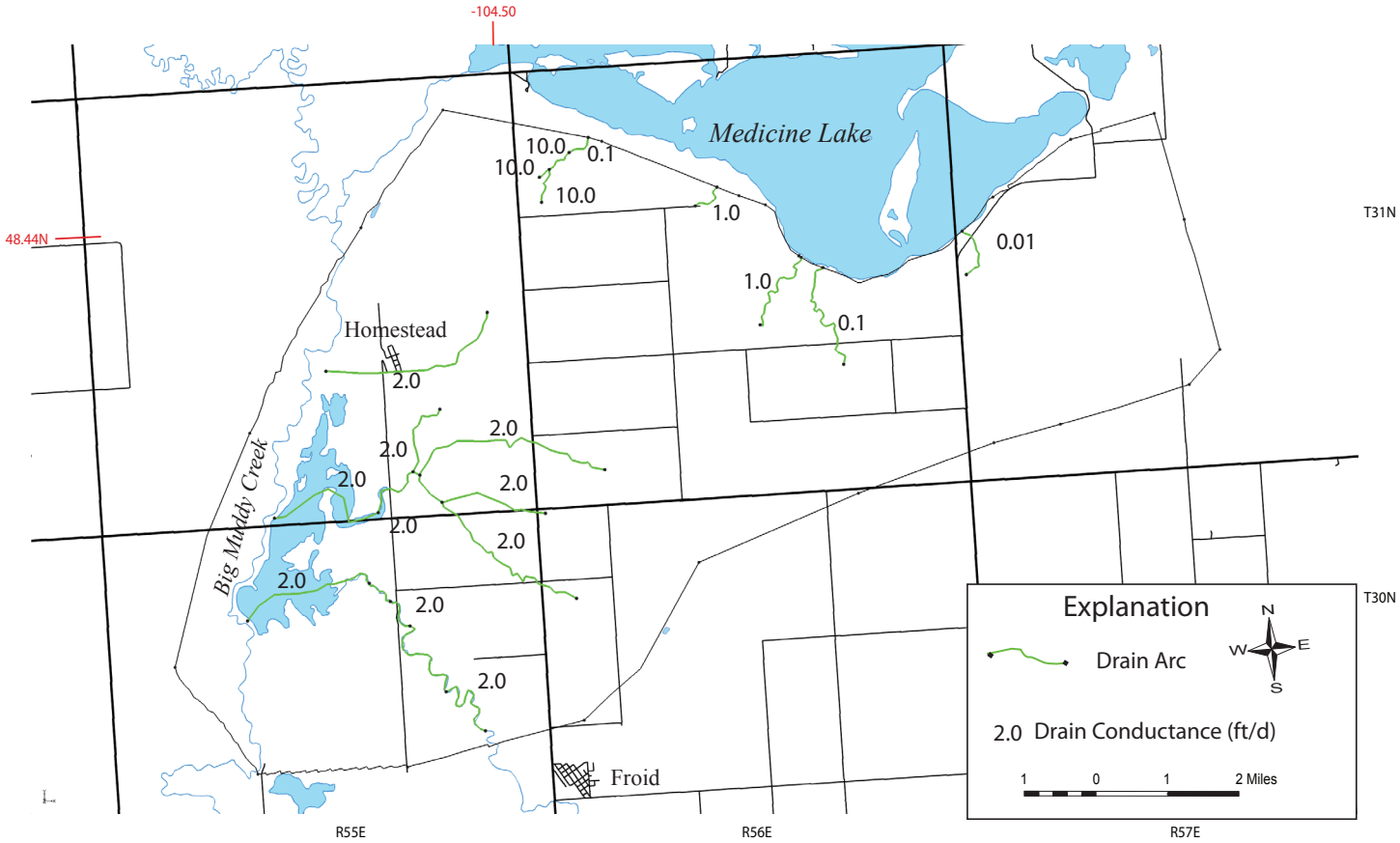

Figure A15. Drain arcs were assigned to layer one at locations where ground water seeps were observed.

Date	Recharge Rate (ft/d)
1/1/15	0.000010
1/15/15	0.000300
2/14/15	0.000700
3/16/15	0.000800
4/15/15	0.000916
5/15/15	0.000050
6/14/15	0.000050
7/14/15	0.000050
8/13/15	0.000050
9/12/15	0.000960
10/12/15	0.000900
11/11/15	0.000327
12/11/15	0.000010
12/31/15	0.000001

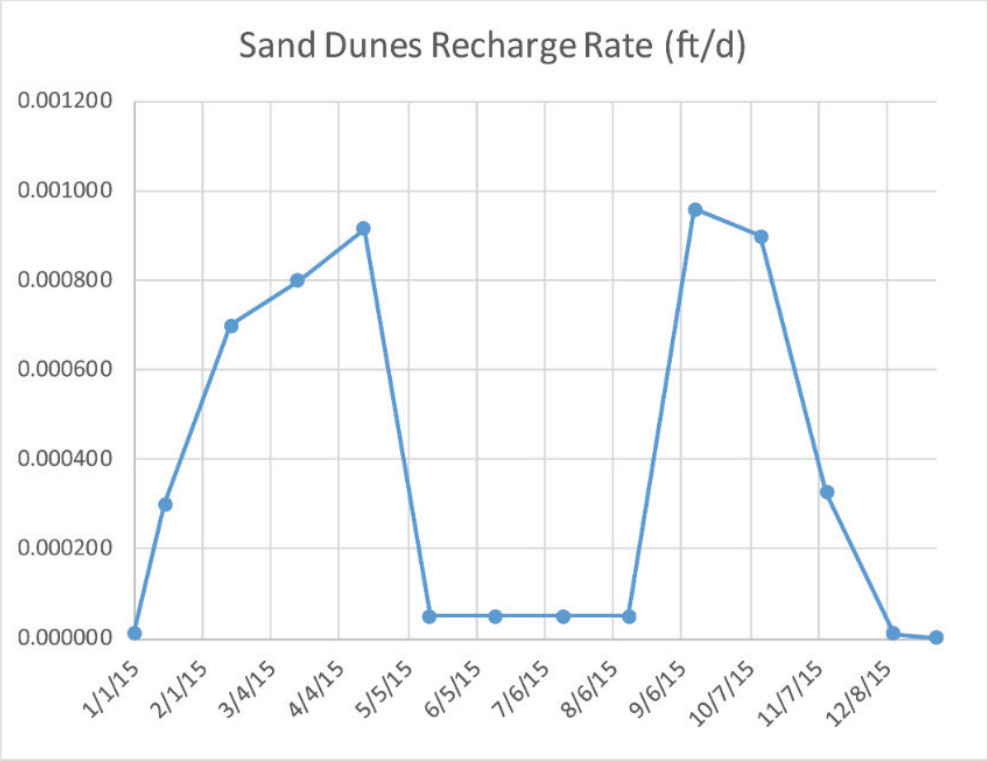

Figure A16. Recharge rates applied to the sand dunes recharge area reflects spring and fall recharge.

Time	Max ETS Rate (ft/d)
1/1/2015 0:00	0
1/30/2015 0:00	0
2/28/2015 0:00	0
3/30/2015 0:00	0.000375
4/30/2015 0:00	0.00075
5/6/2015 0:00	0.0009
5/19/2015 0:00	0.00100125
5/31/2015 0:00	0.0011125
6/15/2015 0:00	0.0012375
6/30/2015 0:00	0.00125
7/15/2015 0:00	0.00155
8/1/2015 0:00	0.001875
8/15/2015 0:00	0.00178125
8/31/2015 0:00	0.00175
9/30/2015 0:00	0.00125
10/30/2015 0:00	1.25E-06
11/30/2015 0:00	0
12/30/2015 0:00	0

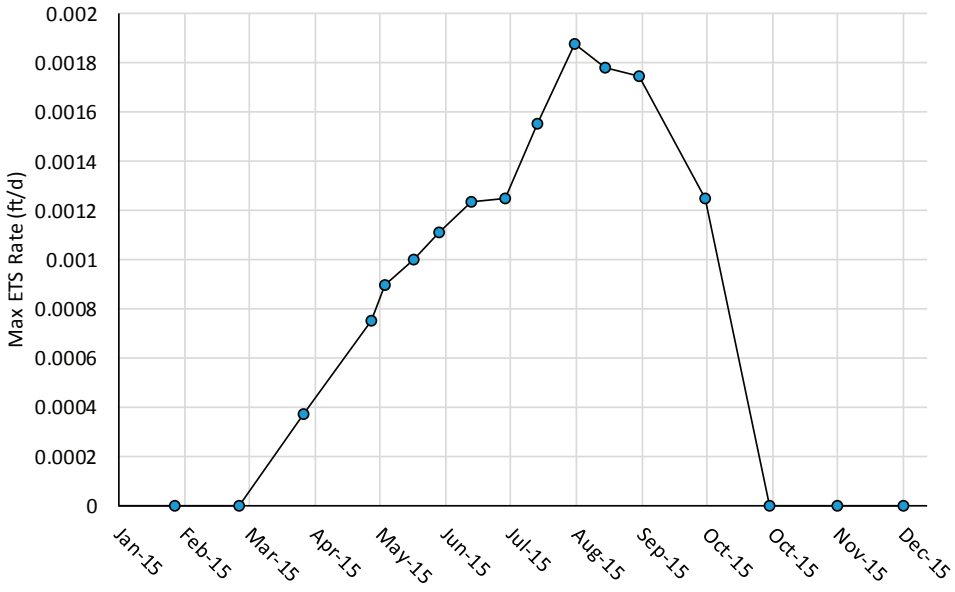

Figure A17. Max ETS rates applied to the Medicine Lake ETS polygon.

Time	Max ETS Rate (ft/d)
1/1/2015 0:00	0
1/15/2015 0:00	0
2/15/2015 0:00	0
3/18/2015 0:00	0.0012
4/18/2015 0:00	0.00245
5/19/2015 0:00	0.0045
6/19/2015 0:00	0.0095
7/20/2015 0:00	0.014
8/20/2015 0:00	0.019
9/20/2015 0:00	0.019
10/21/2015 0:00	0.0048
11/21/2015 0:00	0
12/22/2015 0:00	0
12/30/2015 0:00	0
12/30/2015 0:00	0

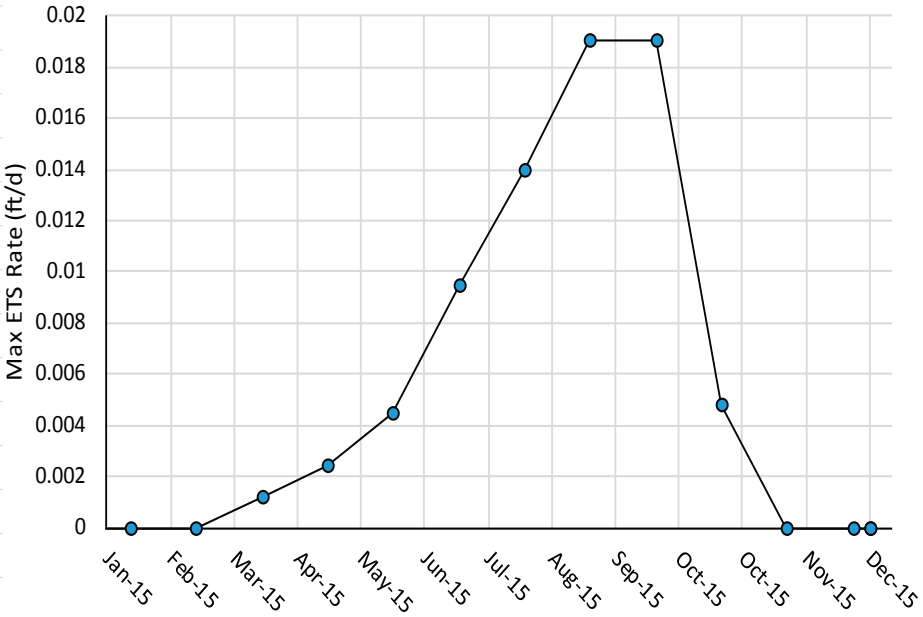

Figure A18. Max ETS rates assigned to the Big Muddy ET polygon.

Table A2. Stress period and time step schedule.

Start Time	Length (days)	No. of Time Steps	Start Time	Length (days)	No. of Time Steps
1/1/2015	29	1	7/1/2015	1	1
1/30/2015	29	1	7/2/2015	1	1
2/28/2015	30	1	7/3/2015	1	1
3/30/2015	31	1	7/4/2015	1	1
4/30/2015	1	1	7/5/2015	1	1
5/1/2015	1	1	7/6/2015	1	1
5/2/2015	1	1	7/7/2015	1	1
5/3/2015	1	1	7/8/2015	1	1
5/4/2015	1	1	7/9/2015	1	1
5/5/2015	1	1	7/10/2015	1	1
5/6/2015	1	1	7/11/2015	1	1
5/7/2015	1	1	7/12/2015	1	1
5/8/2015	1	1	7/13/2015	1	1
5/9/2015	1	1	7/14/2015	1	1
5/10/2015	1	1	7/15/2015	1	1
5/11/2015	1	1	7/16/2015	1	1
5/12/2015	1	1	7/17/2015	1	1
5/13/2015	1	1	7/18/2015	1	1
5/14/2015	1	1	7/19/2015	1	1
5/15/2015	1	1	7/20/2015	1	1
5/16/2015	1	1	7/21/2015	1	1
5/17/2015	1	1	7/22/2015	1	1
5/18/2015	1	1	7/23/2015	1	1

Table A2—*Continued*.

Start Time	Length (days)	No. of Time Steps	Start Time	Length (days)	No. of Time Steps
5/19/2015	1	1	7/24/2015	1	1
5/20/2015	1	1	7/25/2015	1	1
5/21/2015	1	1	7/26/2015	1	1
5/22/2015	1	1	7/27/2015	1	1
5/23/2015	1	1	7/28/2015	1	1
5/24/2015	1	1	7/29/2015	1	1
5/25/2015	1	1	7/30/2015	1	1
5/26/2015	1	1	7/31/2015	1	1
5/27/2015	1	1	8/1/2015	1	1
5/28/2015	1	1	8/2/2015	1	1
5/29/2015	1	1	8/3/2015	1	1
5/30/2015	1	1	8/4/2015	1	1
5/31/2015	1	1	8/5/2015	1	1
6/1/2015	1	1	8/6/2015	1	1
6/2/2015	1	1	8/7/2015	1	1
6/3/2015	1	1	8/8/2015	1	1
6/4/2015	1	1	8/9/2015	1	1
6/5/2015	1	1	8/10/2015	1	1
6/6/2015	1	1	8/11/2015	1	1
6/7/2015	1	1	8/12/2015	1	1
6/8/2015	1	1	8/13/2015	1	1
6/9/2015	1	1	8/14/2015	1	1
6/10/2015	1	1	8/15/2015	1	1
6/11/2015	1	1	8/16/2015	1	1
6/12/2015	1	1	8/17/2015	1	1
6/13/2015	1	1	8/18/2015	1	1
6/14/2015	1	1	8/19/2015	1	1
6/15/2015	1	1	8/20/2015	1	1
6/16/2015	1	1	8/21/2015	1	1
6/17/2015	1	1	8/22/2015	1	1
6/18/2015	1	1	8/23/2015	1	1
6/19/2015	1	1	8/24/2015	1	1
6/20/2015	1	1	8/25/2015	1	1
6/21/2015	1	1	8/26/2015	1	1
6/22/2015	1	1	8/27/2015	1	1
6/23/2015	1	1	8/28/2015	1	1
6/24/2015	1	1	8/29/2015	1	1
6/25/2015	1	1	8/30/2015	1	1
6/26/2015	1	1	8/31/2015	30	1
6/27/2015	1	1	9/30/2015	30	1
6/28/2015	1	1	10/30/2015	31	1
6/29/2015	1	1	11/30/2015	30	1
6/30/2015	1	1			

APPENDIX B

MODEL CALIBRATION CHARTS

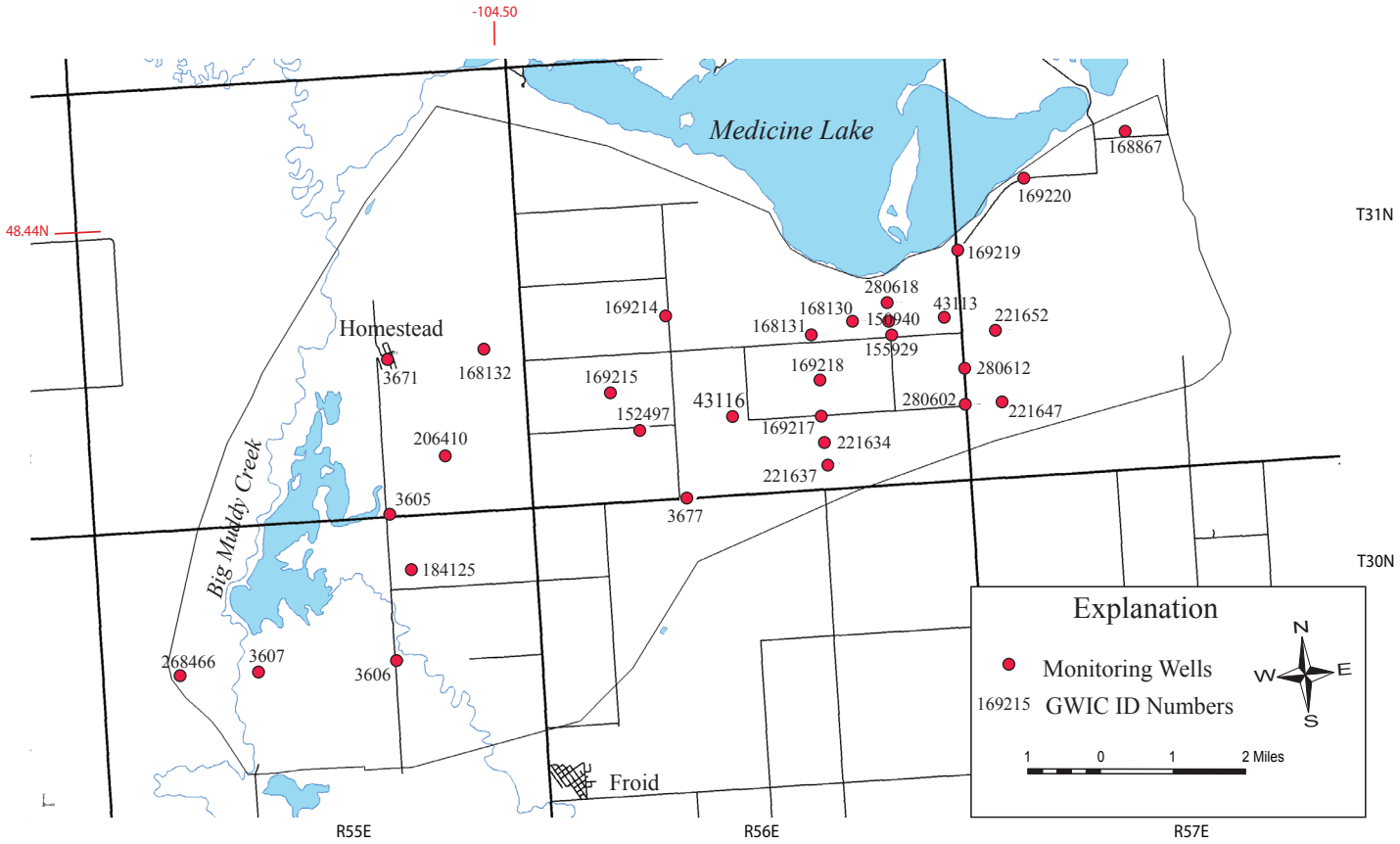

Figure B1. Model observation wells used for calibration with GWIC ID numbers.

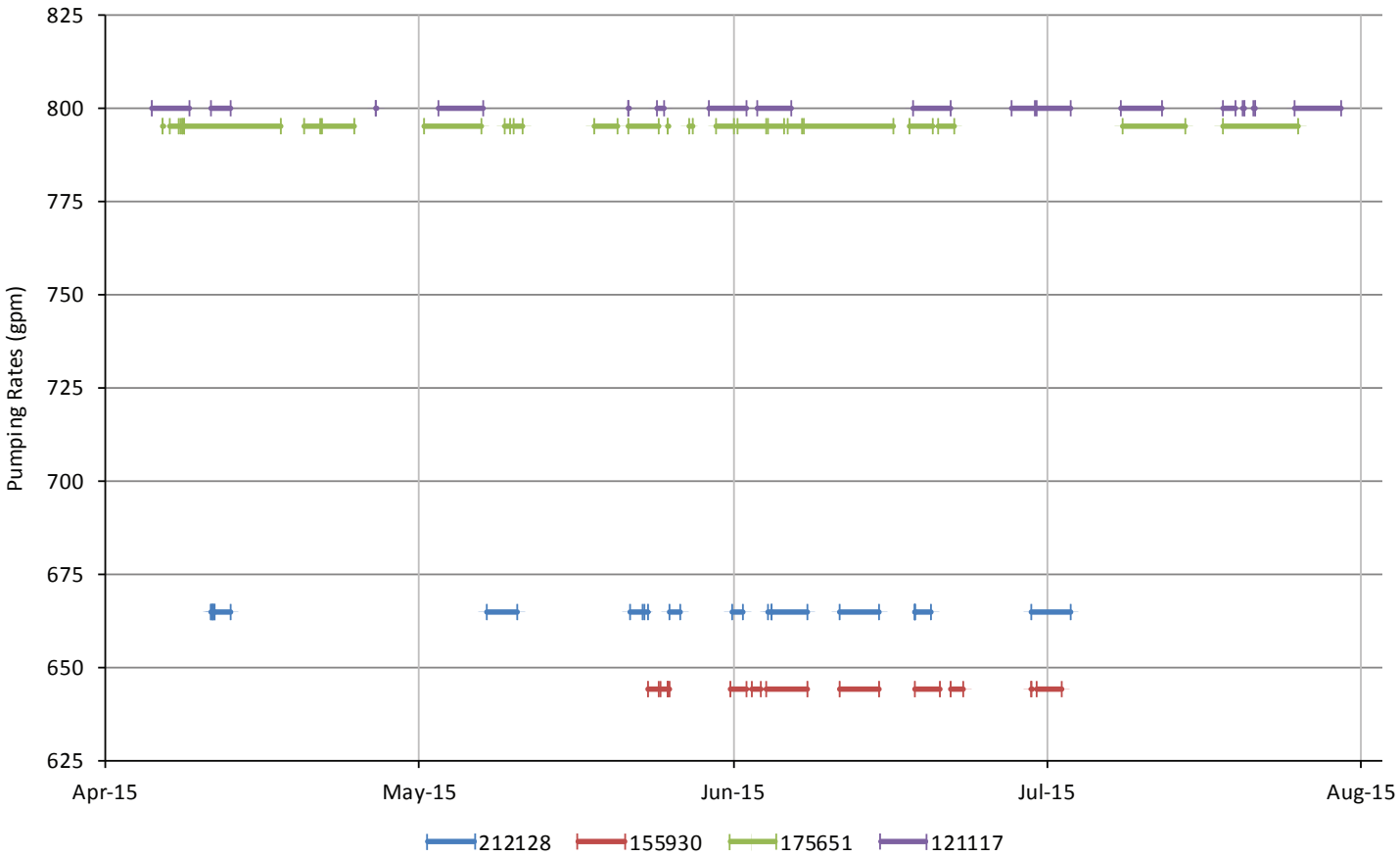

Figure B2. Pumping rates and use timing for the four existing irrigation wells in the model area during the 2015 irrigation season. The wells are listed by their GWIC ID numbers.

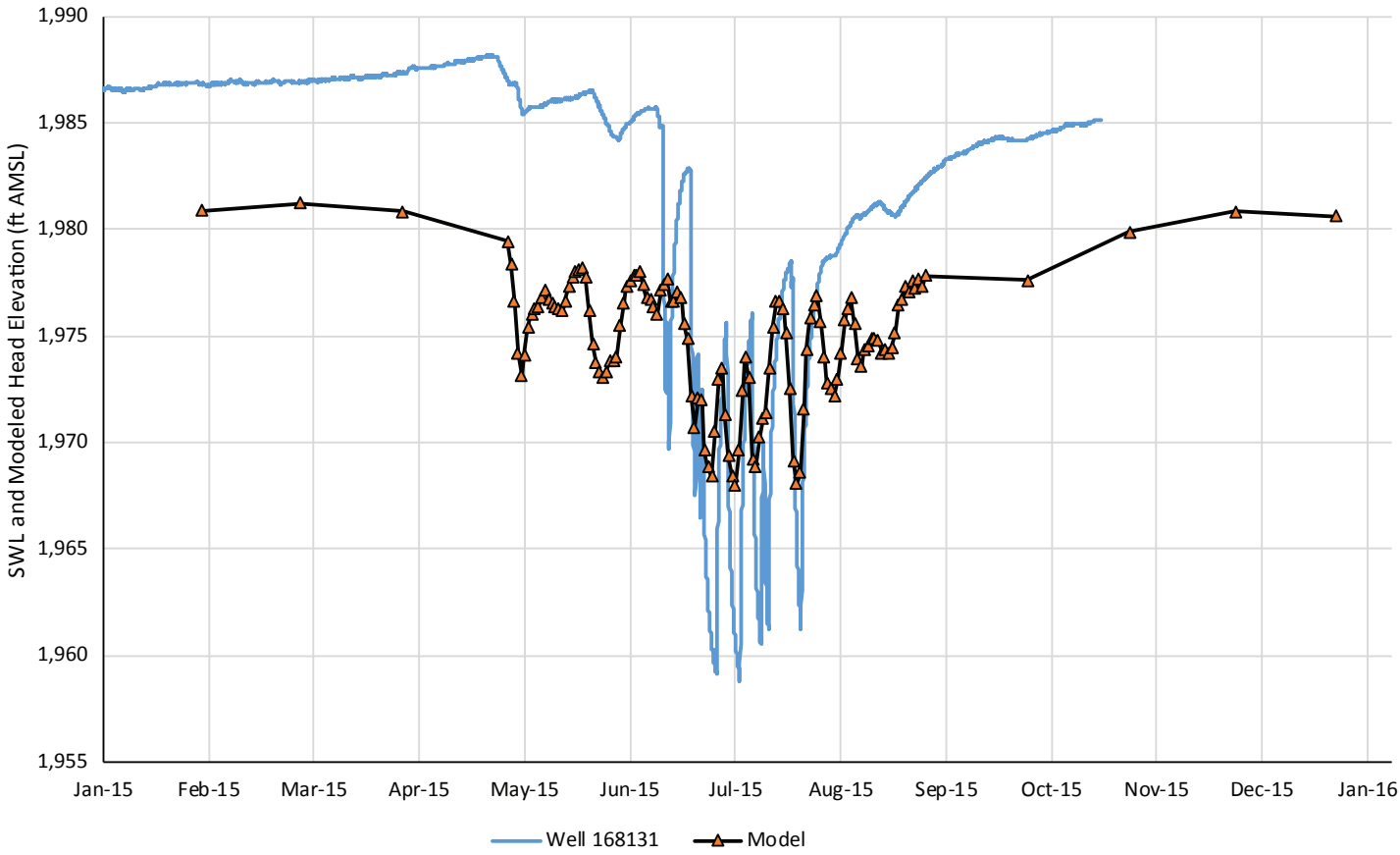

Figure B3. Transient model calibration at well 168131 shows the model response dampened compared to the actual water-level response to pumping.

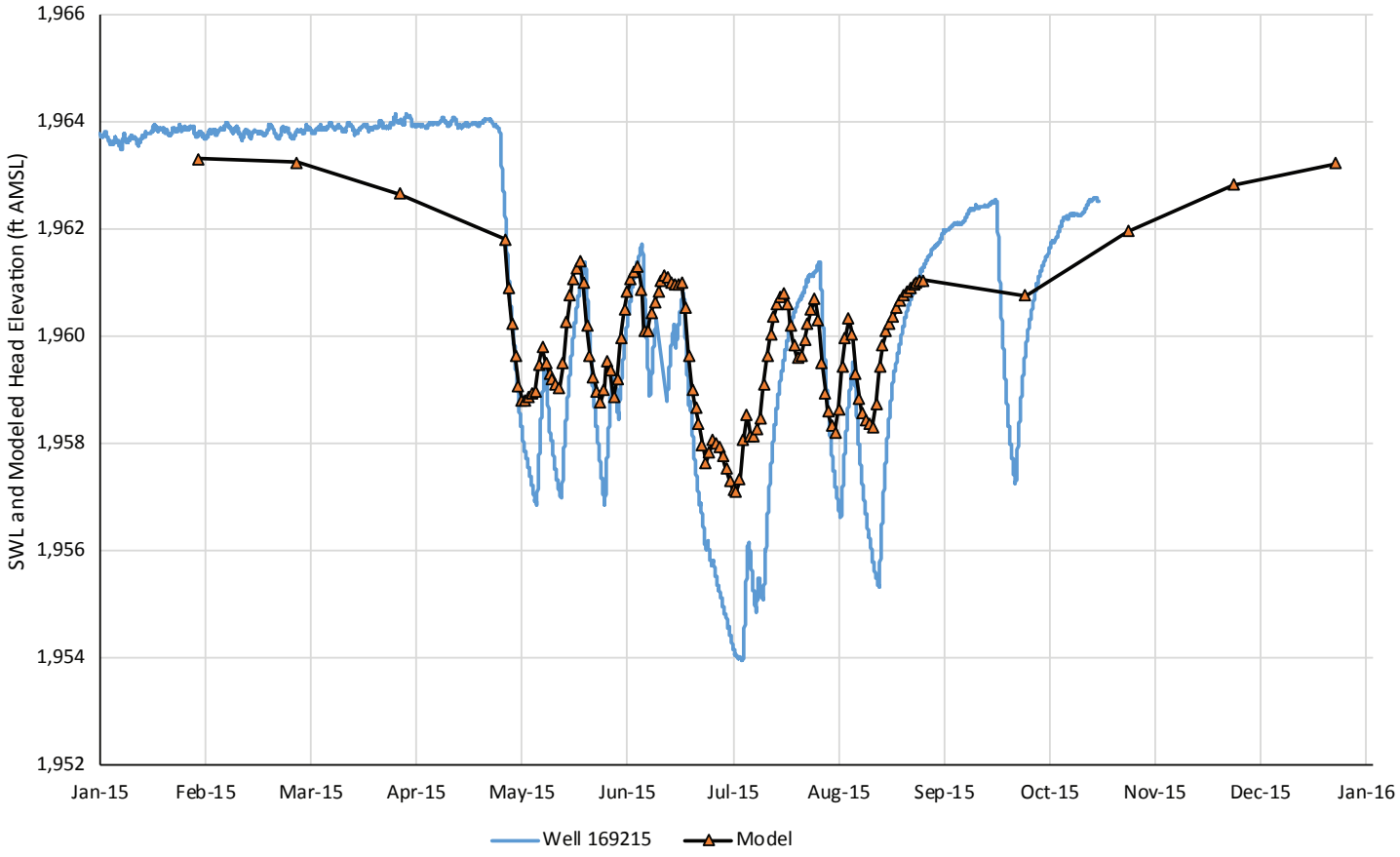

Figure B4. The transient model calibrated closely to 2015 level pumping at well 169215.

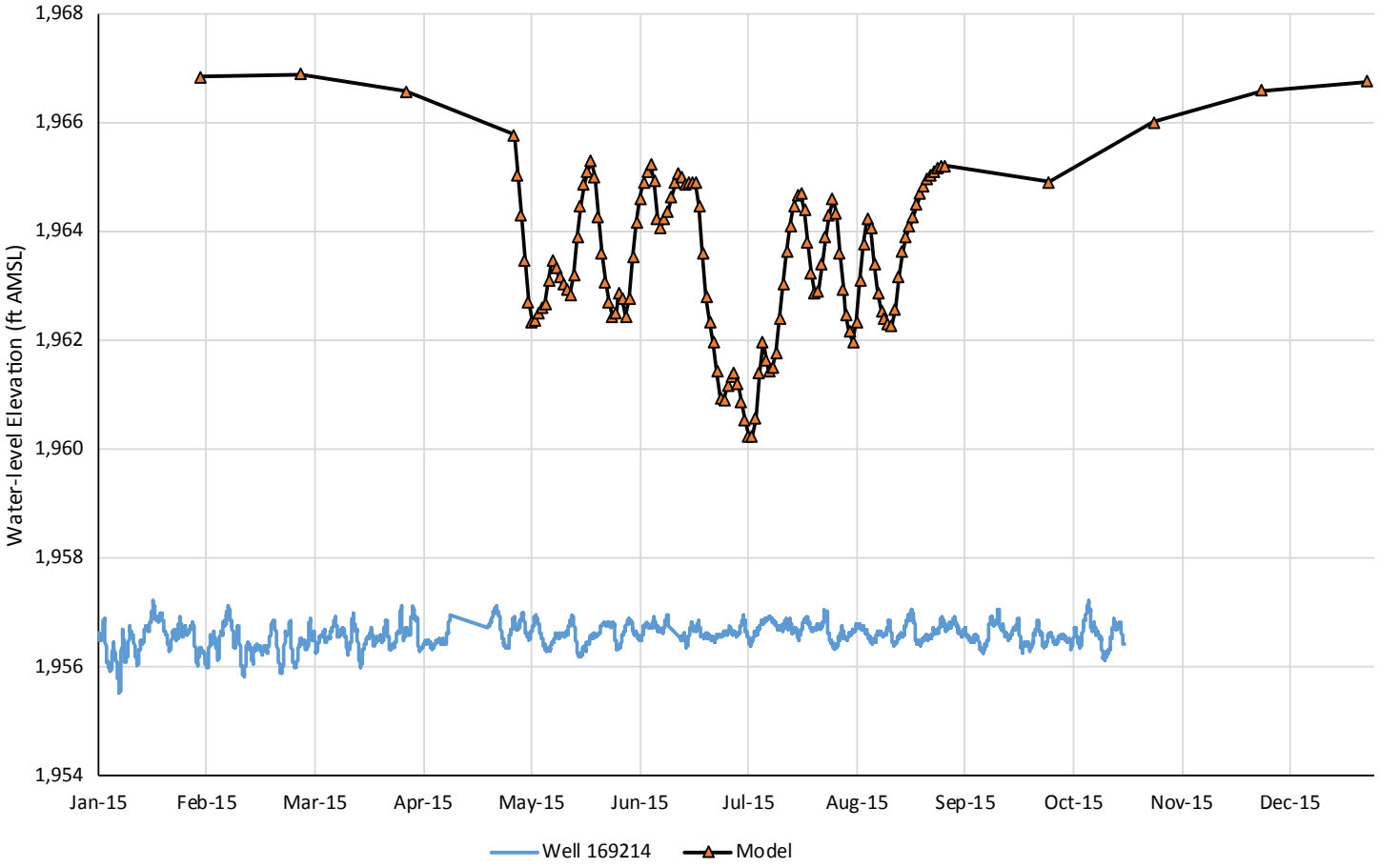

Figure B5. The transient model responded at well location 169214, but the actual well does not respond to irrigation pumping. The well is completed in the upper terrace gravels south of Medicine Lake and not in the Clear Lake aquifer. This shows the model stratigraphy does not adequately isolate the upper terrace aquifer from the Clear Lake aquifer.

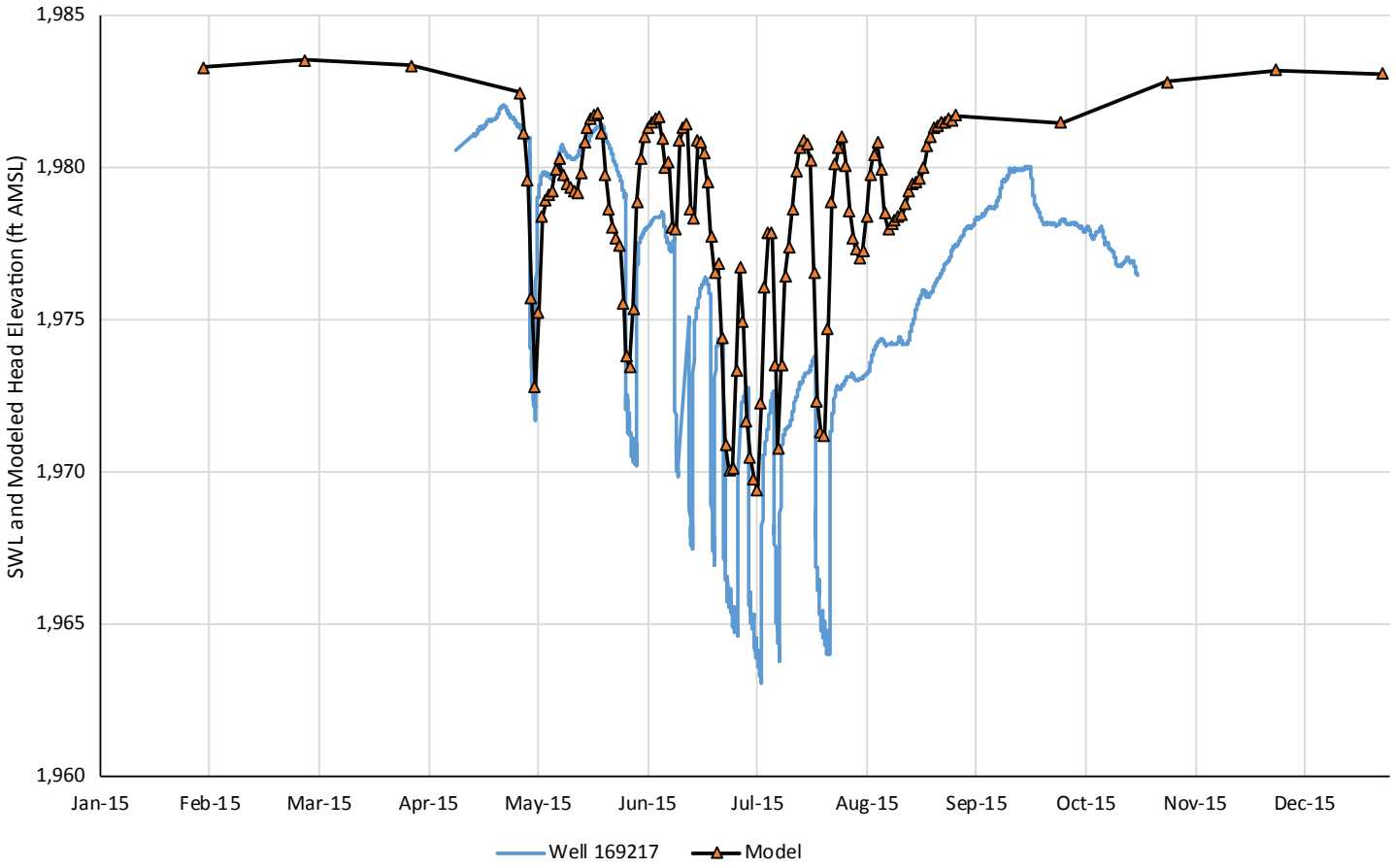

Figure B6. Calibration at well 169217 shows the model matches the drawdown well, but overpredicts aquifer recovery after the irrigation season.

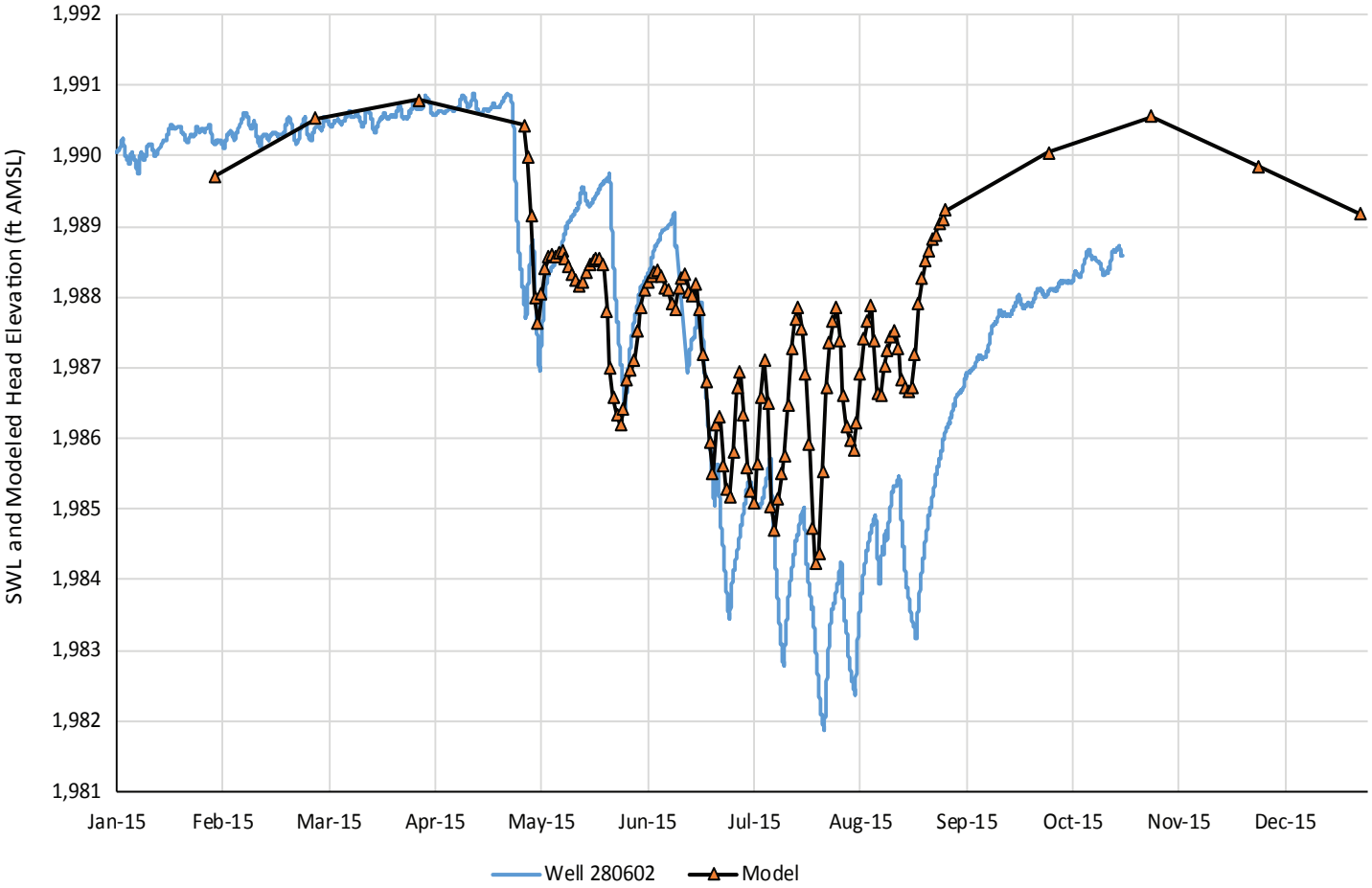

Figure B7. The calibrated transient model matches the early season drawdown but overpredicts aquifer recovery in the late season at well 280602.

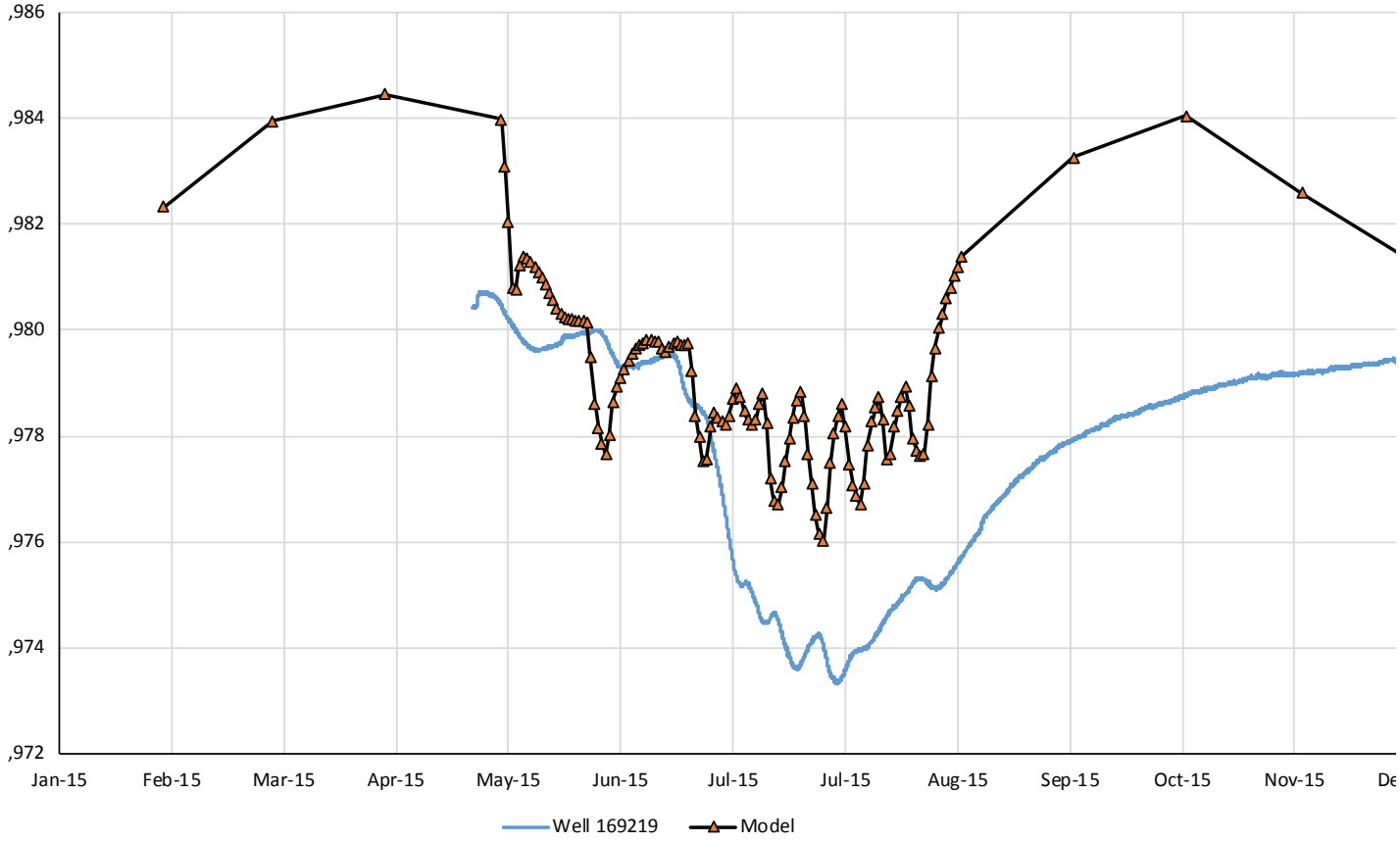

Figure B8. The model response at well 169219 shows the model responds quicker to pumping and recovery than the actual aquifer.

APPENDIX C

MODEL SENSITIVITY CHARTS

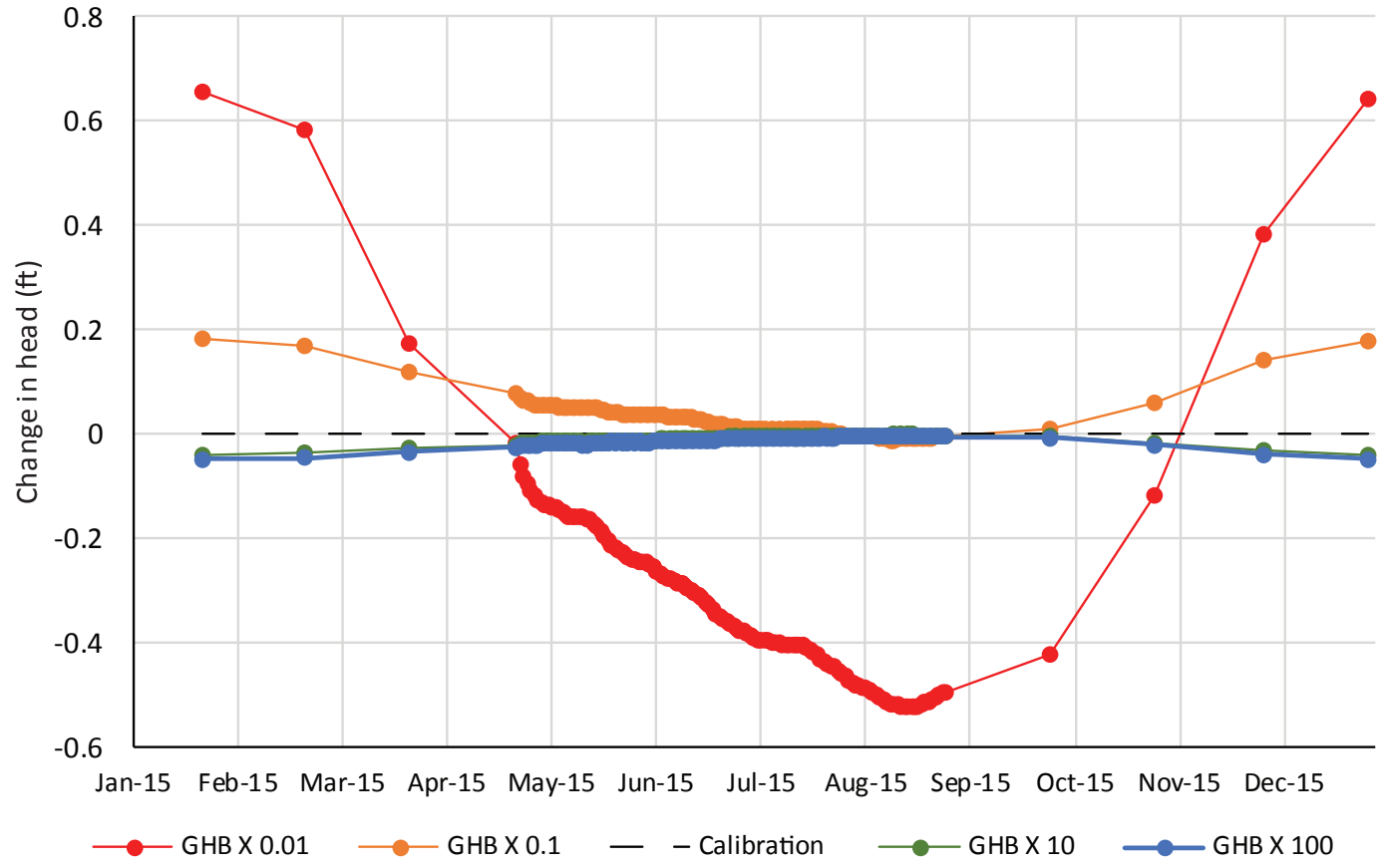

Figure C1. Changes in the GHB conductance only produced small head changes in the Big Muddy Creek area at well 3671 when the value was decreased by two orders of magnitude.

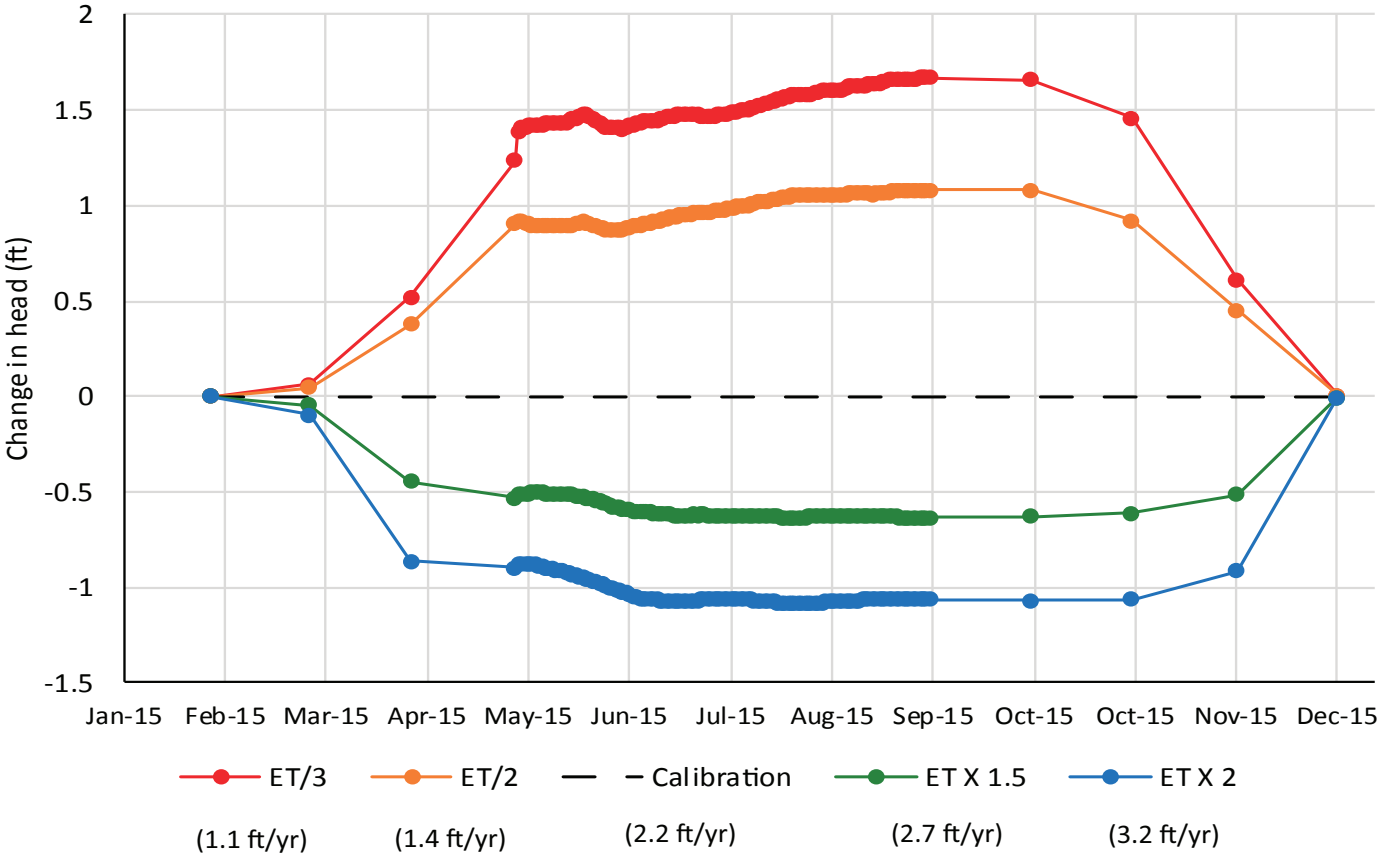

Figure C2. The model heads at cell 8239, layer 1 showed little sensitivity to changes in ET.

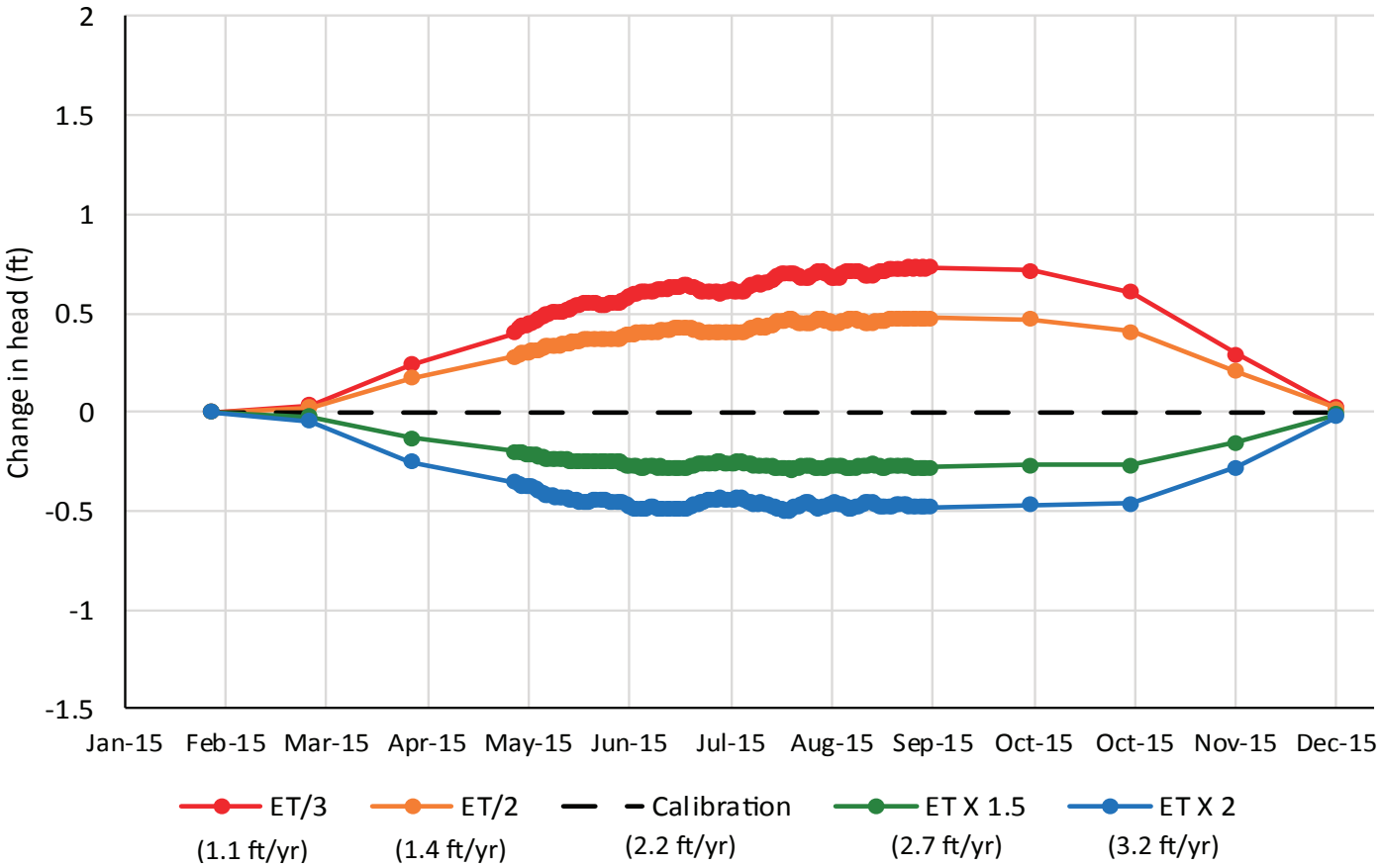

Figure C3. Model heads at cell 83082 in layer 4 showed little sensitivity to changes in ET rates.

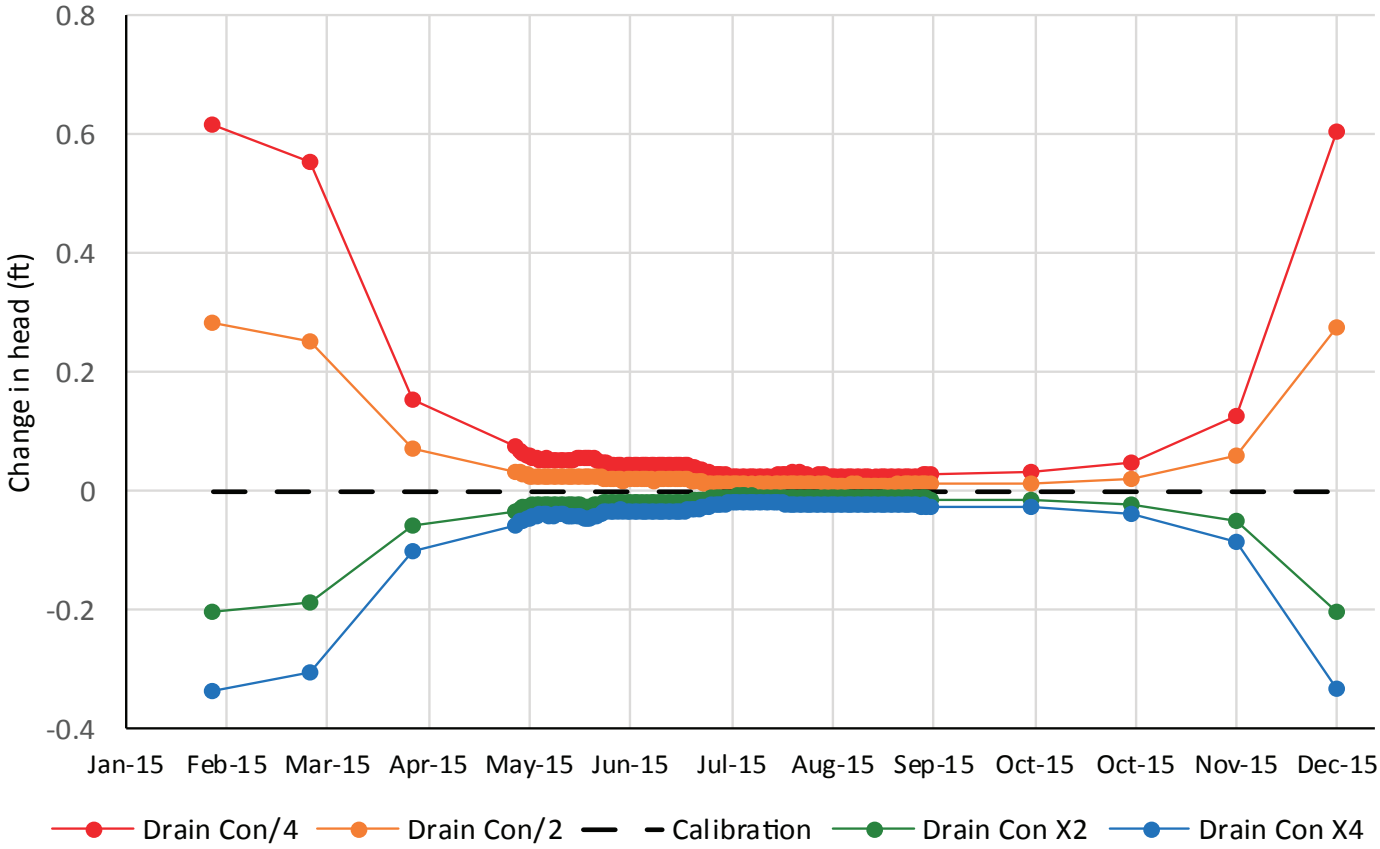

Figure C4. Model heads at cell 8239, layer 1 showed little sensitivity to changes in drain conductance.

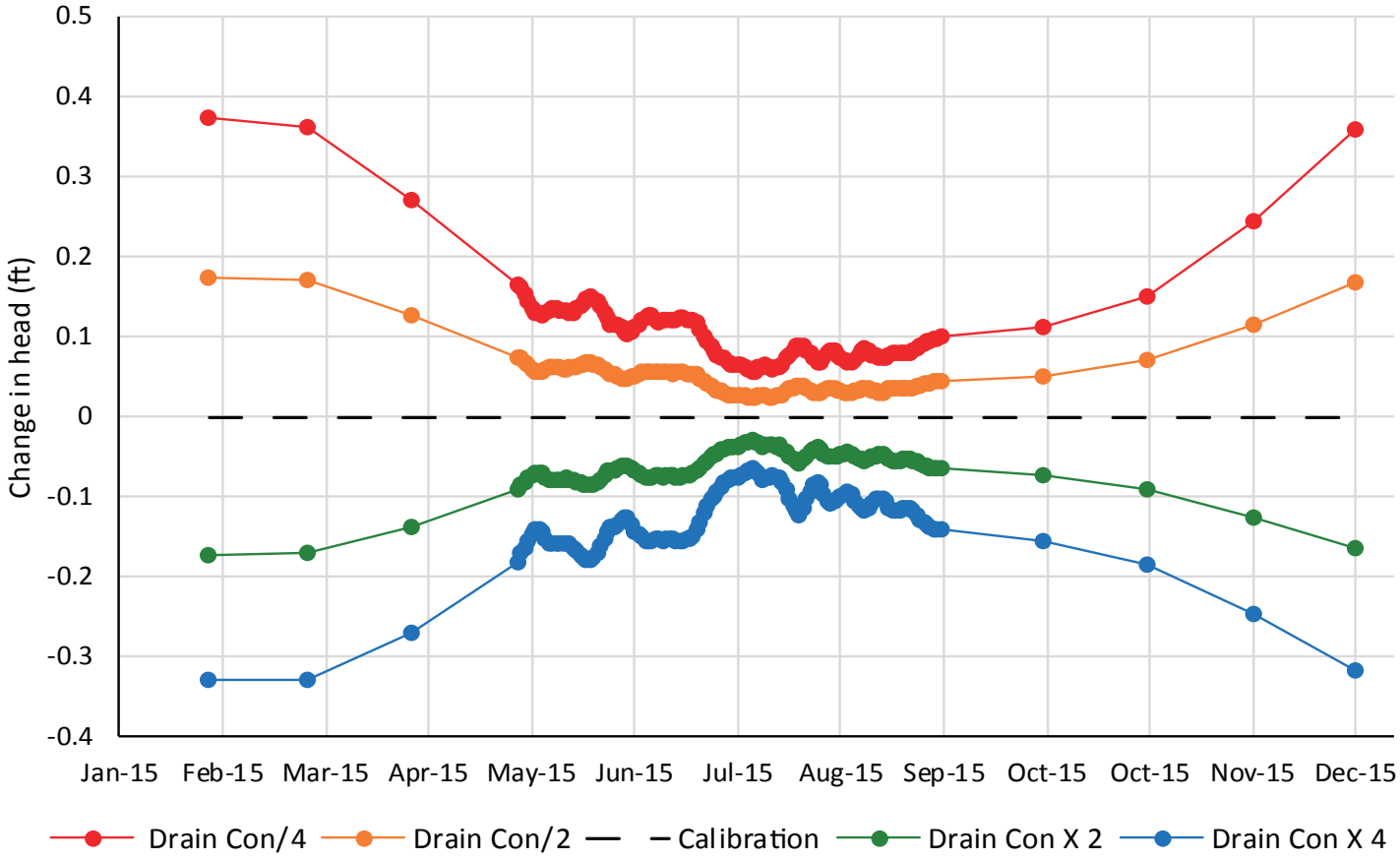

Figure C5. Model heads at cell 83082, layer 4 showed very little sensitivity to changes in drain conductance.

APPENDIX D

MODEL PREDICTIVE SCENARIO RESULTS

Table D1. Comparisons of the increased pumping scenario flow budgets to the flow budget for the 2015 4 well calibrated transient model.

	4 Well 2015 Volume (acre-ft)	4 Well Full Allocation (acre-ft)	Change from 2015 (acre-ft)	Percent Change	8 Well 2015 Volume (acre-ft)	Change from 2015 (acre-ft)	Percent Change	8 Well Full Allocation (acre-ft)	Change from 2015 (acre-ft)	Percent Change
STORAGE IN	152	155	3	1.7%	228	76	49.5%	256	103	67.7%
HEAD DEP BOUNDS IN	10,961	11,674	714	6.5%	11,338	377	3.4%	12,379	1,418	12.9%
RECHARGE IN	1,207	1,207	0	0.0%	1,207	0	0.0%	1,207	0	0.0%
STORAGE OUT	147	150	3	1.7%	222	75	51.0%	248	101	68.3%
HEAD DEP BOUNDS OUT	4,935	4,778	-157	-3.2%	4,832	-103	-2.1%	4,622	-313	-6.3%
WELLS OUT	483	1,500	1,017	210.7%	1,104	621	128.6%	2,585	2,103	435.4%
DRAINS OUT	570	543	-27	-4.8%	547	-23	-4.1%	509	-61	-10.6%
ET OUT	6,191	6106	-85	-1.4%	6,103	-89	-1.4%	5,916	-275	-4.4%

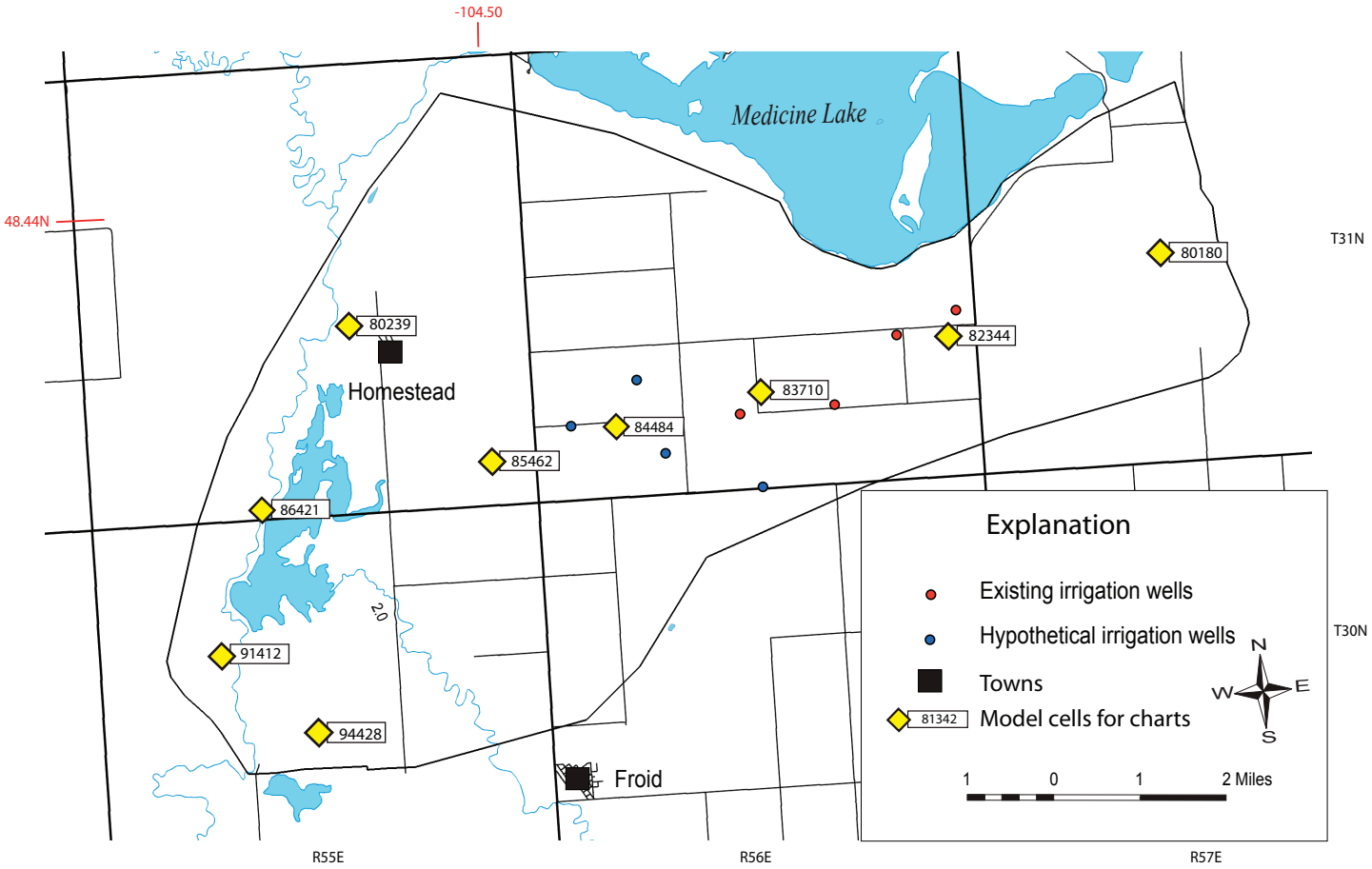

Figure D1. Cell locations used to export model heads for comparison charts. Some of the following charts compare the heads at different locations within the model for a particular simulation. Other charts select a single location to compare the heads for different water-use scenarios. The four existing irrigation wells are shown in red. The blue dots represent hypothetical wells that were added for the increased water-use scenarios.

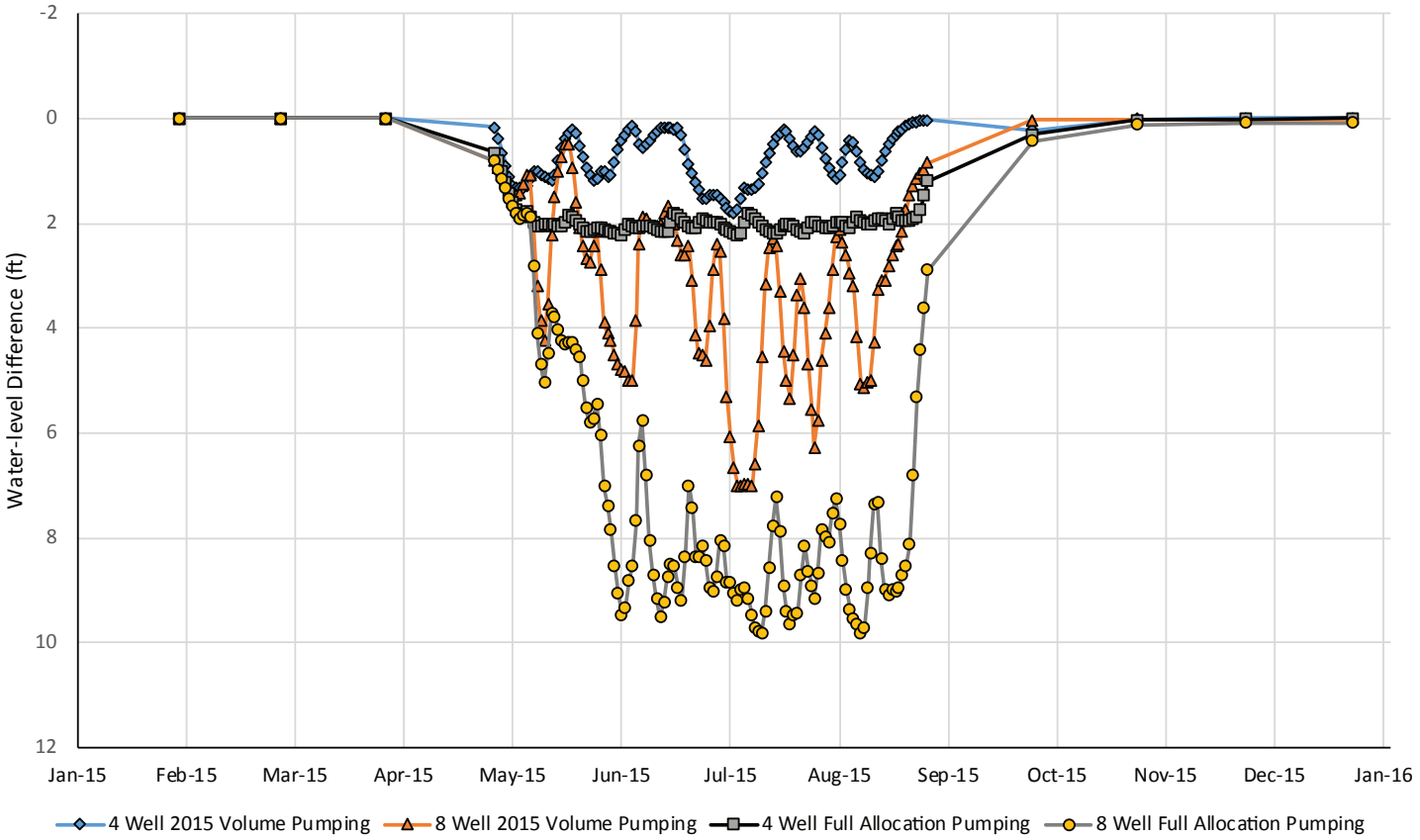

Figure D2. Time-series water-level differences between no irrigation use and the four scenarios, calculated using heads at cell 85462. Cell locations are shown in figure D1.

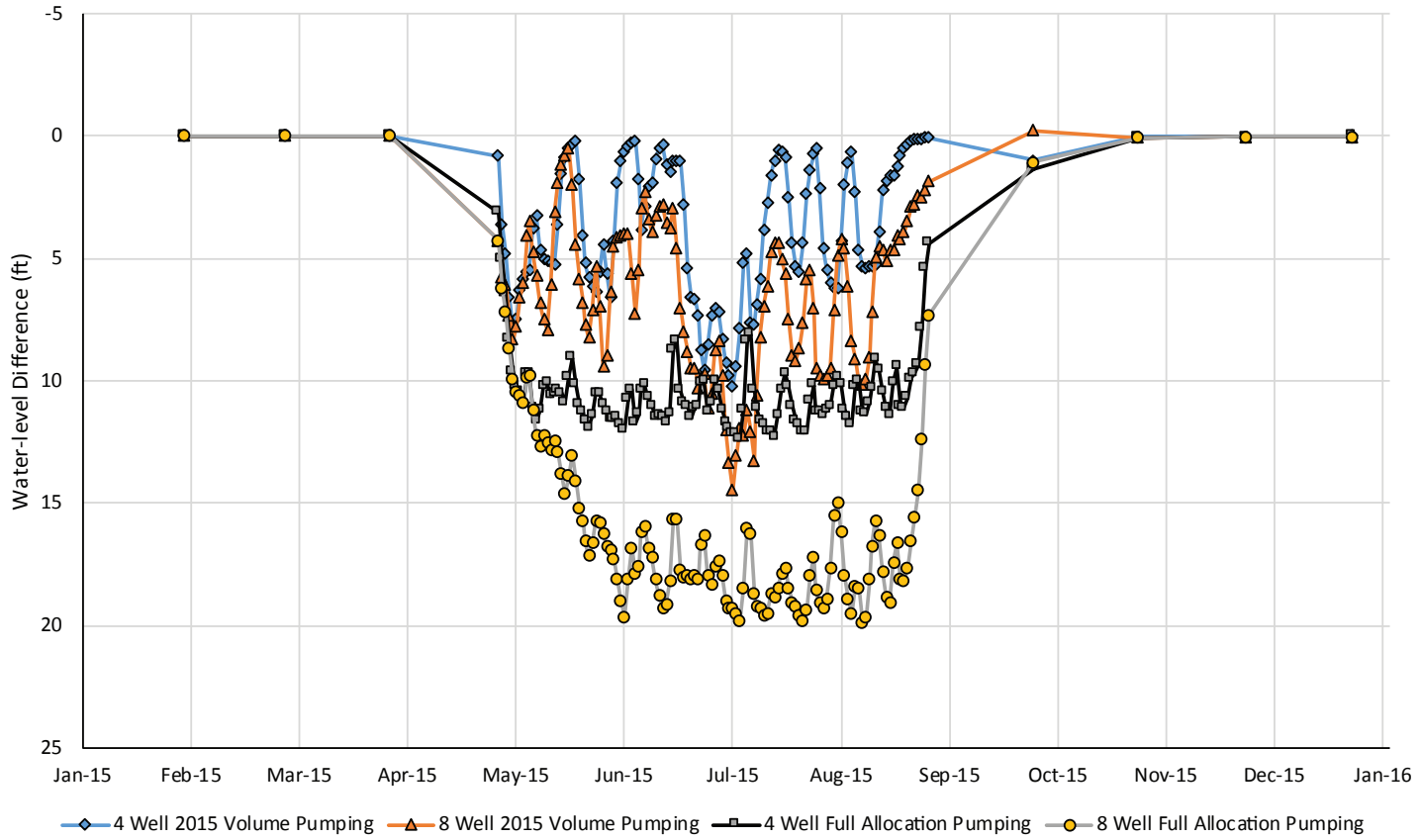

Figure D3. Time-series water-level differences between no irrigation use and the four scenarios calculated using heads at cell 83710. Cell locations are shown in figure D1.

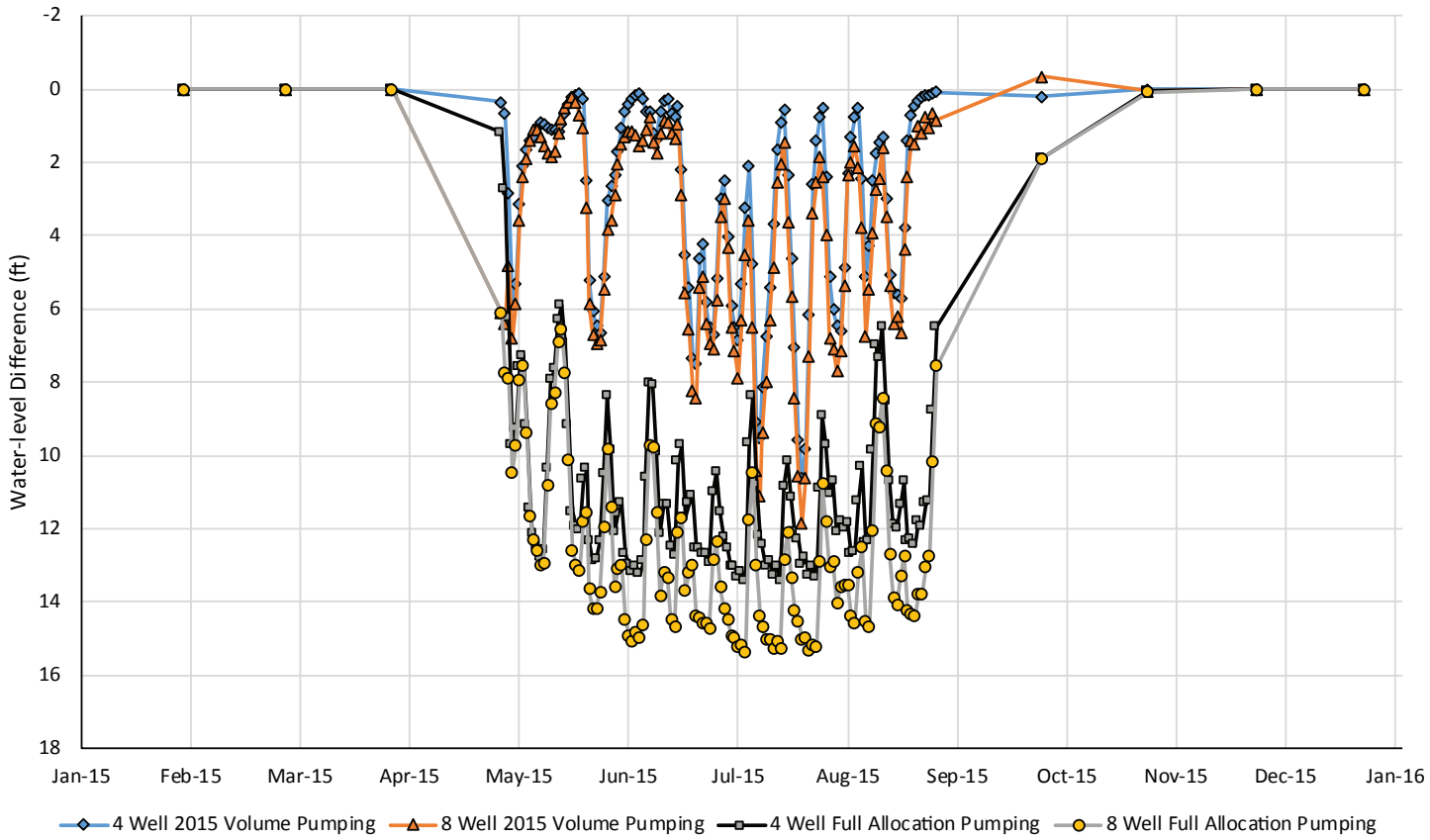

Figure D4. Time-series water-level differences between no irrigation use and the four scenarios calculated using heads at cell 82344. Cell locations are shown in figure D1.

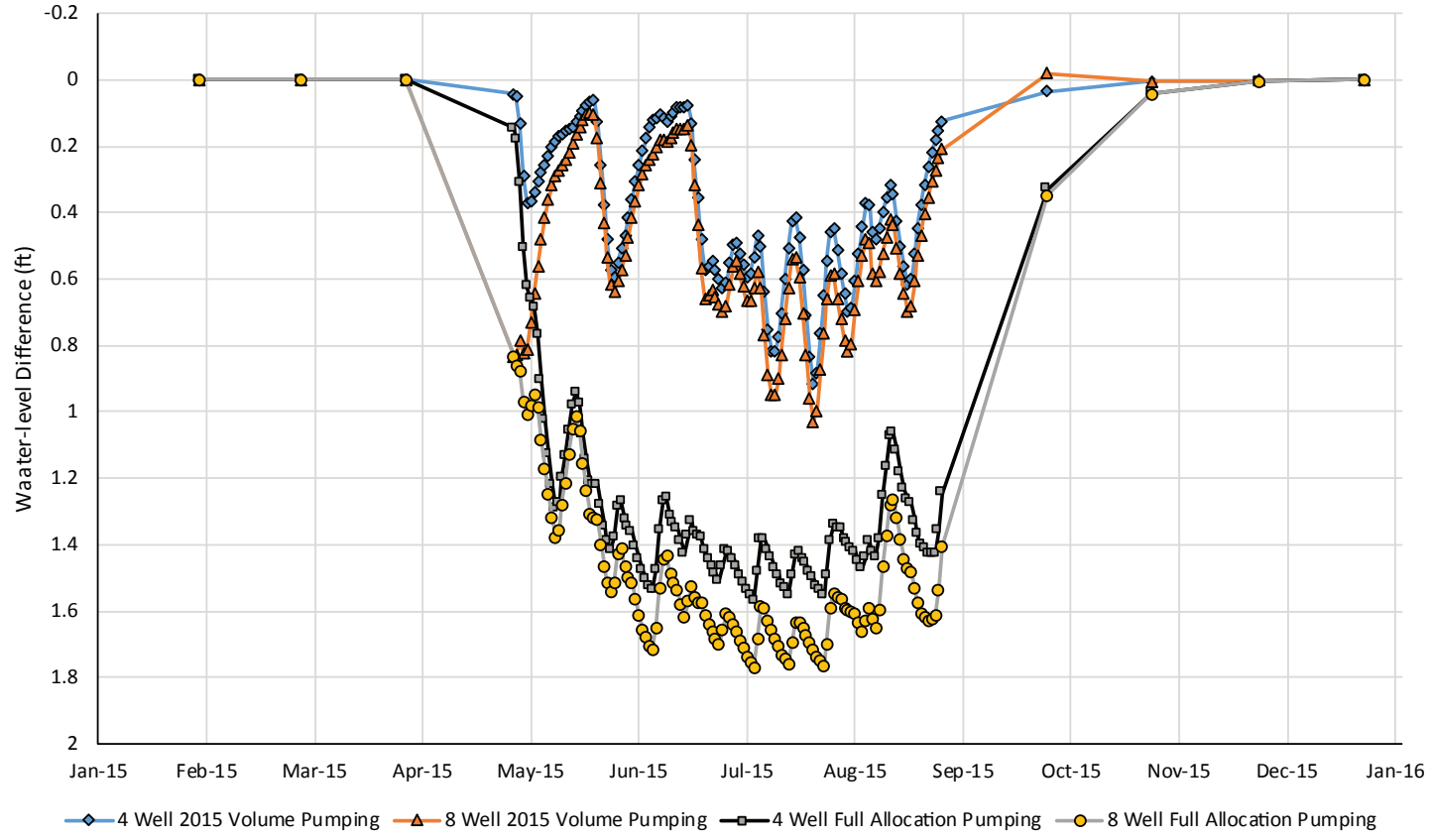

Figure D5. Time-series water-level differences between no irrigation use and the four scenarios calculated using heads at cell 80180. Cell locations are shown in figure D1.

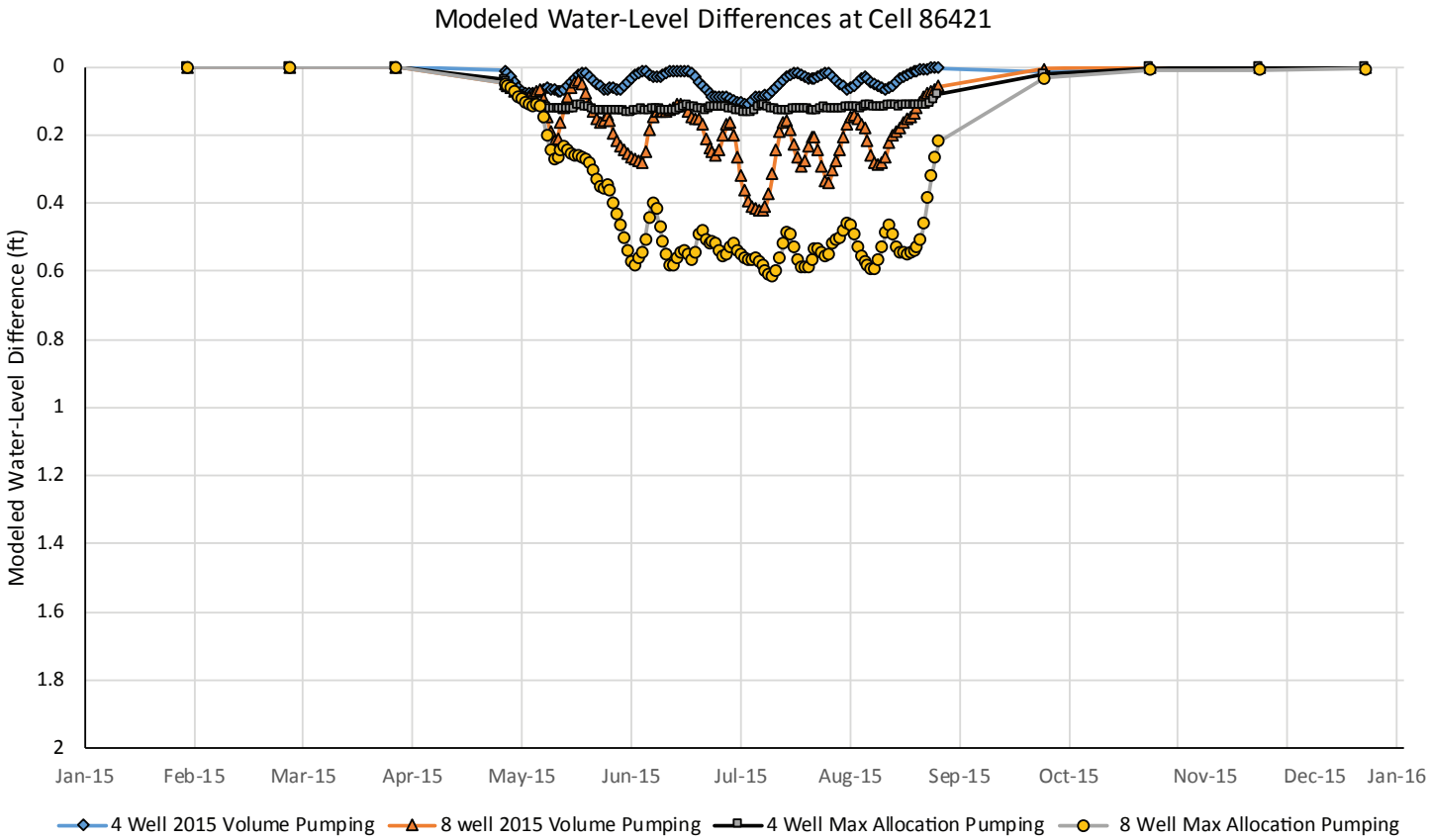

Figure D6. Time-series water-level differences between no irrigation use and the four scenarios calculated using heads at cell 86421. Cell locations are shown in figure D1.

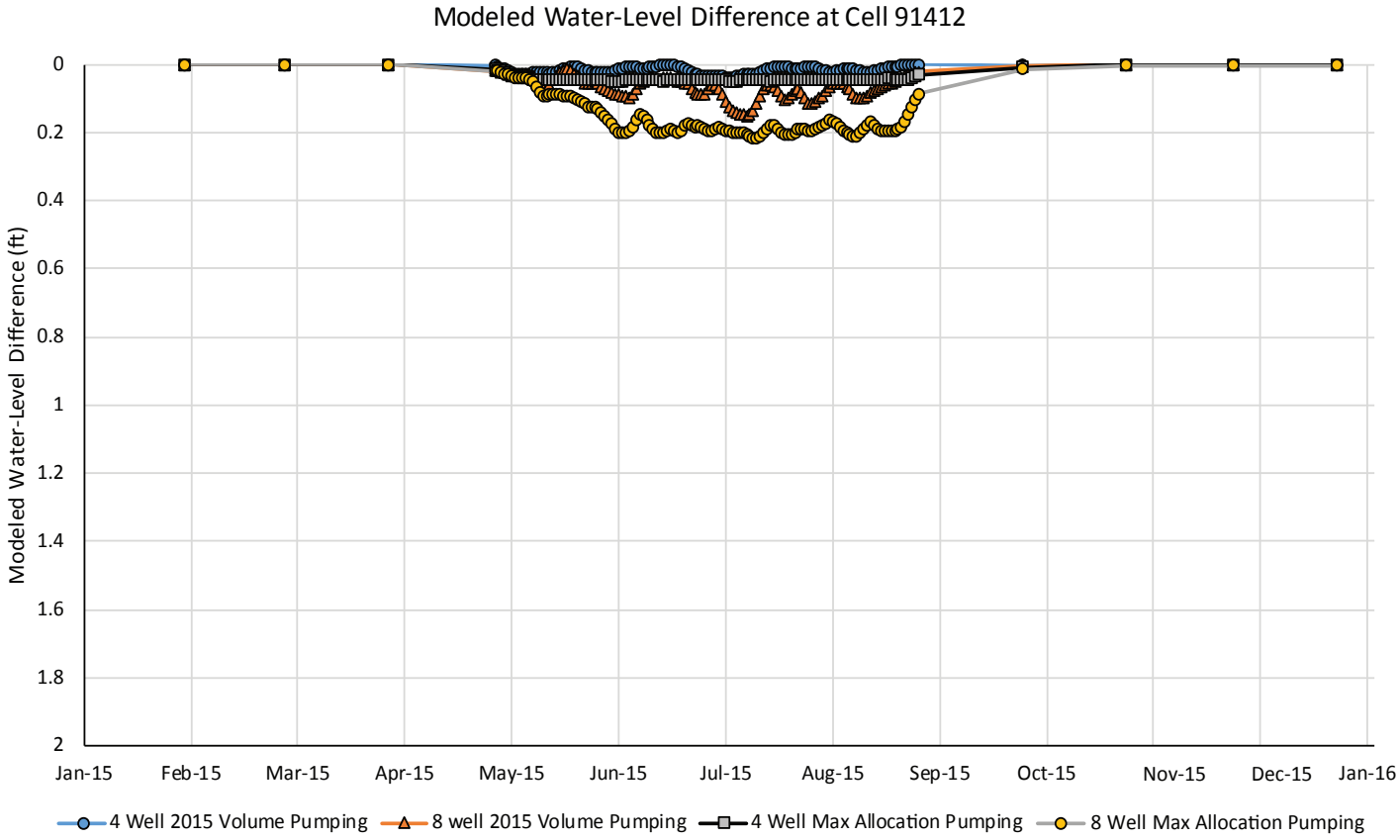

Figure D7. Time-series water-level differences between no irrigation use and the four scenarios calculated using heads at cell 91412. Cell locations are shown in figure D1.

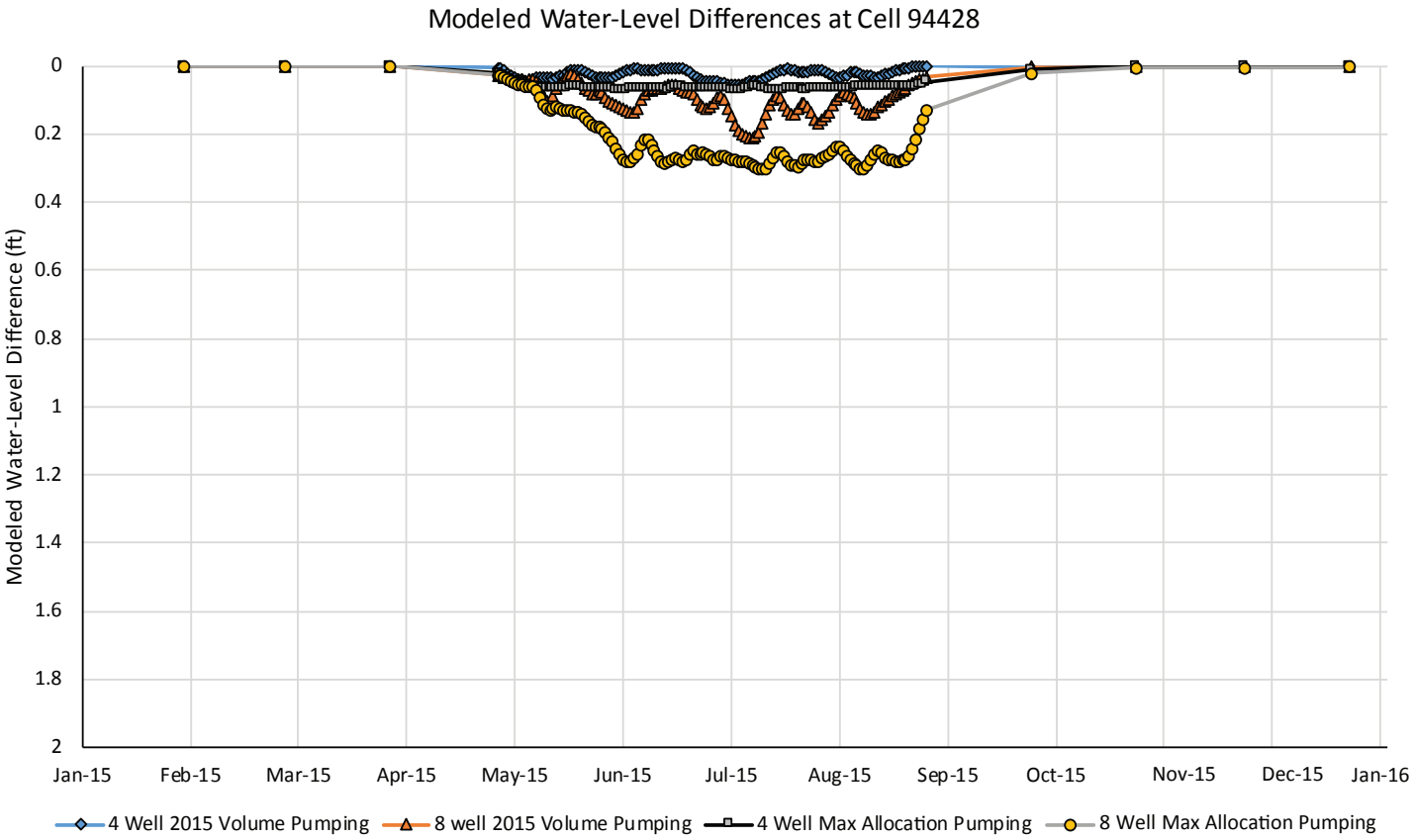

Figure D8. Time-series water-level differences between no irrigation use and the four scenarios calculated using heads at cell 94428. Cell locations are shown in figure D1.

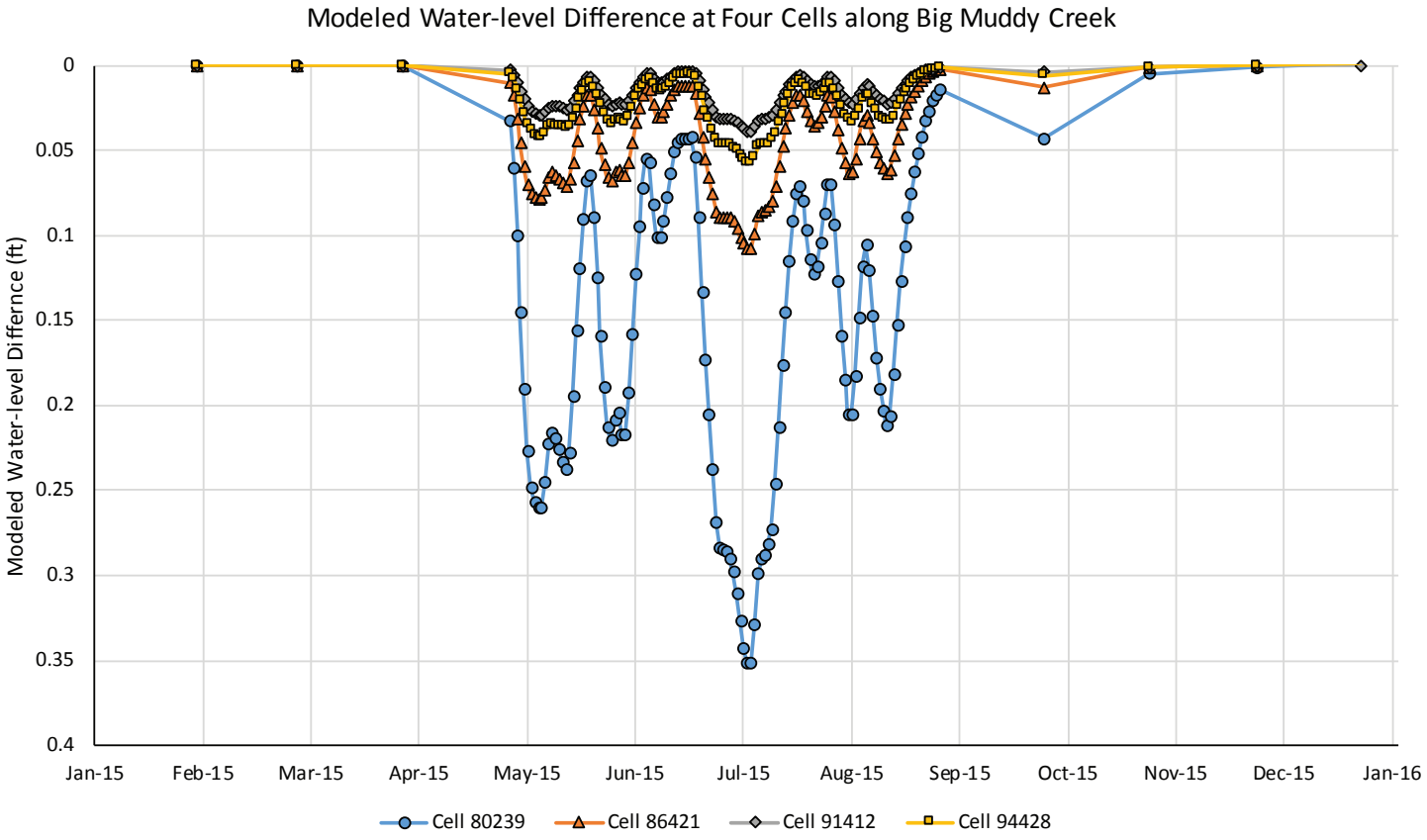

Figure D9. Time-series water-level differences between no irrigation use and 4 well 2015 volume pumping scenarios at four locations close to the Big Muddy. Cell locations are shown in figure D1.